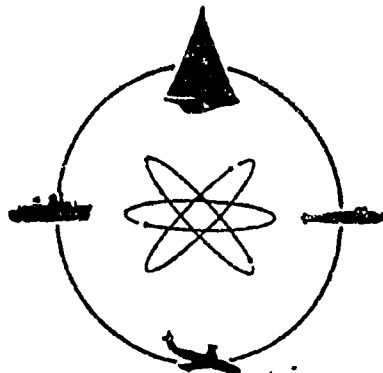


AD708694

R-1275



DAVIDSON LABORATORY

Report 1275

November 1969

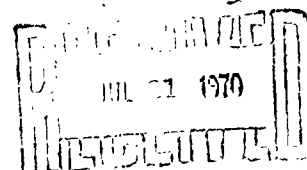
A SYSTEMATIC STUDY OF THE ROUGH-WATER PERFORMANCE
OF PLANING BOATS

by

Gerard Fridsma

This research was carried out under the
Naval Ship Systems Command
General Hydromechanics Research Program
SR 009 01 01, administered by the
Naval Ship Research and Development Center
under Contract N00014-67-A-0202-0010

This document has been approved for public release and
sale; its distribution is unlimited. Application for
copies may be made to the Defense Documentation
Center, Cameron Station, 5010 Duke Street, Alexandria,
Virginia 22314. Reproduction of the document in
whole or in part is permitted for any purpose of the
United States Government.



C -

73



STEVENS INSTITUTE
OF TECHNOLOGY

CASTLE POINT STATION
HOBOKEN, NEW JERSEY

DAVIDSON LABORATORY
STEVENS INSTITUTE OF TECHNOLOGY
Castle Point Station
Hoboken, New Jersey 07030

Report 1275

November 1969

A SYSTEMATIC STUDY OF THE ROUGH-WATER PERFORMANCE
OF PLANING BOATS

by

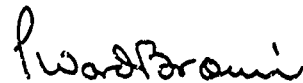
Gerard Fridsma

This research was carried out under the
Naval Ship Systems Command
General Hydromechanics Research Program
SR 009 01 01, administered by the
Naval Ship Research and Development Center
under Contract N00014-67-A-0202-0010

(DL Project 3383/096)

This document has been approved for public release and sale; its distribution is unlimited. Application for copies may be made to the Defense Documentation Center, Cameron Station, 5010 Duke Street, Alexandria, Virginia 22314. Reproduction of the document in whole or in part is permitted for any purpose of the United States Government.

Approved



P. Ward Brown, Manager
Marine Craft Development Group

viii + 38 pages
65 figures

ABSTRACT

A series of constant-deadrise models, varying in length, was tested in smooth water and regular waves to define the effects of deadrise, trim, loading, speed, length-beam ratio, and wave proportions on the added resistance, on heave and pitch motions, and on impact accelerations at the bow and center of gravity. Each of these parameters was varied independently of the others so as to obtain a proper evaluation of the effects of changing a single quantity. The results, presented in the form of response characteristics, cover a wide range of operating conditions; and show, quantitatively, the importance of design parameters on the rough-water performance of planing hulls.

Keywords

Planing Hulls
Hydrodynamic Impact
Marine Craft
Prismatic Surfaces
Motions
Resistance in waves
Linearity

CONTENTS

Abstract	iii
Nomenclature	vii
INTRODUCTION	1
MODELS	3
APPARATUS AND TEST PROCEDURE	5
Smooth-Water Resistance Tests	5
Regular-Wave Tests	6
RESULTS	9
Smooth-Water Resistance Tests	9
Regular-Wave Tests	9
DISCUSSION	11
Linearity	12
Effect of Speed	15
Performance at Speed-Length Ratio = 2	17
Performance at Speed-Length Ratio = 4	19
Performance at Speed Length Ratio = 6	23
CONCLUSIONS	25
RECOMMENDATIONS	29
ACKNOWLEDGEMENTS	31
TABLES	33-38
FIGURES (1-65)	

BLANK PAGE

NOMENCLATURE

b	beam of planing surface, ft
C_v	speed coefficient, V/\sqrt{gb}
C_Δ	load coefficient, Δ/wb^3
C_λ	wavelength coefficient, $L/\lambda [C_\Delta/(L/b)^2]^{1/3}$
g	acceleration of gravity, 32.2 ft/sec ²
H	wave height, crest to trough, ft
h	double amplitude heave motion, ft
I	pitch moment of inertia, slug ft ²
k	pitch gyradius, %L
k_g	non-dimensional factor defined as $C_\Delta/(L/b)^2$
L	model hull length, ft
LCG	longitudinal center of gravity, %L
ℓ_m	mean wetted length, ft
R	resistance in smooth water, lb
R_{aw}	added resistance in waves, $R_w - R$, lb
R_w	total resistance in waves, lb
TR_o	height of transom-wetting above chine at zero speed, %b
V	horizontal forward speed, fps
VCG	vertical center of gravity
V/\sqrt{L}	speed-length ratio, knots/ft ^{1/2}
w	specific weight of water, 62.4 lb/ft ³

β	deadrise angle, deg
Δ	hull displacement, lb
η_{bow}	acceleration at bow, normal to keel, g
η_{cg}	acceleration at center of gravity, normal to smooth-water surface, g
λ	wavelength, ft
φ_h	heave phase angle, lag positive, deg
φ_p	pitch phase angle, lead positive, deg
ρ	density of fresh water, 1.94 slug/ft ³
τ	trim angle, deg
τ_o	static smooth-water trim angle at zero speed, deg
θ_p	double amplitude pitch motion, rad

INTRODUCTION

For many years now, hydrodynamic studies of planing hulls have been directed chiefly toward problems of smooth-water resistance and stability. As a result, there is available, in the literature, extensive information on the basic elemental planing characteristics of prismatic hulls and also on several planing-hull series with excellent smooth-water characteristics. The combination of hydrodynamically efficient hulls and large installed horsepower has resulted in high-performance, high-speed craft which behave very well in smooth water.

The modern planing hull, however, is usually exposed to a rough-water environment, and a good smooth-water boat does not necessarily behave well in a seaway. Since concentrated, systematic studies have not been made to establish the extent to which rough-water performance depends upon boat geometry and operating conditions, there is a continuing controversy among designers on the subject of what constitutes a good rough-water boat. The proponents of the "round bottom" hull are locked in battle with the proponents of the "hard chine" hull, and the recent "deep vee" hull enthusiasts appear content with their particular designs. There is no question but that, for particular combinations of hull loadings, hull trim, speed, and sea state, each of the hull forms can exhibit good rough-water performance. The challenge to the hydrodynamic researcher is to define those loading and operating conditions which, in combination with a given body plan, can make rough-water performance acceptable. Without such qualifying conditions, it seems unreasonable to compare different boats on the basis of such a gross parameter as section shape (i.e., round bottom, hard chine, deep vee, etc.).

Yet the status of research is such that available information on the rough-water performance of planing hulls cannot provide the answers to all of these questions. There are, of course, model- and full-scale test results for specific boat designs, but the variations in test conditions are too limited to allow for any generalized conclusions. In recent years,

several papers have appeared which do attempt to study the effect which systematic variation in hull form and loading has on seakeeping. These studies, although few and circumscribed, provide results that are most useful to a broad investigation of the behavior of planing hulls in a seaway.

A recent survey of the available literature attempted to isolate and define those parameters which significantly influence rough-water behavior.* To eliminate the many serious gaps in the present state of knowledge, this survey strongly recommended that systematic tests be undertaken to study the linearity of response and to learn the effect of hull geometry, of operating loads and trim, of boat speed, and of regular-wave proportions upon rough-water characteristics such as resistance increment, trim and heave motions, and hydrodynamic impact accelerations. An attendant analysis of the systematically collected experimental data obtained in such studies would produce results immediately applicable to the rational design of planing hulls intended for rough-water operation.

The Department of the Navy, acting on the recommendations of the survey, contracted with the Davidson Laboratory for an investigation of the kind described above. The study was conducted as part of the Navy's General Hydromechanics Research Program, and involved the testing of simple, constant-deadrise models. The results, presented in the form of response operators, relate planing-boat performance to the hull and wave characteristics over a sizable range of speed. The work was performed in the Davidson Laboratory's Tank 3, over the period of March-December 1968.

*For a report of the survey, see Daniel Savitsky's paper "On the Seakeeping of Planing Hulls," presented at the May 1966 meeting of the Southeast Section of the Society of Naval Architects and Marine Engineers. The report contains a good bibliography.

MODELS

Three models with 9-in. beams were built by the Davidson Laboratory according to the lines drawing of Fig. 1. Airplane plywood and balsa were used throughout, in an effort to keep the models light yet strong enough to absorb the pounding of waves. The outside surface of each model was given five coats of varnish and rubbed to a smooth finish. The bow of each (hollowed out from solid balsa) was one beam in length and of constant deadrise. Sections aft of the bow were constant hard-chine prismatic forms with deadrise angles of 10, 20, and 30 degrees, respectively, for the three models. The 20-deg deadrise model was built with three transom sections, for investigation of length-beam ratios of 4, 5, and 6. Photographs of the models appear as Fig. 2.

The bows were unconventional, since constant deadrise is unrealistic from a practical viewpoint. In a study of this kind, however, it becomes increasingly apparent that if the deadrise effect is to be isolated, particularly during bow accelerations, it must be made a feature of the test models (incorporating a family of more realistic bow shapes would throw another variable into the program and make evaluation more difficult). All the bows had identical planforms and elliptical keel profiles.

The hulls were constructed with U-shaped bulkheads, so that there would be clearance for the arrangement of ballast and room to adjust the LCG (50 to 80 percent of the model length after station zero). Two longitudinal rails made of hardwood were installed parallel to the keel; they spanned the bulkheads along the entire inside of the model. These rails were fitted with a plate engineered to slide and clamp along their length. The plate could accept a standard pivot box, as well as threaded steel rods for the positioning of weights at given distances from the pivot or the LCG. With the model so light, and with most of its displacement deriving from the ballast on the threaded rods, the LCG could be shifted without greatly affecting the magnitude of the pitch moment of inertia. Model construction and plate are shown in Fig. 3.

To obtain the length-beam ratios for the model with 20-deg deadrise, this model was cut at station 7, and three transom sections were constructed with lengths of 0.5, 1.5, and 2.5 beams (1, 3, and 5 stations). Hardwood bulkheads on the sides of the joint ensured against leakage and provided firm support for clamps used to fasten the forward and aft sections together. A thick silicone grease, sandw'ched between the butted bulkheads, further ensured against the entry of water.

The models were ballasted so that in each case the pivot became the center of gravity of the hull. The VCG was held constant for all models (0.294 beams above the keel). For the smooth-water tests, the LCG was changed simply by shifting ballast from one threaded rod to another. In the rough-water phase, the plate was moved until the pivots came to the specified LCG; then the proper amount of ballast was inserted in the model to obtain the correct CG, displacement, and moment of inertia, simultaneously. The gyradius was set at 25%L for the $L/b = 5$ models at $C_{\Delta} = 0.608$ design displacement. For other loadings, changes in ballast were made at the CG to maintain the same inertia value. The only time the inertia was allowed to change was in going to models with other length-beam ratios; for these models, the gyradius per unit length was held constant, so that the inertia would vary as the square of the length.

Each model was equipped with a bubble level mounted parallel to the keel (which also served as the reference for zero trim); and with mounting plates for accelerometers. The accelerometers were installed at the longitudinal center of gravity just above the pivots and at the bow, 10 percent of the length aft of the stem. For the rough-water tests, a clear plastic cover was fitted over the deck to keep water from sloshing into the model.

APPARATUS AND TEST PROCEDURE

SMOOTH-WATER RESISTANCE TESTS

If one is to use a parametric study for comparing the performance of planing boats in rough water, a matrix of smooth-water operating conditions must be developed. When comparing planing hulls that have different deadrise angles, it is, for example, necessary to evaluate them at the same speed, load, length-beam ratio, moment of inertia, and running trim. The LCG position that a 30-deg deadrise boat requires for operation at 4-deg trim will be different from that required by a boat with 10-deg deadrise at the same condition. The smooth-water tests, therefore, were designed to cover a wide range of loading, speed, and LCG positions, so that cross-plotting would make it possible to choose a number of specific running conditions for later investigation in regular waves.

These tests were conducted in the Davidson Laboratory's Tank 3. The standard free-to-heave and -trim resistance carriage was used, together with a (0-20 lb) drag balance. Because of the nature of the study, no provision was made for the stimulation of turbulence.

The rise of the CG, the trim, and the drag were measured over a constant-speed range of zero to 20 fps ($C_v = 0-4.0$), at $C_\Delta = 0.304, 0.608$, and 0.912 , and for LCG positions at from 50 to 80 percent of the hull length. Values for wetted keel-and-chine intersections, and for the extent of side-wetting, were obtained after each run, from polaroid pictures. All models were assumed to have thrust lines parallel to the smooth-water surface, and it is therefore not necessary to account for unloading related to the vertical component of the thrust.

While testing, small irregularities were noted in running plots of the drag data. It was discovered that the flow was wrapping up along the side-wall, because there was no separation at the chine. A thin celluoid strip taped to and projecting 0.030 inches below the chine helped to

alleviate this problem. Such strips were later attached to all models.

REGULAR-WAVE TESTS

The "free to surge" servo-carriage was used to study the performance of the planing-hull models in regular head seas. This carriage allows the model complete longitudinal freedom as well as the usual freedom in heave and trim. The longitudinal freedom is provided by a servo-controlled system which keeps a small, lightweight, model carriage centered on an auxiliary subrail. The subrail, suspended from the main carriage beneath and parallel to the monorail of the tank, provides a travel of ± 2 feet. With this freedom, the model arrives at its own speed when a balance between the applied thrust (a falling weight) and the hydrodynamic resistance force is reached. And with freedom to surge, the model can "check" in the wave system, instead of being "forced through" the waves as it would be if it were towed at constant speed. The applied thrust, which is equivalent to model resistance once constant speed is attained, exerts a constant horizontal force at the model's center of gravity or tow point. Figure 4 is a photograph of the test setup.

Once the model was set up for the desired test condition (Table 1), it was attached to the servo subcarriage. The tank was then filled with waves, and the model brought up to the desired constant speed. At a given position in the tank, solenoids released the subcarriage and allowed the model freedom to surge. Time histories were then taken of speed, heave and pitch motions, wave profile, and bow and CG accelerations (these were recorded on oscillograph tape). Since the model had to seek an average equilibrium speed, for the corresponding applied thrust, it was not always possible to choose that particular thrust-speed combination which would produce the desired speed-made-good in the seaway. A number of trials were usually necessary to arrive at the desired test condition.

The apparatus was run without the model, for a routine determination of air tares; and a few model runs were made to check smooth-water resistance and trim. Two of the model configurations were run in irregular waves to check the correlation of the response amplitude operators in the

regular and the irregular seas.

The models were tested in regular waves at wavelength to hull-length ratios of 1, 1.5, 2, 3, 4, and 6; at speed-length ratios of 2, 4, and 6; with deadrise angles of 10, 20, and 30 degrees; with length-beam ratios of 4, 5, and 6; and with running trim angles of 4 and 6 degrees and displacements corresponding to C_{Δ} 's of 0.608 and 0.912. Wave height was varied initially from 1 to 3 inches, to determine linearity; then it was fixed at 1 inch or 0.11 beam for the remainder of the tests. The rough-water test configurations are given in Table 1 (p. 33).

A wave wire was mounted on the carriage abreast of the LCG and about a beam's distance to port of the model centerline. This wire was used exclusively for the phasing of the motion-time histories relative to the wave.

RESULTS

SMOOTH-WATER RESISTANCE TESTS

The results for these tests are plotted as a function of V/\sqrt{L} in Figs. 5 to 17. In most cases, the model data have been non-dimensionalized by standard methods. Barriers located on the plots indicate porpoising at the higher trims or excessive bow-wetting at the lower trims.

The running trims later used in the rough-water test were selected after a study of the smooth-water results. The selection took into account the need to prevent diving at the lower speeds and porpoising at the high speeds. Values of 4 degrees and 6 degrees were finally selected for running trim, and the appropriate LCG positions were obtained from cross-plots.

REGULAR-WAVE TESTS

The wave-test results are tabulated in Table 2 and plotted in Figs. 18 to 65. They were obtained by averaging the peaks of ten consecutive cycles once the speed was constant and a regular periodic time-history pattern was established. The double amplitude heave motions were non-dimensionalized by wave height (crest to trough), and the double amplitude pitch motions by twice the wave slope. The phasing of the motions is defined below.

- (a) Zero phase angle for heave and pitch: The maximum heave or pitch motions occur with the wave crest at the longitudinal center of gravity.
- (b) Phase lag: Pitch or heave has reached a maximum amplitude after the wave crest has passed the LCG.
- (c) Phase lead: Pitch or heave has reached a maximum before the wave crest arrives at the LCG.

PRECEDING PAGE BLANK

The accelerations presented are in the up direction (tending to lift the boat), and are measured from the zero "g" or still-water condition. The added resistance, R_{aw} , is the difference between the smooth- and rough-water values after removal of air tares.

The results are plotted as a function of the parameter

$$C_{\lambda} = \frac{L}{\lambda} \left[\frac{C_{\Delta}}{(L/b)^3} \right]^{1/3}$$

A value of $C_{\lambda} = 0$ corresponds to an infinitely long wave, with the boat assumed to contour the wave perfectly. Thus the asymptotic solution for long waves becomes another datum point on the plot; and the various responses can be presented over the entire range of significant wavelengths.

The correlation between regular and irregular seas was studied by comparing the heave response amplitude operators of a given model condition, as found by tests in each wave system. The response amplitude operators in irregular seas were determined by standard spectral-analysis techniques and evaluated on an IBM 360 computer.

DISCUSSION

Figures 18 through 65 are presented in a sequence that facilitates logical and systematic discussion of results. The first block of figures, Figs. 18 to 24, has to do with the linearity of the measured quantities with wave height. The second block, Figs. 25 to 35, illustrates the effect of speed. Then, beginning with Fig. 36, the remaining plots are divided into regimes of speed-length ratio 2, 4, and 6, or C_v 's of 1.3, 2.7, and 4.0. At a speed-length ratio of 2, the planing hull behaves much like a displacement ship (Figs. 36 to 43). This is a "pre-hump" condition, with the buoyancy forces playing the major role. Some lift is generated, and the flow breaks clean of the transom, but there is a significant amount of side-wetting. At a speed-length ratio of 4, the boat is beginning to plane (Figs. 44 to 60). This is a "post-hump" condition in which the dynamic and buoyant forces on the hull are both significant. Some side-wetting may still appear at this speed. At a speed-length ratio of 6, the hull is fully planing, the buoyancy plays only a minor role, and no side-wetting is observed (Figs. 61 to 65).

Within the various blocks of figures, the measured quantities of resistance, heave, pitch, and acceleration are presented in order. The effect of load, trim, deadrise, and length-beam ratio are illustrated at each particular speed-length ratio. Not all combinations of parameters could be tested, because of the immensity of the test program that would be required and the physical impossibility of running certain conditions.

In the course of analysis, a non-dimensional factor was discovered that collapsed the motion data with respect to load and length-beam ratio. This factor was $C_\lambda = L/\lambda [C_\Delta/(L/b)^2]^{1/3}$. The term C_λ may be thought of as a frequency-ratio coefficient which relates the load and the geometry of the hull to the wavelength. The term inside the brackets is the familiar k_2 -factor associated with the loading of seaplane hulls. In its essential form, C_λ is equal to $1/\lambda (\nabla L/b)^{1/3}$. Although a function of λ , ∇ , L , and b , the coefficient is not strongly dependent on ∇ , L , and b .

because they are raised to the $1/3$ power. Thus a 100-percent or a 50-percent increase in the magnitudes of these three quantities only changes C_λ by 26 percent and 14.4 percent, respectively.

Unfortunately, the introduction of a new non-dimensional coefficient means that the designer wastes some of the practical experience he has gained in relating rough-water performance to the ratio of wavelength to hull length (L/λ). But the step is necessitated by the fact that the length of a planing boat is not the only significant parameter. To conserve the experience gained with the L/λ ratio, for the range of conditions tested in these studies, the following approximation may be taken:

$$L/\lambda \approx 3.4 C_\lambda$$

LINEARITY (Figs. 18-24)

Configurations H, A, and B (Table 1) were used to check linearity at speed-length ratios of 2, 4, and 6 respectively. Although H is a 10-deg-deadrise model condition and A and B are 20-deg model conditions, it was presumed that any one of these deadrise models could be tested to determine the linearity of the results. For the speed-length ratio of 2, and small wave heights, the effect of deadrise turned out to be insignificant.

Added Resistance

The variation of added resistance with wave height is shown in Fig. 18 for V/\sqrt{L} values of 2, 4, and 6. For the most part, the results show that added resistance has a non-linear dependence on wave height, although some exceptions do appear. At a $V/\sqrt{L} = 2$, the added resistance varies as the wave height raised to the 1.67 power, while at $V/\sqrt{L} = 4$ the power is 1.35. No great importance should be assigned to these particular values except as they indicate the type of non-linearity. At a $V/\sqrt{L} = 6$, only two wavelengths were investigated. At the shorter of the two, the added resistance is linear with wave height, but at the longer it is discontinuous because the model is leaving the water surface.

Heave and Pitch Response

Figures 19 and 20 show that both the heave and the pitch motions are linear with wave height at $V/\sqrt{L} = 2$, over all wavelengths. This is not surprising, since the model behaves like a displacement ship at this speed, and displacement ships generally have linear motion response.

At $V/\sqrt{L} = 4$, however, the motion response is linear only at the very short and long wavelengths. The non-linear behavior at $\lambda/L = 2$ and 3 is characterized by an attenuation of the motions with wave height. For both the heave and the pitch, the response increases at some fractional power of the wave height, usually between 0.7 to 0.85.

At the still higher speed, $V/\sqrt{L} = 6$, and wavelengths of two and four model lengths (the wavelength range of marked non-linear behavior), the trend with wave height is similar to that at $V/\sqrt{L} = 4$, with one exception -- the motions increase as wave height to the 0.7 to 0.8 power, except for the pitch motion in the shorter of the two waves, where the variation increases as $H^{0.4}$. It would appear that at this speed-length ratio the wavelength range of non-linear behavior is shifted toward the longer wavelengths.

To further study the linearity of the motions, response characteristics like that shown in Fig. 21 can be plotted from the regular wave data. The ordinate, which is known as a response amplitude operator (RAO), indicates the system's response to input throughout the range of significant frequencies or wavelengths. In a linear system, the RAO is independent of the impressed amplitude and thus becomes a very useful tool in predicting response to any type of input function. The lack of linearity is evidenced in Fig. 21 by the dependence of the heave RAO on the wave height. The response amplitude operator may also be generated by testing the model in irregular waves instead of in a series of regular waves, in which case spectral-analysis techniques are used to determine the RAO's (the RAO's should be identical to those found for regular waves if the response is linear with wave height). A comparison of the two methods, then, becomes a measure of the system's linearity.

Such a comparison is shown in Fig. 22. Configuration A (at the bottom of the figure) was tested in a relatively large irregular sea, and the

RAO's from the spectral analysis are compared with linearized RAO's from the regular-wave tests. Agreement is poor. This is not too surprising, since the average wave height of the irregular sea was 0.202 beam, which placed a good deal of the wave spectrum beyond the linear response of the model hull. Configuration 1, the 10-deg deadrise model (top of Fig. 22), was tested in a smaller irregular sea with an average wave height of 0.118 beam. Since a great deal more of this wave's energy lies within the linear range, the comparison of the RAO's from the regular and the irregular waves shows better agreement.

Accelerations

The accelerations at the CG and bow (Figs. 23 and 24) are non-linear with wave height, again with some exceptions. At a $V/\sqrt{L} = 2$, the accelerations increase sharply for the 10-deg deadrise model. No consistent power function of wave height was apparent, although accelerations for $\lambda/L = 1.5$ and 2 appear to vary as wave height to the 4th power. At long wavelengths, however, there is a tendency for the accelerations to be linear with wave height. This can be shown more readily at a speed-length ratio of 4, where linear behavior is found for the CG accelerations at $\lambda/L = 3, 4$, and 6 and for the bow accelerations at $\lambda/L = 4$ and 6. At other wavelength values where the behavior is non-linear, both CG and bow accelerations increase as the 1.6 power of the wave height. This is also true at the speed-length ratio of 6.

Summary

The added resistance, motion response, and accelerations are, in general, non-linear functions of the wave height, although there is a tendency for these quantities to behave linearly at the longer and the shorter wavelengths. The one exception is at a $V/\sqrt{L} = 2$, where the motions are linear over all wavelengths. Where they are linear, the performance of the planing boat can be characterized as approaching either the limiting condition of "contouring" (i.e., exhibiting motion that follows the waves) at long wavelengths, or "platforming" (exhibiting motion that is independent of the waves) at short wavelengths. Provided the wave heights are small (< 0.15 beam), the motion responses can be assumed

linear, with little error.

EFFECT OF SPEED (Figs. 25-35)

The effect of speed was determined by testing the 10-, 20-, and 30-deg deadrise models at speed-length ratios of 2, 4, and 6. While it is apparent that these speed-length ratios correspond to three distinct flow regimes, it is nonetheless interesting to observe how speed affects the added resistance, motions, and accelerations for the three deadrise models.

One rather unusual phenomenon occurred at $V/\sqrt{L} = 6$ for the 10-deg deadrise model, at a wavelength value equal to one and a half hull lengths ($C_\lambda = 0.194$). The model was observed to rebound from a wave crest, completely "fly over" a second wave crest, and land again on the third. This pattern was perfectly periodic and repeatable over many cycles. The result is shown in the figures as another resonant or peaking condition.

Added Resistance

For the 10-deg deadrise model, added resistance (Fig. 25) increases with speed over all wavelengths greater than a hull length. This is also true for the 20- and 30-deg models in long waves up to $C_\lambda = 0.10$. At the shorter wavelengths, added resistance for the two higher-deadrise models increases with speed up to a maximum at $V/\sqrt{L} = 4$, then decreases at $V/\sqrt{L} = 6$.

The wavelength at which the maximum added resistance is reached shifts with speed-length ratio and follows the same trend for each deadrise model. The figures show the maximum added resistance to occur at $0.2 \leq C_\lambda \leq 0.3$ for $V/\sqrt{L} = 2$, at $0.15 \leq C_\lambda \leq 0.2$ for $V/\sqrt{L} = 4$, and at $C_\lambda = 0.1$ for $V/\sqrt{L} = 6$.

A possible explanation for this shift in the maximum resistance, as well as for the leveling off of resistance at short wavelengths, is that at high speeds and short wavelengths the model cannot fall into the wave as readily. Consequently, it skims across the wave crests, with greatly

reduced motions and improved resistance characteristics. It should be noted that the wavelength corresponding to maximum resistance is consistently shorter than the wavelength corresponding to maximum motions (this will be referred to later).

Heave and Pitch Motions

The trend of heave and pitch motions with speed, plotted in Figs. 27 to 31, shows all three deadrise models exhibiting similar behavior. Increasing the speed magnifies the motions to a great degree, near resonance -- in a manner analogous to the removal of damping from the system. With higher speeds, the resonant peak shifts to longer wavelengths.

Maximum motions in all cases occur at wavelengths equal to three to four times the hull length ($0.07 \leq C_\lambda \leq 0.1$). At the shorter wavelengths ($C_\lambda > 0.145$), increasing the speed tends to reduce the motion, until, at wavelengths of the order of a hull length, the effect of speed is very small.

These results are in line with the experience of operators, who find that planing boats commonly get stiffer at high speed-length ratios.

For phase, the plots show a consistent trend that bears no similarity to that for a single-degree-of-freedom system with simple harmonic motion. The phase has its predicted value at long wavelengths (contouring), passes through a maximum lag in the vicinity of $C_\lambda = 0.15$ to 0.20 , and then appears to level off at some intermediate value. Increasing the speed increases the magnitude of the phase lag.

Accelerations

Figures 32 to 35 show the marked capacity that speed has for increasing the accelerations at all wavelengths and for all three deadrise models. The wavelengths at which the accelerations reach a maximum are similar to the wavelengths at which the maximum added resistance is obtained. The extremely large accelerations experienced at $V/\sqrt{L} = 6$ by the 10-deg deadrise hull should be noted. Despite the low wave height, large and intolerable accelerations can be developed on the hull.

Summary

Speed is and continues to be the limiting factor in the design of rough-water planing craft. At high speed-length ratios the sharply tuned resonant peaks in the motion and acceleration responses prohibit practical operations, particularly for low-deadrise boats. Higher speeds also account for greater added resistance at the longer wavelengths, for all three deadrise models.

The results do not exhibit any properties that would indicate a complete collapse of the data with speed. For the short wavelengths, ($C_\lambda > 0.25$), there does appear to be some correlation with speed. In this wavelength range, the motions are small and independent of speed; and the accelerations are power functions of speed. It is interesting to note that the accelerations increase as the square of the velocity, for the 10-deg deadrise model, but are linear with speed for the 30-deg deadrise model.

PERFORMANCE AT SPEED-LENGTH RATIO = 2 (Effect of Deadrise and Trim; Figs. 36-43)

It has already been established that at this speed the motions are linear with wave height but the added resistance and accelerations tend to be non-linear. Within the linear range and at a constant wave height, the effects of deadrise and trim variations on planing-hull performance were studied as a function of wavelength.

Examination of Figs. 36 to 43 shows that a distinctive frequency exists at $C_\lambda = 0.194$ or at a wavelength one and one-half times the hull length. For one thing, the added resistance is greatest at this wavelength. In addition, there is a maximum phase shift in the motions, together with a peak in the accelerations. The motions, however, peak at longer waves of the order of $C_\lambda = 0.085$, which is in the area of the craft's natural frequency. At this condition, the motions are damped, with little or no overshoot.

For displacement ships, maximum added resistance is usually associated with maximum motions. This is not true for the planing boat at this speed.

The data indicate the added resistance to be greatest at a wavelength half that for maximum motions; and to occur at a wavelength where the motions are attenuated by at least 50 percent.

Effect of Deadrise

Configurations H, C, and L were the model conditions tested at $V/\sqrt{L} = 2$. These represent the 10-, 20-, and 30-deg deadrise models, respectively. Each model had a length-beam ratio of 5, a C_{Δ} of 0.608, smooth-water running trim of 4 degrees, and a gyradius of 25%L. The respective LCG positions for the 10-, 20-, and 30-deg models were 62 percent, 61.5 percent, and 62.5 percent of the length aft of station zero.

Deadrise has virtually no effect on the response of the planing hull at this speed. Although the total resistance in waves increases with increasing deadrise (see bottom of Fig. 36), this is just a reflection of the higher smooth-water resistance which is known to increase with deadrise. Isolating the added increment in rough water (Fig. 36, top) reveals little deadrise effect.

The motions, too, are unaffected by deadrise (Figs. 37 and 38). However, the heave response does indicate slightly higher motions with increasing deadrise. The pitch response and the phasing for both heave and pitch are identical for the three deadrise models.

The bow and CG accelerations (Fig. 39) are also independent of deadrise, at this speed and wave height.

Effect of Trim

Configurations C and D, representing a 4- and 6-deg smooth-water running trim respectively, were tested at identical values of length-beam ratio (5), load ($C_{\Delta} = 0.608$), deadrise (20-deg) and gyradius (25%L). The increased trim was obtained by shifting ballast from an LCG position of 61.5%L to one of 67.5%L.

The effect of trim on resistance is presented in Fig. 40. The total resistance in waves is significantly increased when the trim is increased;

and the rough-water increment, because of a 2-deg increase in trim, is larger by 50 percent, over the C_λ range from 0.1 to 0.3.

The motions (Figs. 41 and 42) are affected by trim to some degree, but to a significant degree only in the region of resonance. The comparable heave response for the condition with 6-deg trim is slightly larger in magnitude than that for the 4-deg trim condition. On the other hand, the pitch motions are consistently higher, particularly at resonance, where there is a 20-percent increase in the pitch motions. Heave phases for the 6-deg and 4-deg trim cases are identical for all wavelengths. The phase angles for the pitch motions show the lag for the model with 6-deg trim falling behind that for the 4-deg model.

Figure 43 shows that CG accelerations are unaffected by the 2-deg increase in running trim. The bow accelerations, however, are increased by an average of 50 percent, over the wavelength spectrum.

PERFORMANCE AT SPEED-LENGTH RATIO = 4 (Effects of Deadrise, Trim, Length-Beam Ratio, and Load; Figs. 44-60)

Most of the parametric study was carried out at the speed-length ratio of 4, because this speed is more typical in planing craft operations than are speeds of 2 or 6. Linearities at this speed have already been discussed, and shown to be dependent on wavelength. Within the linear range, at a constant wave height of 0.11 beam, the deadrise, trim, load, and length-beam ratio were varied. At this speed the collapsing factor C_λ was discovered.

As in the case of lower speed, certain trends with wavelength appear. A distinctive frequency is again observed, not defined as well as at $V/\sqrt{L} = 2$ but appearing to have shifted toward $C_\lambda = 0.15$ ($\lambda/L = 2$). A good deal of the data for added resistance, motion phase angle, and accelerations peak in the range $0.14 \leq C_\lambda \leq 0.2$. The motions again reach their maximum amplitudes near resonance, at a C_λ equal to 0.09; and are more sharply peaked than at $V/\sqrt{L} = 2$. It is clear, here also, that the maximum added resistance and maximum motions do not occur at the same wavelength, but differ by a factor of about 2.

Effect of Deadrise

The family of model conditions (I, A, and K) was tested under the same conditions as at $V/\bar{L} = 2$, except for a doubling of speed. The LCG positions for the 10-, 20-, and 30-deg deadrise models were, respectively, 59.5%L, 59.0%L, and 59.5%L.

The deadrise effect becomes more pronounced with speed, although some of the performance features found at $V/\bar{L} = 2$ are also found at this speed. The added resistance, for example (Fig. 44), remains independent of deadrise even though the total resistance in waves increases with deadrise. The resistance data for Configuration A (the first condition tested) scatter about the plotted line to a considerable degree, and are somewhat suspect. The data were faired to the line shown, for two reasons: (1) the data become consistent with data for similar configurations; and (2) the phasing wire was, for this test only, towed ahead of the model. It was found, during the course of testing, that the position of the wave wire introduced errors in resistance values. Consequently, the wire was moved to a position abeam of the hull. Unfortunately, repeat runs for Configuration A were not carried out to obtain more accurate resistance values.

Deadrise also has small effect on motions -- virtually none on the magnitude of heave and pitch response (Figs. 45 and 46). There does, however, appear to be a trend in the motion phases at $0.15 \leq C_\lambda \leq 0.30$. The motions of the lower-deadrise model lag the wave motion to a greater degree. For $C_\lambda \leq 0.15$, deadrise has no effect on motion phases.

It is in reducing the magnitudes of the accelerations that deadrise can be used to good advantage (Fig. 47). At this speed-length ratio, accelerations in the shorter waves are considerably lower for the higher-deadrise models. On CG acceleration, deadrise has no effect in the longer waves ($C_\lambda \leq 0.15$), but for shorter waves there is at least a 50-percent reduction of impacts in going from a 10- to a 30-deg deadrise model. The bow accelerations are independent of deadrise for $C_\lambda \leq 0.1$. At the shorter wavelengths, a 30-deg deadrise model has only 35 percent to 55 percent of the acceleration levels experienced by the 10-deg model.

Effect of Trim

The 20-deg deadrise model was tested in regular waves at smooth-water running trims of 4 degrees (A) and 6 degrees (E), with other conditions the same. The respective LCG positions were 59%L and 65.5%L.

At this speed-length ratio, the total resistance of the 4-deg configuration and that of the 6-deg trim configuration overlap (Fig. 48). It would appear that the 4-deg condition has less resistance at the longer wavelengths ($C_\lambda \leq 0.15$), and that the 6-deg condition has less resistance at wavelengths shorter than this value. This may be due to a coupling with the motions where the motions of the 6-deg trim configuration are higher -- in the region of resonance (see Figs. 49 and 50). That is, a 2-deg increase in the running trim, at resonance, accounts for a 45-percent increase in heave motions and a 60-percent increase in pitch motions. Yet in this range of waves the phase angles are unchanged. Trim has no effect on heave and pitch motions for $C_\lambda \geq 0.15$. However, the motions of the 6-deg trim model now show a notably greater lag behind the wave motion than do the motions of the 4-deg trim model.

The effect of a 2-deg change in trim on the values of acceleration is quite pronounced (Fig. 51). Over the C_λ range of from 0.08 to 0.3, an increase in trim from 4 to 6 degrees produces a 50- to 100-percent higher level of CG and bow accelerations.

These findings confirm what has been intuitively known from experience -- that the ride in rough water is smoother when the planing craft is trimmed down by the bow; and furthermore, that this effect becomes more significant as the speed increases.

Effect of Length-Beam Ratio and Load

The effect of load was evaluated at the two length-beam ratios of 5 and 6. In each case, the model ballast was adjusted when the load was changed, to maintain the same running trim and the same value of pitch inertia. Of course when this is done the gyradius changes. When the length-beam ratio was changed, however, the pitch inertia was increased or decreased as the square of the length, so that the gyradius would remain constant.

Configurations E and F illustrate the effect of load at $L/b = 5$, with C_{Δ} 's of 0.608 and 0.912, respectively, and constant smooth-water running trims of 6 degrees. The comparison here is between a normally loaded hull (E) and a heavily loaded hull (F). For the $L/b = 6$ model, configurations N and O were tested at C_{Δ} 's of 0.608 and 0.912 with running trim of 4 degrees. This comparison is between a normally loaded (O) and a lightly loaded (N) hull. Configurations P, A, and N are used to compare the effects of length-beam ratios of 4, 5, and 6, for the same load ($C_{\Delta} = 0.608$), trim (4 deg), and deadrise (20 deg).

The resistance in rough water for the configuration with a length-beam ratio of 4 (P) could not be obtained, because this heavily loaded boat had an excessively high hump resistance.

Figure 52 shows the effect of L/b on resistance, for $L/b = 5$ and 6. No appreciable change is found in the added resistance, but the total resistance is lower for the $L/b = 5$ model in wavelengths greater than two model lengths.

The effect of load on resistance (Figs. 53 and 54) is intuitively known. There is no way of loading a boat without paying the penalty of more drag. This is true for both smooth water and rough water, including the added component in waves. The absolute amount of the increase in resistance can be found by multiplying the ordinates by the respective displacements.

If the terms R_w/Δ and R_{aw}/Δ may be considered a drag-lift ratio and an added drag-lift ratio in waves (these are an inverse measure of the efficiency of the hull), then when the load is increased the R_{aw}/Δ versus C_{λ} plot shows a deterioration of efficiency in waves for both of these length-beam ratio models when C_{λ} values are above 0.15.

The significance of the C_{λ} factor is clearly seen in Figs. 55 and 56, where both the heave and pitch motions and phase are collapsed onto one line for all three length-beam-ratio conditions. A change in load is also collapsed onto the line except in the area of resonance, where a reduction in motions is attained without any change in phase. Thus in a given wave, at an encounter frequency smaller than resonance, higher values in load and length, or smaller beams, will increase the motions. On the other side of

resonance, these same changes will decrease the motions.

The effect of load on the motions can also be seen in Figs. 57 and 58 where displacement is varied at a smooth-water running trim of 6 degrees. Here again the motions are significantly reduced. At resonance the heave motions are reduced 25 percent and the pitch motions 30 percent. At this trim condition, moreover, the phase angles for the lighter of the two loads indicate motions lagging behind those for the heavy load.

Another look at the motion responses, in the plots comparing Configurations A and F, shows that a 2-deg trim increase (from 4 to 6 degrees), together with a 50-percent load increase, produces motions of about the same magnitude and phase. That is, the smaller motions associated with greater load compensate for the larger motions associated with higher trims.

Figure 59 contains another collapse of data, this time with accelerations. When the accelerations in g's are multiplied by $C_{\Delta}/(L/b)$ (sometimes referred to as the K_1 -factor), and plotted versus C_{λ} , a single line is obtained for both CG and bow-acceleration data. This is true, of course, for the combination of parameters given ($V/\sqrt{L} = 4$, $\tau = 4$ deg, $\beta = 20$ deg). What is gained is that for $C_{\lambda} > 0.2$, or wavelengths smaller than one and a half hull lengths, the magnitudes of the accelerations are proportional to $(L/b)/C_{\Delta}$.

The same kind of comparison with load at a different trim (Fig. 60) indicates a collapse of the CG accelerations, but a marked decrease of the bow accelerations in the range $0.08 < C_{\lambda} < 0.2$.

PERFORMANCE AT SPEED-LENGTH RATIO = 6 (Effect of Deadrise; Figs. 61-65)

At the fully planing speed of $V/\sqrt{L} = 6$, the behavior of the planing boat is quite non-linear, more so than at the lower speeds. The boat can better negotiate the smaller wavelengths, since it doesn't tend to fall into the wave troughs. However, there is little damping in the hull; and the craft rebounds, pitches, and heaves in a dangerous manner, at certain critical frequencies. Acceleration levels are high and would limit the operation of low-deadrise boats at this speed. The constant-height wave

of 0.11 beam was used to evaluate the effect of deadrise at this speed, over a range of wavelengths.

The major characteristic of planing-boat performance at this speed is the highly tuned behavior at a wavelength at or near the resonant frequency. In this case, it occurs at a wavelength of four hull lengths, $C_\lambda = 0.085$. Motions peak at this frequency. Resistance and accelerations peak at a slightly smaller wavelength value of three hull lengths or $C_\lambda = 0.1$, which again points up the fact that resistance and accelerations do not peak at the same frequency or wavelength as do motions. Maximum phase lag still occurs in the wavelength range of one and a half to two hull lengths or C_λ values of 0.15 to 0.20.

Configurations J, B, and M, representing deadrise angles of 10, 20, and 30 degrees, were tested at the same load, trim, inertia, and length-beam ratio. Corresponding LCG positions were 68%L, 62%L, and 60.5%L, respectively.

While the total resistance for higher-deadrise boats in waves is still large (Fig. 61), the added resistance decreases as the deadrise increases. This is not so at $V/\sqrt{L} = 2$ and 4, where added resistance in waves is independent of deadrise. Thus, once the decision has been made to go to deep-vee hulls and the penalty has been paid for using greater installed horsepower to run at high speed in smooth water, the percentage increase of resistance in waves is very small.

The effect of deadrise on motions appears in Figs. 62 and 63. The heave and pitch motions are drastically reduced with increasing deadrise. Resonant motions are smaller, and the tendency of the boat to "fly" and leave the water surface is lessened. At resonance ($C_\lambda = 0.085$), the heave motions are lessened by 25 percent and the pitch motions by 50 percent in going from a 10- to a 30-deg deadrise boat. Associated with the smaller motions are smaller phase lags for the 30- versus the 10-deg boat.

The deadrise effect is most significant in the case of accelerations (Figs. 64 and 65). For the 30-deg deadrise boat, the peak at $C_\lambda = 0.1$ virtually disappears, and the accelerations at other wavelengths are consistently about 75 percent (or more) smaller than for the 10-deg boat.

CONCLUSIONS

A series of constant-deadrise models of varying length was tested to define the effect of deadrise, trim, load, speed, length-beam ratio, and wave proportions on the resistance, motion, and accelerations of a planing craft in waves. Although it was not possible to test all combinations of parameters (because of the extensive testing that would have been required), extreme care was taken, in changing a single parameter from one value to another, to keep other model parameters the same. Thus in evaluating each of the three deadrise models, the load, running trim, and length-beam ratio were kept constant.

One important finding concerns the extent of the linearity of the results with wave amplitude. Linearity is found to be, in general, a function of speed and wavelength. Accelerations and added resistance in waves are generally non-linear at all speeds, although there is a tendency for these quantities to behave linearly at the longer and shorter wavelengths away from resonance. The accelerations and the added resistance are, in the main, power functions of the wave height, with the actual power subject to speed and model configuration.

The same is true of the motions, except that in the displacement range of speeds ($V/\sqrt{L} = 2$) the motions are linear with wave height over all wavelengths. Where the responses are linear, the performance of the planing boat can be characterized as approaching the limiting condition of "contouring" the waves at long wavelengths, or "platforming" the waves at short wavelengths. In between, the responses are non-linear, particularly near resonance, and again may be said to vary according to some power law of the wave height. Despite this non-linearity, the results may be applied for small wave heights and in wave spectra whose energies fall within the linear ranges.

After the extent of linearity was established, the major effort in this study was directed toward evaluation of the significance of known

model parameters at a constant wave height of 0.111 beam as a function of speed and wavelength. Speed continues to be the limiting factor in the design of rough-water planing craft. At high speed-length ratios, sharply tuned resonant peaks in the motion and acceleration responses prohibit practical operations, particularly for boats with low deadrise. In attenuating the motions associated with higher speed, certain combinations of load, trim, and deadrise can be used to good advantage.

Most of the results of this investigation are presented as response curves similar to those used in textbooks on vibration. The non-dimensional parameter or factor used as the abscissa may be considered a frequency-ratio coefficient which relates load and hull geometry to wavelength.

This factor, $C_\lambda = L/\lambda [C_\Delta / (L/b)^2]^{1/3}$, was discovered at a speed-length ratio of 4 and was found to collapse the load and length-beam variations. Inside the brackets is the familiar k_Δ -relation used in the design of seaplane hulls.

Associated with each speed-length ratio ($V/\sqrt{L} = 2, 4, 6$) is a wavelength at which the motions reach a maximum (resonance). Also associated with each speed is a frequency or wavelength at which the accelerations, added resistance, and motion phases peak. Such a frequency may be as little as one-half the resonant frequency. (This is not so for a displacement ship, where maximum added resistance is usually associated with maximum motions.)

One of the parameters important to planing-boat design is deadrise. It is responsible for greater total resistance, from a strictly smooth-water point of view. At speed-length ratios of 2 and 4, the added resistance due to waves is independent of deadrise, and at a V/\sqrt{L} of 6 it is considerably less for the boat with a 30-deg deadrise than for the boat with a 10-deg deadrise. Thus, if the designer is able to install enough horsepower to overcome the higher smooth-water resistance associated with high deadrise, the percentage increase of resistance in waves will be small and the boat should be able to maintain speed in rough water.

The motions of the planing boat are also independent of deadrise at a speed-length ratio of 2, and very nearly independent at 4 (amplitudes are the same but phases are slightly different). It is at a $V/\sqrt{L} = 6$ that

motions become drastically reduced with increasing deadrise, and the planing boat has less of a tendency to leave the water surface. At resonance, the heave motions are less by 25 percent and the pitch motions by 50 percent in going from a 10- to a 30-deg deadrise boat.

Deadrise has its greatest effect on accelerations, at the higher speeds. At a $V/\sqrt{L} = 2$, deadrise apparently has no effect on accelerations. At $V/\sqrt{L} = 4$, a 50-percent reduction in the CG and a 35- to 55-percent reduction in the bow accelerations is attained at the shorter wavelengths in going from a 10- to a 30-deg deadrise hull. Reductions on the order of 75 percent and higher can be expected at a speed-length ratio of 6.

For this study, the load and length-beam-ratio effects are evaluated at a speed-length ratio of 4. Significant here is the C_λ coefficient which collapses the motions onto one line for three different length-beam ratios. This means that higher values of load and length, or smaller beams, will increase the motions at encounter frequencies less than the resonant frequency, but will decrease the motions at encounter frequencies greater than resonant. A similar kind of collapse was discovered for the accelerations where, for $C_\lambda \geq 0.2$, the magnitude of the accelerations is proportional to $(L/b)/C_\Delta$. The C_λ coefficient also collapses the motion and acceleration data with respect to load, except in the area of resonance where it is shown that higher loads significantly reduce the motion peaks and acceleration levels.

Trim is another parameter important to planing boat design. Present results confirm the effects of trim as known to those experienced in the operation of planing boats. At a speed-length ratio of 2, increasing the trim from 4 to 6 degrees increases the total and added resistance in waves. Motions and accelerations at the CG for this speed-length ratio do not change appreciably for the 2-deg increase in trim. The pitch motions and bow accelerations are affected most. Results indicate a 20-percent increase in the pitch motions at resonance and a 50-percent increase in the bow accelerations over the wavelength spectrum.

As the speed increases, trim takes on more significance. At a speed-length ratio of 4, an increase in the smooth-water running trim from

4 to 6 degrees accounts for differences in the total resistance which are wavelength-dependent. This increase also results in higher motions at or near resonance, there being 45-percent greater heave motions and 60-percent greater pitch motions in this range. At shorter wavelengths, the motions are almost independent of trim. Accelerations for the same case at both the CG and bow are 50- to 100-percent higher over a good part of the wavelength range, because of the 2-deg increase in trim.

RECOMMENDATIONS

Because the planing boat operating in rough water represents a very complicated system which until now has received little systematic treatment, the results of the present study (a systematic one based primarily on experiment) are of general and immediate value to those responsible for current decision-making, and should be made available at the earliest possible date. It is, of course, possible that further rational analysis might lead to the formulation of design recommendations. But such analysis could be premature and cause unwarranted delay, whereas guidelines based upon the results of this report can be applied now.

A feature of the planing boat's rough-water behavior is its resonant response to certain combinations of wave, speed, and loading conditions, characterized by the value of C_λ . Since the energy in actual random seas is concentrated in a rather narrow frequency spectrum, part of the solution may be to design planing hulls so that resonant peaks do not coincide with the maximum energy frequency of the wave system. This, of course, cannot be avoided entirely. However, the designer can still attenuate motions by exploiting the obvious damping properties of load, deadrise, and trim. He also has recourse to heading changes, which alter the encounter frequencies sensed by the hull.

As is common in the case of a complex system, a number of contradictory requirements demand attention. An examination of the results at a speed-length ratio of $V/\sqrt{L} = 4$, for instance, makes it clear that if one is to obtain minimum motion and avoid resonance, C_λ should be > 0.2 . This is precisely the area to be avoided, however, if accelerations are to be minimized. It may also be important to minimize the added resistance in waves, which can place further limits on the value of C_λ . Thus the designer is faced with the necessity of making decisions which can only be resolved by carefully weighing the alternatives to arrive at some optimum performance.

Because of the non-linear response of planing craft to wave height, future effort should be directed toward studies in irregular seas. But despite the non-linear behavior, the present findings concerning the effect of hull parameters on performance are valid and extremely important. The response operators which have been plotted do tend to overpredict the motions in large waves and hence will give conservative results. Accelerations will be underpredicted and for this reason are not presented as response operators. Caution must therefore be exercised in predicting absolute acceleration magnitudes in large waves.

ACKNOWLEDGEMENTS

The author is grateful to the many individuals who assisted him in the course of this study. He is particularly indebted to Mr. P. Ward Brown, for guidance during the testing period and for help in the preparation of the report.

TABLE 1. CONFIGURATIONS

SYMBOL	L/b	β (deg)	C_{Δ}	LCG (%L)	τ (deg)	k (%L)	V/\sqrt{L} (knots/ft ^{1/2})	$k_g^{1/3}$	τ_o (deg)	TR _o (%b)	R/ Δ
A	5	20	0.608	59.0	4	25.1	4	0.290	0.86	8.0	0.158
B	5	20	0.608	62.0	4	25.5	6	0.290	1.50	10.0	0.206
C	5	20	0.608	61.5	4	25.3	2	0.290	1.40	10.0	0.113
D	5	20	0.608	67.5	6	26.5	2	0.290	2.70	16.7	0.125
E	5	20	0.608	65.5	6	26.2	4	0.290	2.30	13.3	0.156
F	5	20	0.912	58.0	6	20.4	4	0.332	1.00	14.5	0.150
G	5	20	0.912	58.0	5	20.4	6	0.332	1.00	14.5	0.178
H	5	10	0.608	62.0	4	25.6	2	0.290	1.36	15.6	0.111
I	5	10	0.608	59.5	4	25.0	4	0.290	0.84	13.3	0.147
J	5	10	0.608	68.0	4	26.2	6	0.290	2.90	20.6	0.156
K	5	30	0.608	61.0	4	24.7	4	0.290	1.40	4.5	0.177
L	5	30	0.608	62.5	4	24.9	2	0.290	1.64	6.7	0.118
M	5	30	0.608	60.5	4	24.8	6	0.290	1.20	4.5	0.264
N	6	20	0.608	64.5	4	24.8	4	0.256	1.56	10.0	0.166
O	6	20	0.912	60.0	4	20.0	4	0.294	1.10	13.3	0.149
P	4	20	0.631	52.5	4	23.7	4	0.341	-1.40	5.5	-

PRECEDING PAGE BLANK

TABLE 2. RESULTS IN REGULAR WAVES

Configuration	H/b	λ/L	R_w/Δ	h/H	$\frac{\theta_p}{2\pi H/\lambda}$	η_{cg} (g)	η_{bow} (g)	R_{aw}/Δ	φ_h (deg)	φ_p (deg)
A	0.111	1	0.182	0.18	0.11	0.25	1.05	0.024	11	46
	0.167		0.195	0.17	0.10	0.45	1.95	0.037	24	17
	0.222		0.208	0.17	0.09	0.75	2.90	0.050	5	67
	0.056	2	0.169	0.93	0.85	0.15	0.35	0.011	-	49
	0.111		0.184	0.84	0.79	0.25	0.90	0.026	55	9
	0.167		0.209	0.81	0.75	0.40	1.80	0.051	47	21
	0.167		0.207	0.74	0.73	0.40	1.90	0.049	46	28
	0.222		0.232	0.73	0.68	0.85	3.15	0.074	49	33
	0.334		0.276	0.59	0.57	1.75	5.25	0.118	54	39
	0.334		0.277	0.61	0.56	1.85	5.20	0.119	-	-
	0.111	3	0.173	1.18	1.29	0.20	0.45	0.015	36	42
	0.222		0.201	1.13	1.24	0.40	1.45	0.043	26	47
	0.334		0.238	1.05	1.16	0.60	2.65	0.078	26	44
	0.111	4	0.169	1.23	1.21	0.15	0.25	0.011	9	65
	0.222		0.175	1.11	1.21	0.25	0.40	0.017	9	65
	0.334		0.190	1.07	1.21	0.40	0.90	0.032	15	63
B	0.111	6	0.161	1.04	1.13	0.10	0.15	0.003	-3	68
	0.334		0.169	0.97	1.23	0.25	0.45	0.011	6	83
	0.111	1	0.225	0.16	0.06	0.50	1.45	0.019	-	-
	0.111	1.5	0.225	0.37	0.21	0.70	2.00	0.019	-	-
	0.111	2	0.231	0.64	0.54	0.80	2.55	0.025	-	-
	0.222		0.256	0.50	0.36	2.70	5.90	0.050	67	-21
	0.334		0.281	0.45	0.26	3.75	7.45	0.075	71	-30
	0.111	3	0.242	1.45	1.68	0.90	2.85	0.036	-	-
	0.111	4	0.224	1.75	2.39	0.35	1.25	0.018	0	48
	0.222		0.270	1.63	2.05	1.65	5.05	0.064	33	42
	0.334		0.282	1.47	1.50	4.25	9.65	0.076	47	18
	0.111	6	0.211	1.08	1.51	0.15	0.25	0.005	-7	95

TABLE 2 (Cont'd)

Configuration	H/b	λ/L	R_w/Δ	h/H	$\frac{\theta_p}{2\pi h/\lambda}$	η_{cg} (g)	η_{bow} (g)	R_{aw}/Δ	φ_h (deg)	φ_p (deg)
C	0.111	1	0.126	0.07	0.13	0.05	0.35	0.013	-26	77
		1.5	0.125	0.49	0.58	0.10	0.45	0.012	39	35
		2	0.119	0.38	0.59	0.10	0.30	0.006	25	49
		3	0.117	1.00	1.21	0.10	0.10	0.004	1	78
		4	0.116	0.99	1.21	0.05	0.05	0.003	-6	89
		6	0.115	0.91	1.19	0.05	0.07	0.002	0	81
D	0.111	1	0.140	0.11	0.14	0.05	0.40	0.015	-6	53
		1.5	0.147	0.59	0.68	0.15	0.80	0.022	39	24
		2	0.143	0.98	1.11	0.15	0.45	0.018	26	42
		3	0.132	1.04	1.37	0.10	0.20	0.007	7	68
		4	0.128	1.04	1.45	0.05	0.13	0.003	5	75
		6	0.126	0.93	1.41	0.05	0.05	0.001	13	81
E	0.111	1	0.174	0.20	0.13	0.45	1.50	0.018	76	-38
		1.5	0.173	0.47	0.41	0.45	1.60	0.017	82	-36
		2	0.179	0.81	0.84	0.45	1.75	0.023	68	-16
		3	0.177	1.56	2.02	0.30	1.15	0.021	38	24
		4	0.172	1.38	1.91	0.15	0.35	0.016	14	60
		6	0.166	0.99	1.39	0.10	0.15	0.010	8	71
	0.111	1	0.180	0.18	0.14	0.30	1.10	0.030	3	44
		1.5	0.179	0.37	0.38	0.20	0.90	0.029	53	5
		2	0.177	0.68	0.75	0.25	0.85	0.027	63	3
		3	0.171	1.13	1.33	0.20	0.40	0.021	29	51
		4	0.169	1.21	1.44	0.15	0.20	0.019	21	60
		6	0.158	1.00	1.21	0.10	0.10	0.008	5	90
		6	0.159	1.06	1.19	0.05	0.10	0.009	7	80

TABLE 2 (Cont'd)

Configuration	H/b	λ/L	R_w/Δ	b/H	$\frac{\theta_p}{2\pi H/\lambda}$	η_{cg} (g)	η_{bow} (g)	R_{aw}/Δ	φ_h (deg)	φ_p (deg)
G	0.111	1	0.193	0.19	0.10	0.55	1.60	0.015	47	-12
		1.5	0.193	0.41	0.30	0.60	1.80	0.015	67	-16
		2	0.193	0.69	0.63	0.55	1.90	0.015	82	-29
		3	0.200	1.56	1.82	0.50	1.95	0.022	48	18
		4	0.190	1.96	2.59	0.35	1.05	0.012	10	63
		6	0.183	1.27	1.64	0.15	0.20	0.005	7	75
H	0.111	1	0.118	0.08	0.12	0.10	0.35	0.007	-30	59
	0.212	1	0.135	0.08	0.12	0.30	1.60	0.024	13	50
	0.111	1.5	0.122	0.36	0.46	0.10	0.35	0.011	35	49
	0.222	1.5	0.144	0.43	0.49	0.40	2.10	0.033	51	21
	0.334	1.5	0.170	0.45	0.48	2.30	7.00	0.059	57	13
	0.111	2	0.118	0.80	0.86	0.10	0.35	0.007	24	54
	0.222	2	0.137	0.90	0.93	0.25	1.10	0.026	17	53
	0.339	2	0.164	1.03	0.95	1.40	5.60	0.053	31	45
	0.111	3	0.113	0.87	1.13	0.10	0.15	0.002	-15	65
	0.111	4	0.112	0.91	1.15	0.05	0.05	0.001	-3	88
	0.222	4	0.118	1.01	1.16	0.15	0.15	0.007	-4	86
	0.328	4	0.121	1.04	1.16	0.20	0.25	0.010	-5	83
I	0.111	6	0.114	0.82	1.10	0	0.05	0.003	-6	96
	0.111	1	0.157	0.21	0.14	0.60	1.70	0.010	30	13
		1.5	0.164	0.44	0.41	0.50	1.60	0.017	40	13
		2	0.163	0.76	0.78	0.25	1.15	0.016	51	15
		3	0.157	1.13	1.24	0.20	0.45	0.010	-	-
		4	0.151	1.14	1.22	0.15	0.20	0.004	9	67
		6	0.148	1.07	1.11	0.10	0.05	0.001	-1	83

TABLE 2 (Cont'd)

Configuration	H/b	λ/L	R_w/Δ	h/H	$\frac{\theta_p}{2\pi h/\lambda}$	η_{cg} (g)	η_{bow} (g)	R_{aw}/Δ	φ_h (deg)	φ_p (deg)
J	0.111	1	0.182	0.23	0.08	1.20	3.70	0.026	60	-40
		1.5	0.199	1.74	1.21	1.30	2.90	0.043	152	-70
		2	0.187	0.57	0.62	1.35	5.20	0.031	100	-64
		3	0.211	1.51	2.06	3.40	13.10	0.055	90	-45
		4	0.198	2.05	3.32	0.60	2.85	0.042	1	73
		6	0.171	1.19	2.53	0.20	0.50	0.015	-	-
K	0.111	1	0.193	0.13	0.09	0.20	0.55	0.016	4	52
		1.5	0.196	0.34	0.32	0.25	0.65	0.019	27	35
		2	0.196	0.72	0.70	0.30	0.65	0.019	55	19
		3	0.187	1.23	1.22	0.30	0.35	0.010	22	55
		4	0.180	1.17	1.19	0.20	0.20	0.003	-1	77
		6	0.177	0.99	1.12	0.15	0.10	0	6	73
L	0.111	1	0.124	0.05	0.11	0.10	0.20	0.006	-10	78
		1.5	0.128	0.54	0.54	0.15	0.35	0.010	32	33
		2	0.124	0.95	0.97	0.20	0.30	0.006	6	62
		3	0.120	1.02	1.18	0.15	0.15	0.002	-12	90
		4	0.119	0.99	1.13	~	0.10	0.001	-8	94
		6	0.118	0.96	1.13	0.10	0.05	0	-5	86
M	0.111	1	0.274	0.13	0.06	0.30	0.85	0.010	30	27
		1.5	0.278	0.30	0.20	0.40	1.00	0.014	64	3
		2	0.278	0.59	0.46	0.45	1.05	0.014	81	-16
		3	0.284	1.31	1.30	0.45	1.05	0.020	60	8
		4	0.275	1.50	1.72	0.35	0.55	0.011	15	57
		6	0.272	1.07	1.28	0.20	0.20	0.008	3	85

TABLE 2 (Cont'd)

Configuration	H/b	λ/L	R_w/Δ	h/H	$\frac{\theta_p}{2\pi h/\lambda}$	η_{cg} (g)	η_{bow} (g)	R_{av}/Δ	φ_h (deg)	φ_p (deg)
N	0.111	1	0.180	0.25	0.17	0.35	1.30	0.014	40	12
		1.5	0.180	0.52	0.47	0.30	1.20	0.014	46	19
		2	0.184	0.97	0.95	0.30	1.20	0.018	49	20
		3	0.177	1.24	1.26	0.15	0.35	0.011	25	54
		4	0.171	1.11	1.15	0.10	0.20	0.005	3	72
		6	0.166	0.96	1.16	0.10	0.10	0	1	68
O	0.111	1	0.170	0.19	0.13	0.20	0.90	0.021	13	47
		1.5	0.170	0.44	0.43	0.20	0.85	0.021	49	11
		2	0.170	0.75	0.80	0.20	0.65	0.021	47	24
		3	0.165	1.14	1.17	0.15	0.25	0.016	19	57
		4	0.161	1.10	1.11	0.10	0.15	0.012	10	71
		6	0.153	0.98	1.06	0.05	0.10	0.004	-2	87
P	0.111	1	-	0.14	0.09	0.30	0.90	-	21	30
		1.5	-	0.34	0.27	0.30	0.90	-	61	0
		2	-	0.50	0.49	0.25	0.75	-	70	-5
		3	-	0.95	0.99	0.20	0.40	-	42	33
		4	-	1.15	1.20	0.20	0.20	-	24	59
		6	-	1.15	1.18	0.10	0.10	-	15	60

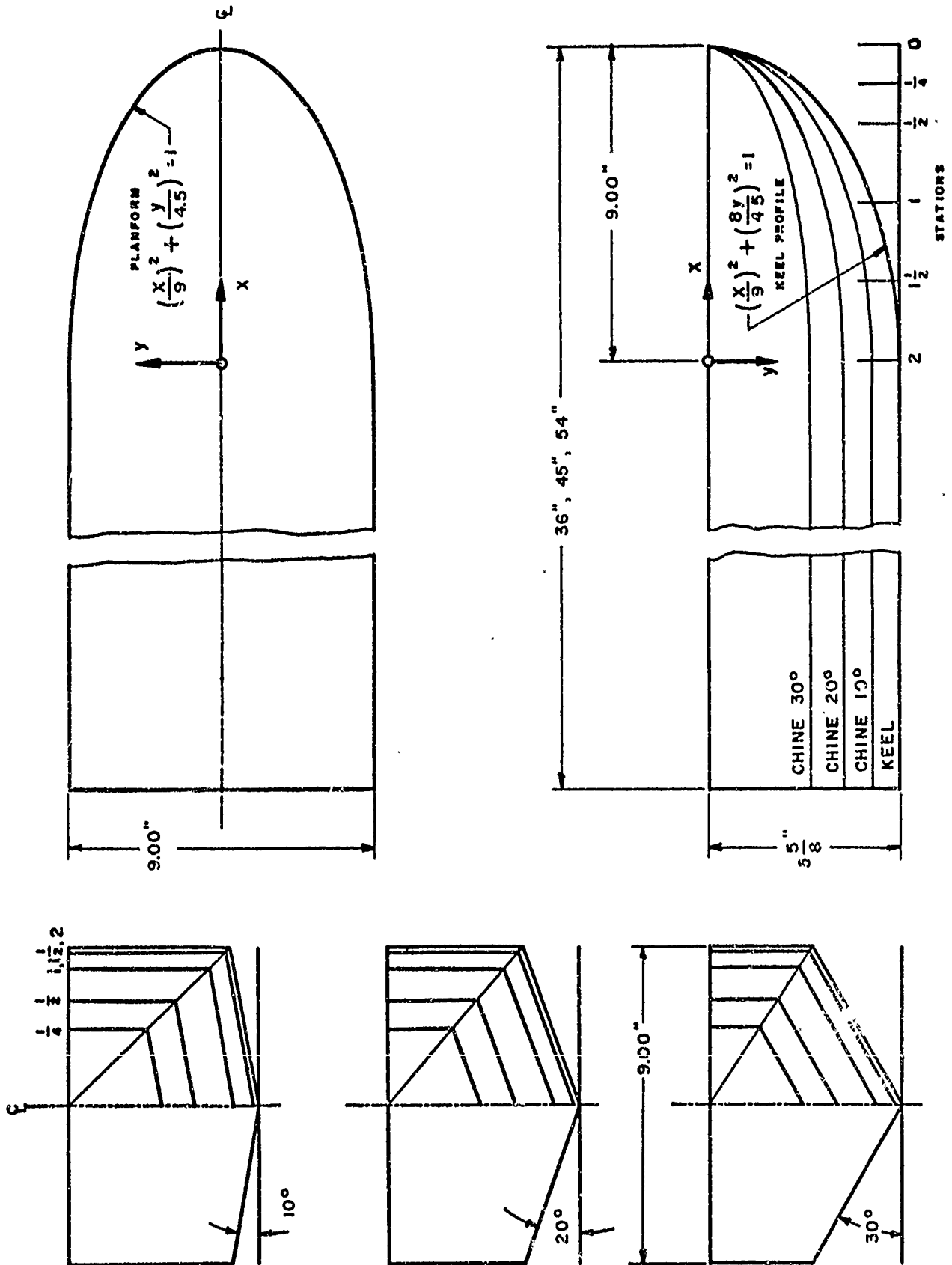
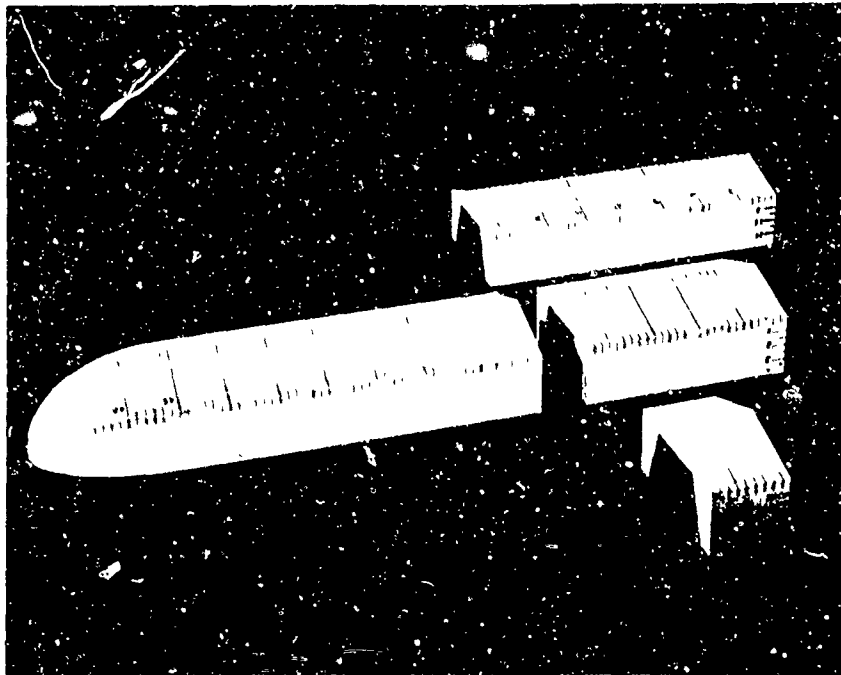
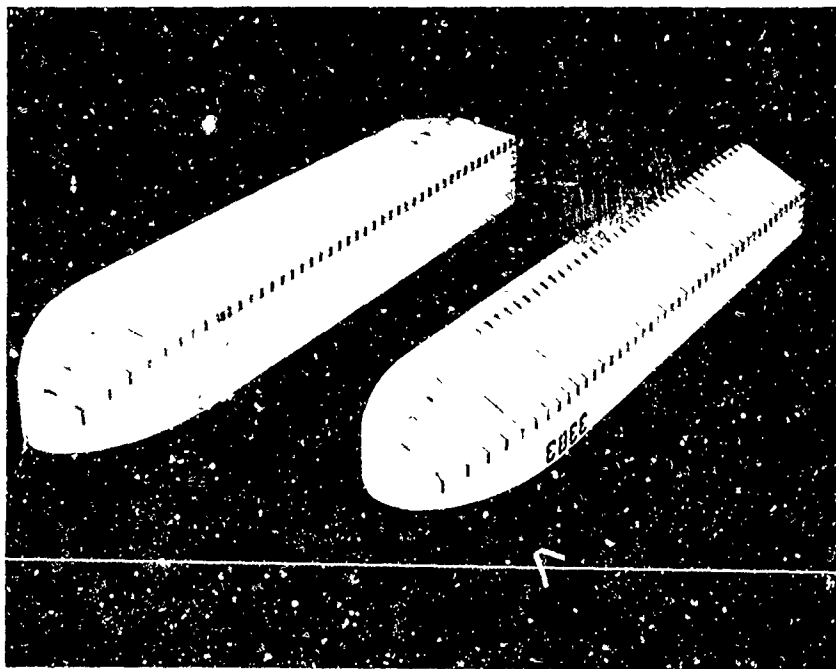


FIG. 1. LINES OF PRISMATIC MODELS



20° DEADRISE MODELS



10° AND 30° DEADRISE MODELS

FIG. 2 PHOTOGRAPHS OF TEST MODELS

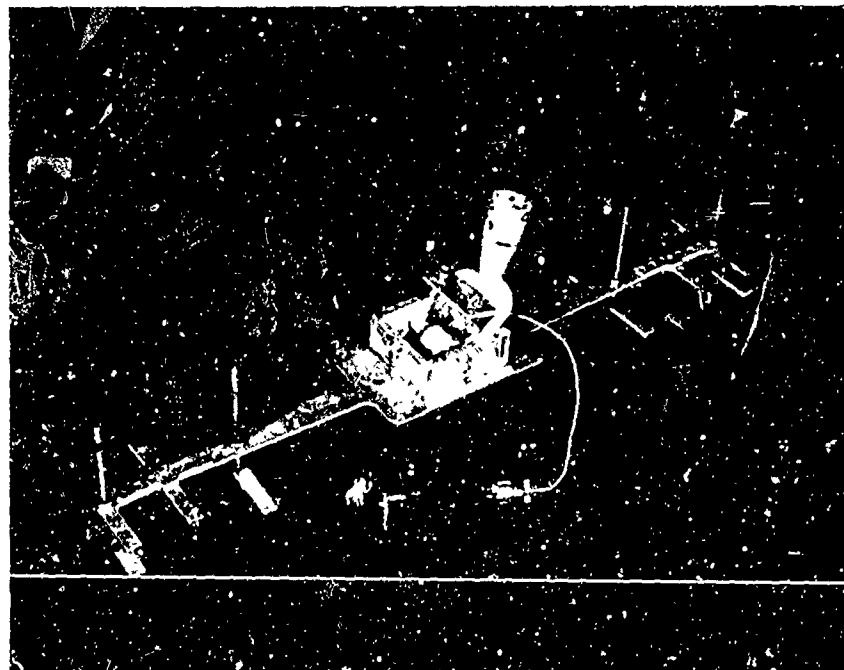
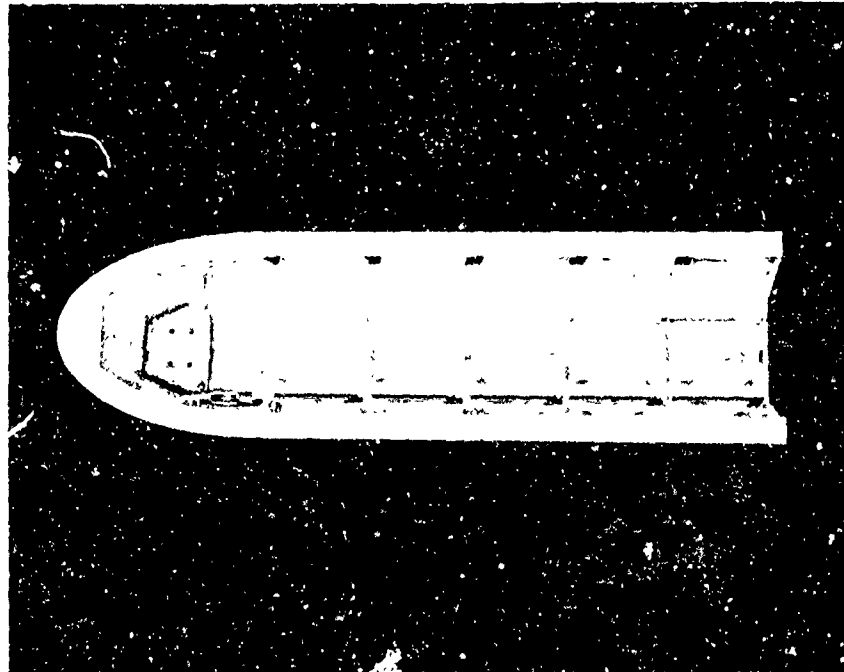


FIG. 3. TYPICAL MODEL CONSTRUCTION AND ATTACHMENT PLATE

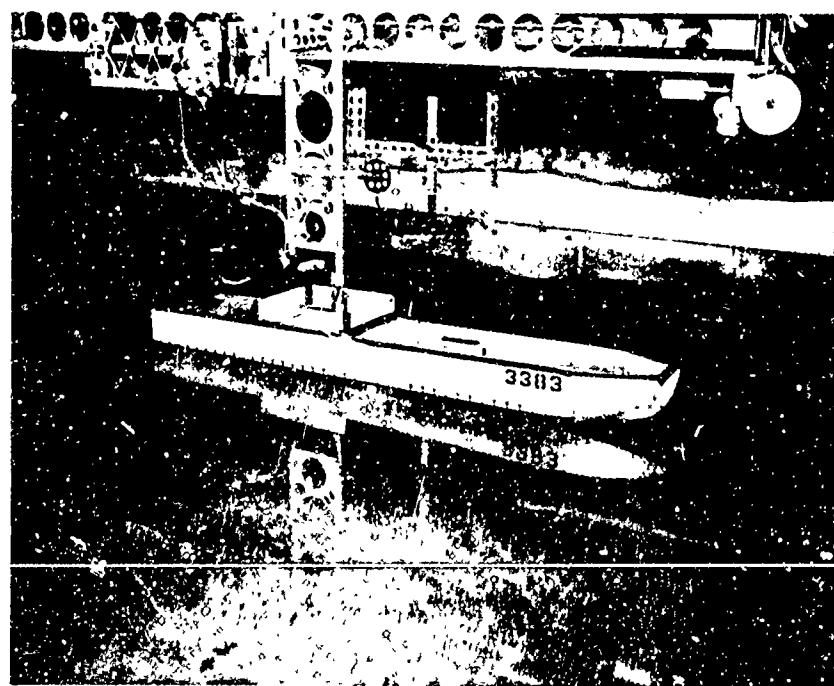
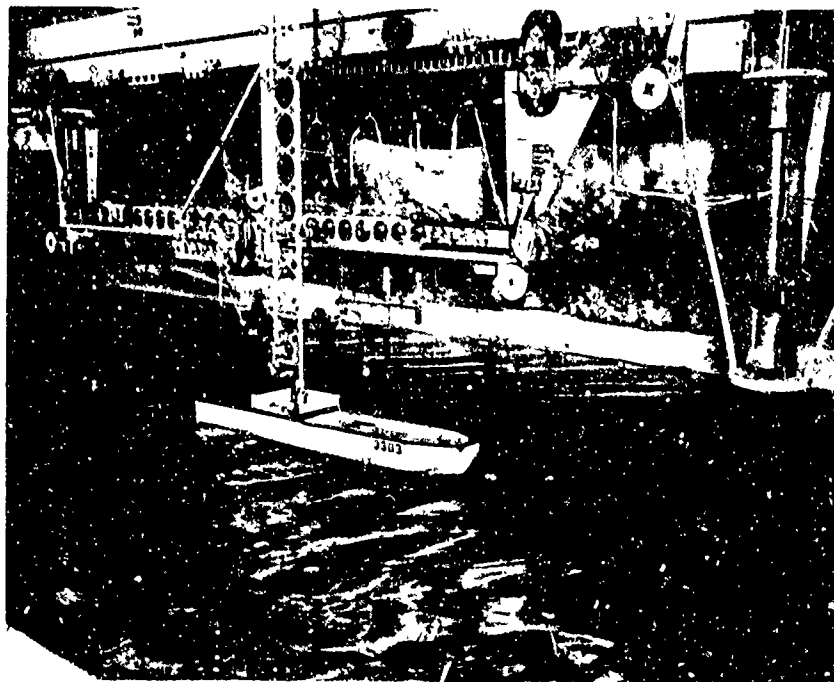


FIG. 4. ROUGH-WATER TEST SETUP

R-1275

PARAMETERS

$C_{\Delta} = 0.304$ $\beta = 10^{\circ}$ $L/b = 5$

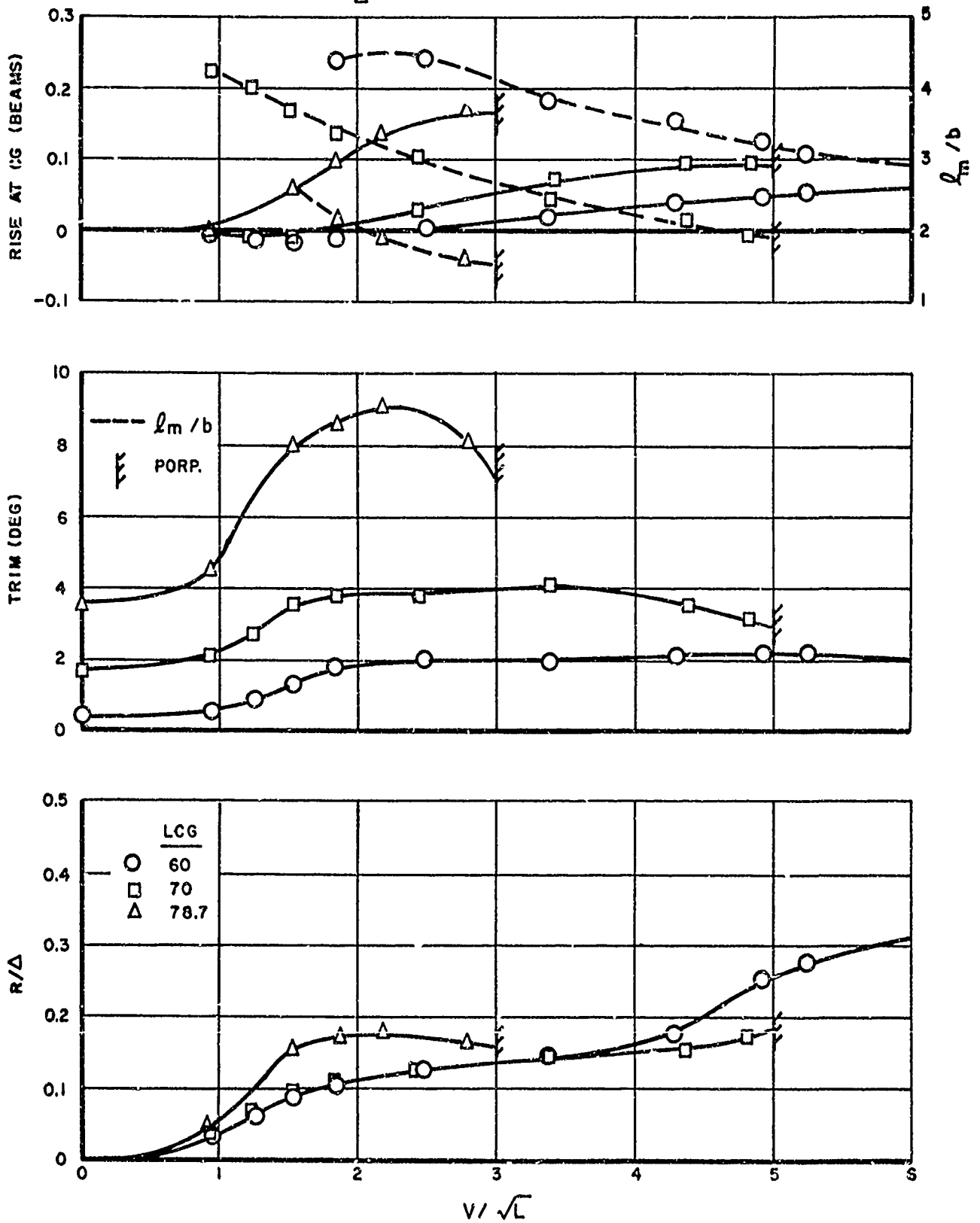


FIG. 5. SMOOTH-WATER PERFORMANCE

R-1275

PARAMETERS

$C_{\Delta} = 0.608$ $\beta = 10^{\circ}$ $L/b = 5$

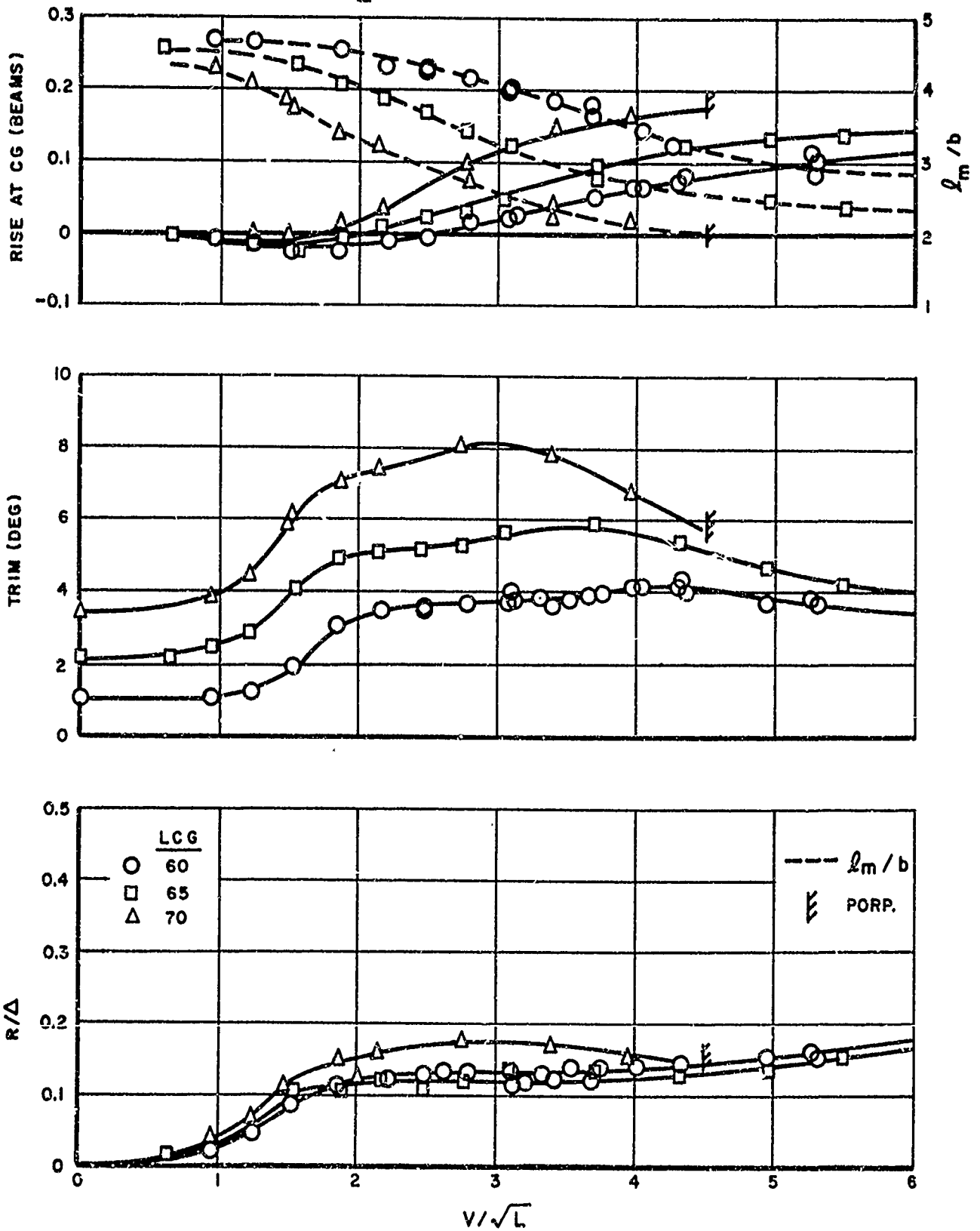


FIG. 6. SMOOTH WATER PERFORMANCE

R-1275

PARAMETERS

$C_{\Delta} = 0.912$ $\beta = 10^{\circ}$ $L/b = 5$

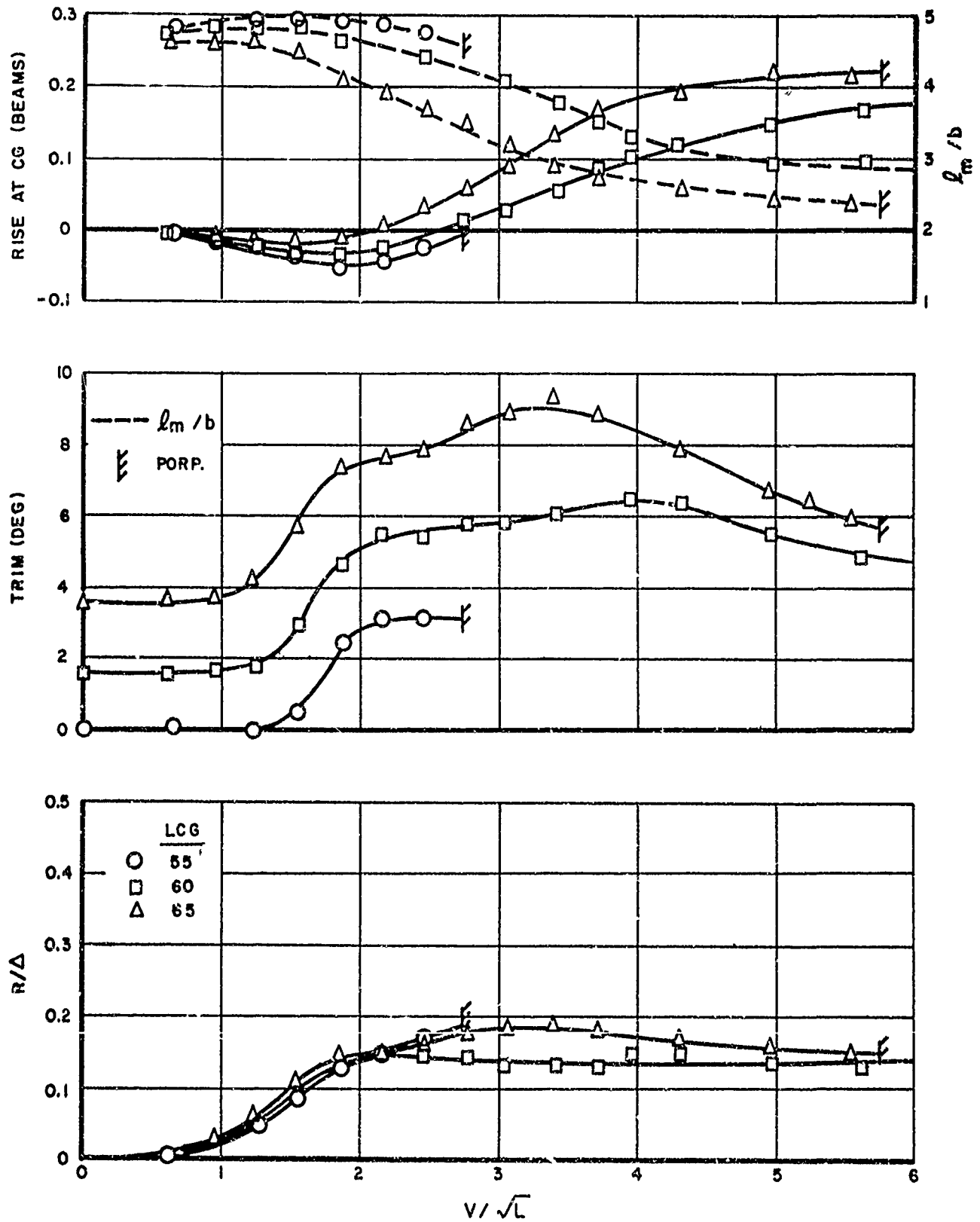


FIG. 7. SMOOTH WATER PERFORMANCE

R-1275

PARAMETERS

$C_{\Delta} = 0.304$ $\beta = 20$ $L/b = 4$

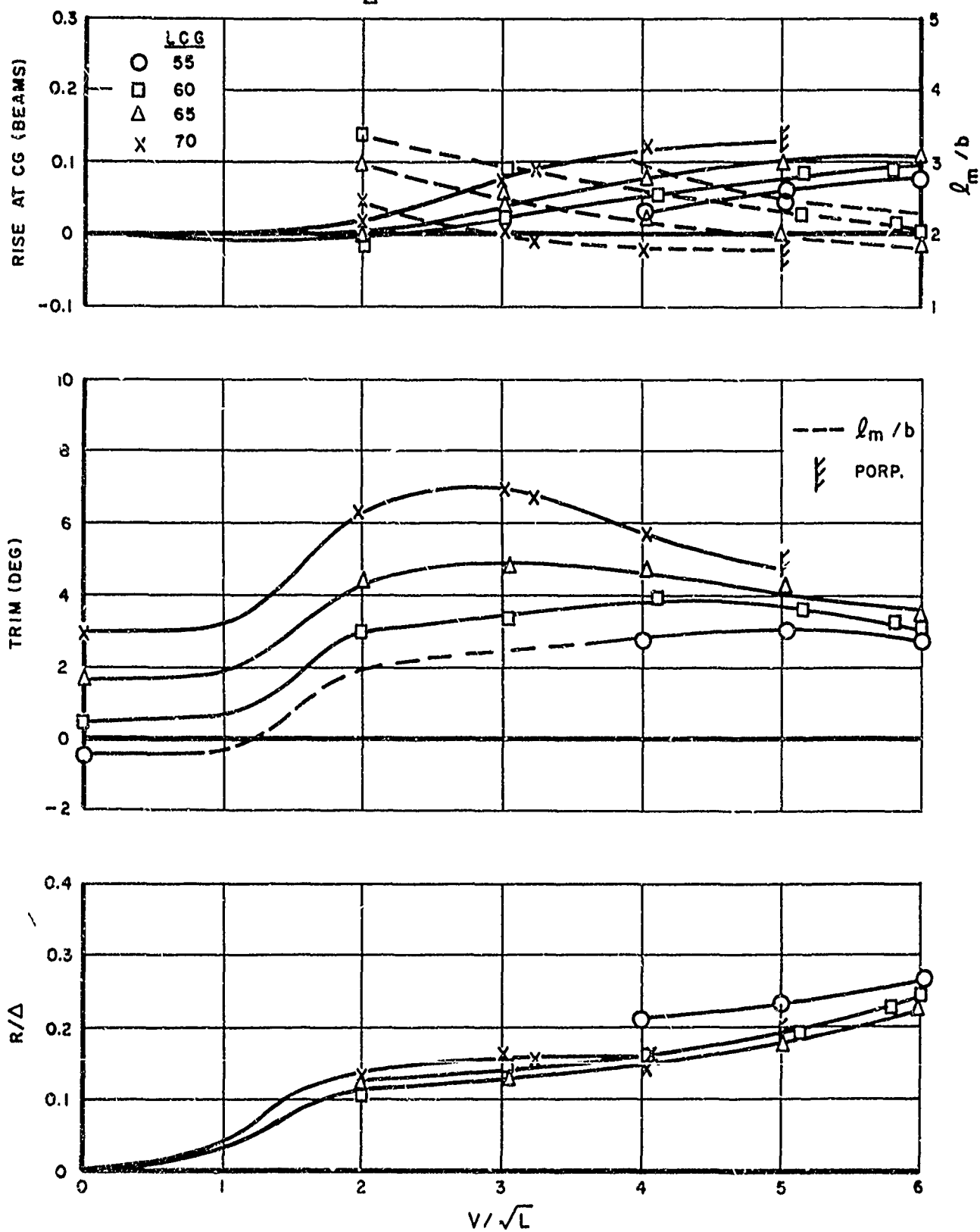


FIG. 8. SMOOTH WATER PERFORMANCE

R-1275

PARAMETERS

$C_{\Delta} = 0.508$ $\beta = 20$ $L/b = 4$

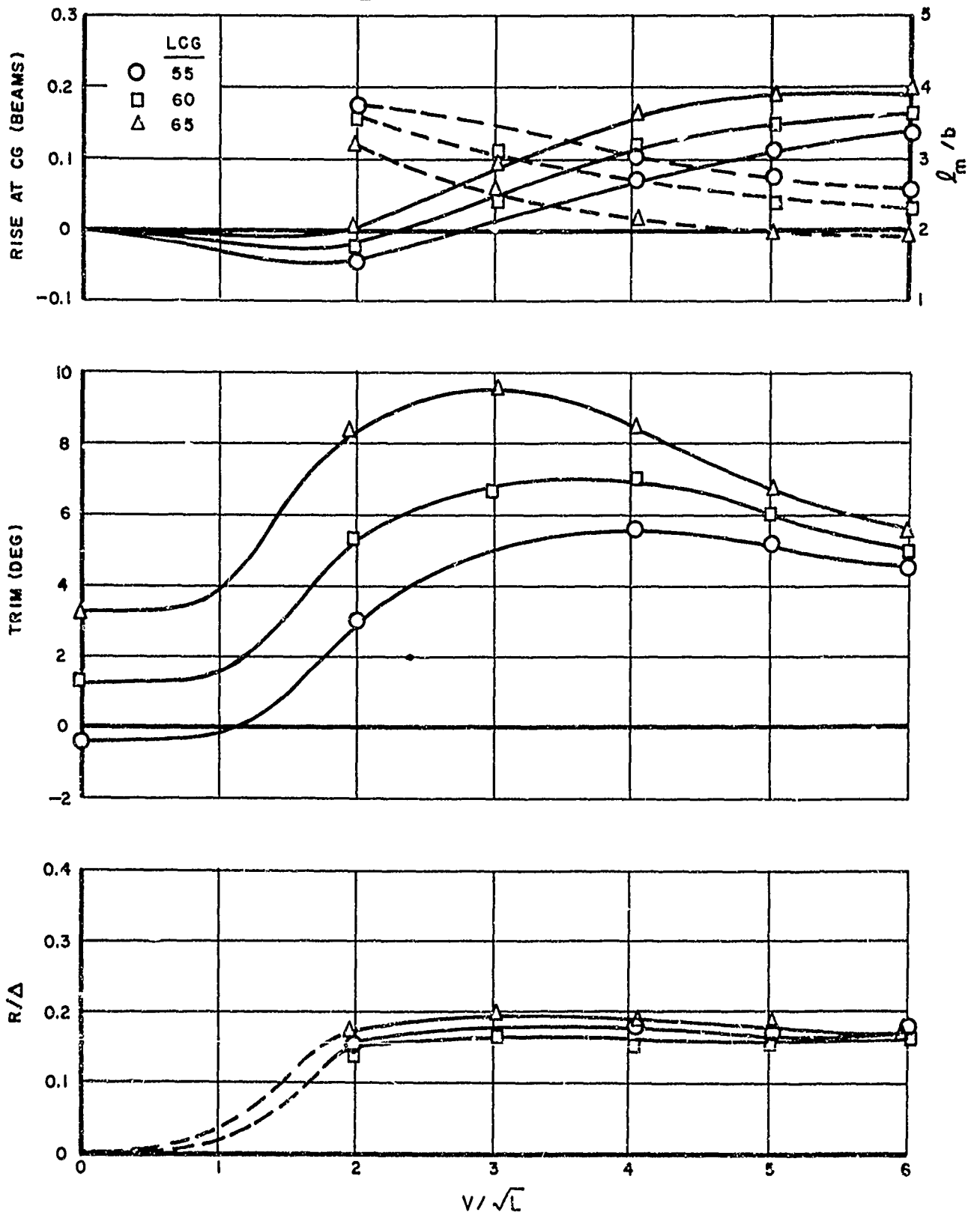


FIG. 9. SMOOTH WATER PERFORMANCE

R-1275

PARAMETERS

$C_{\Delta} = 0.304$ $\beta = 20$ $L/b = 5$

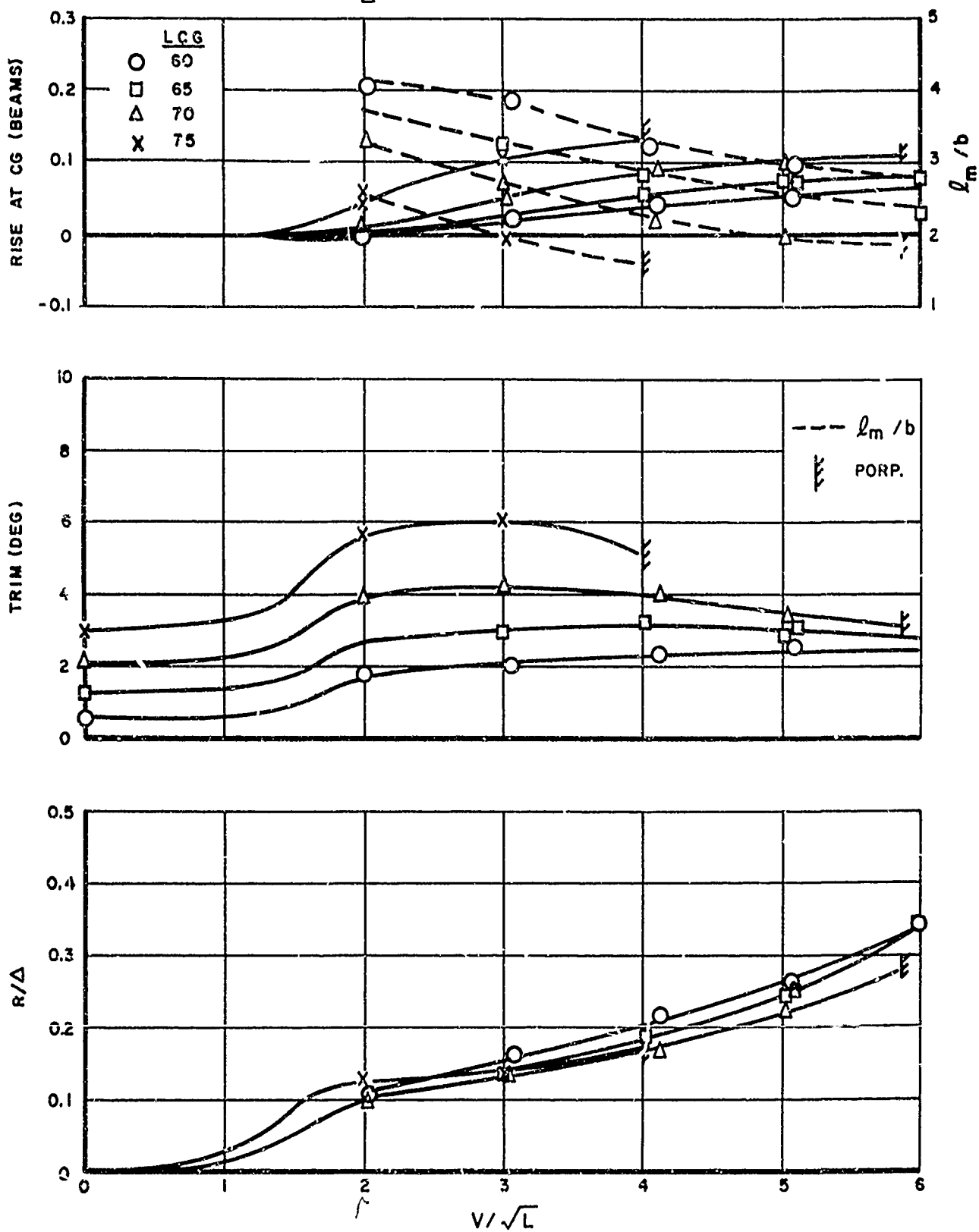


FIG. 10., SMOOTH WATER PERFORMANCE

R-1275

PARAMETERS

$C_{\Delta} = 0.608$ $\beta = 20$ $L/b = 5$

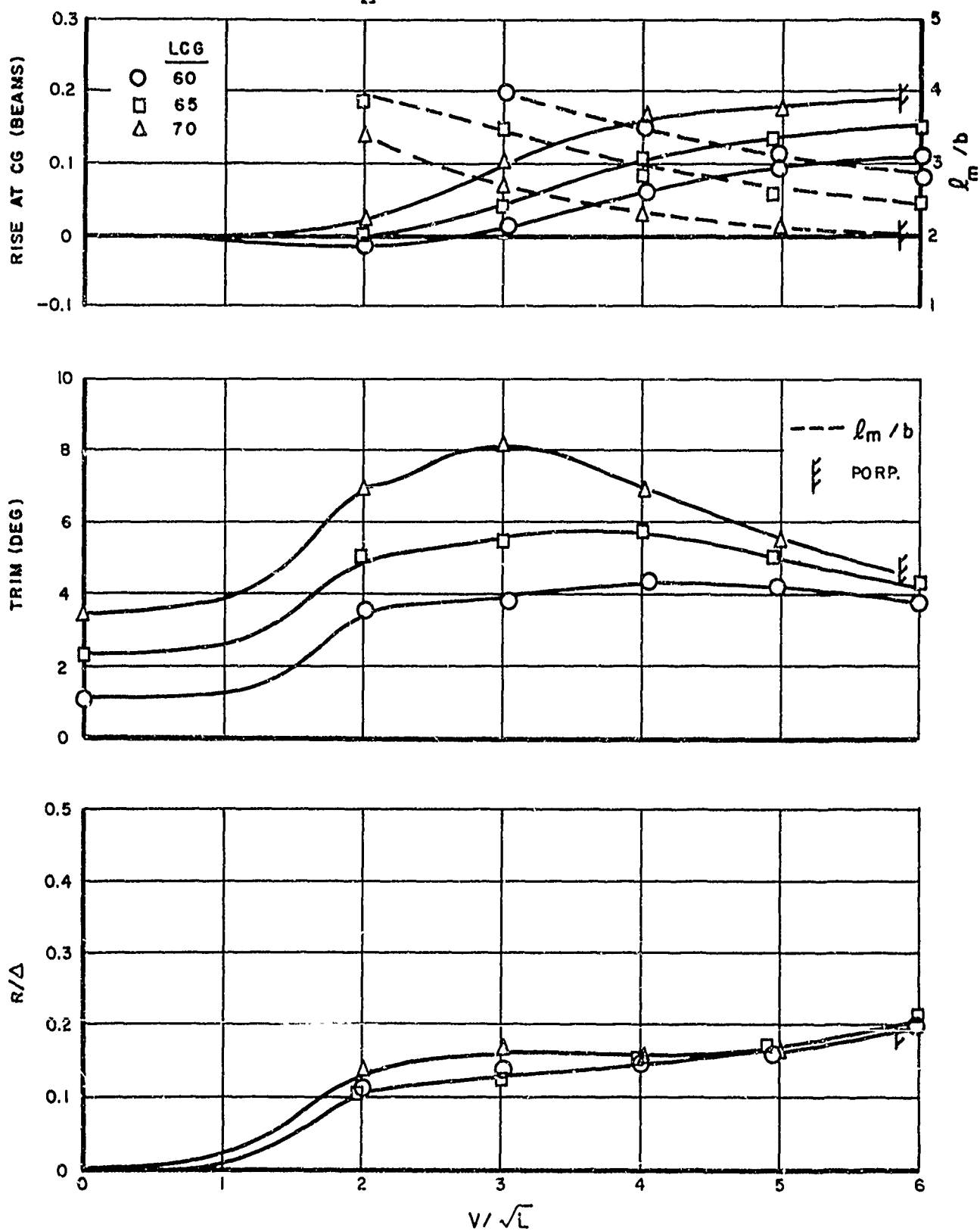


FIG.11. SMOOTH WATER PERFORMANCE

R-1275

PARAMETERS

$C_{\Delta} = 0.912$ $\beta = 20$ $L/b = 5$

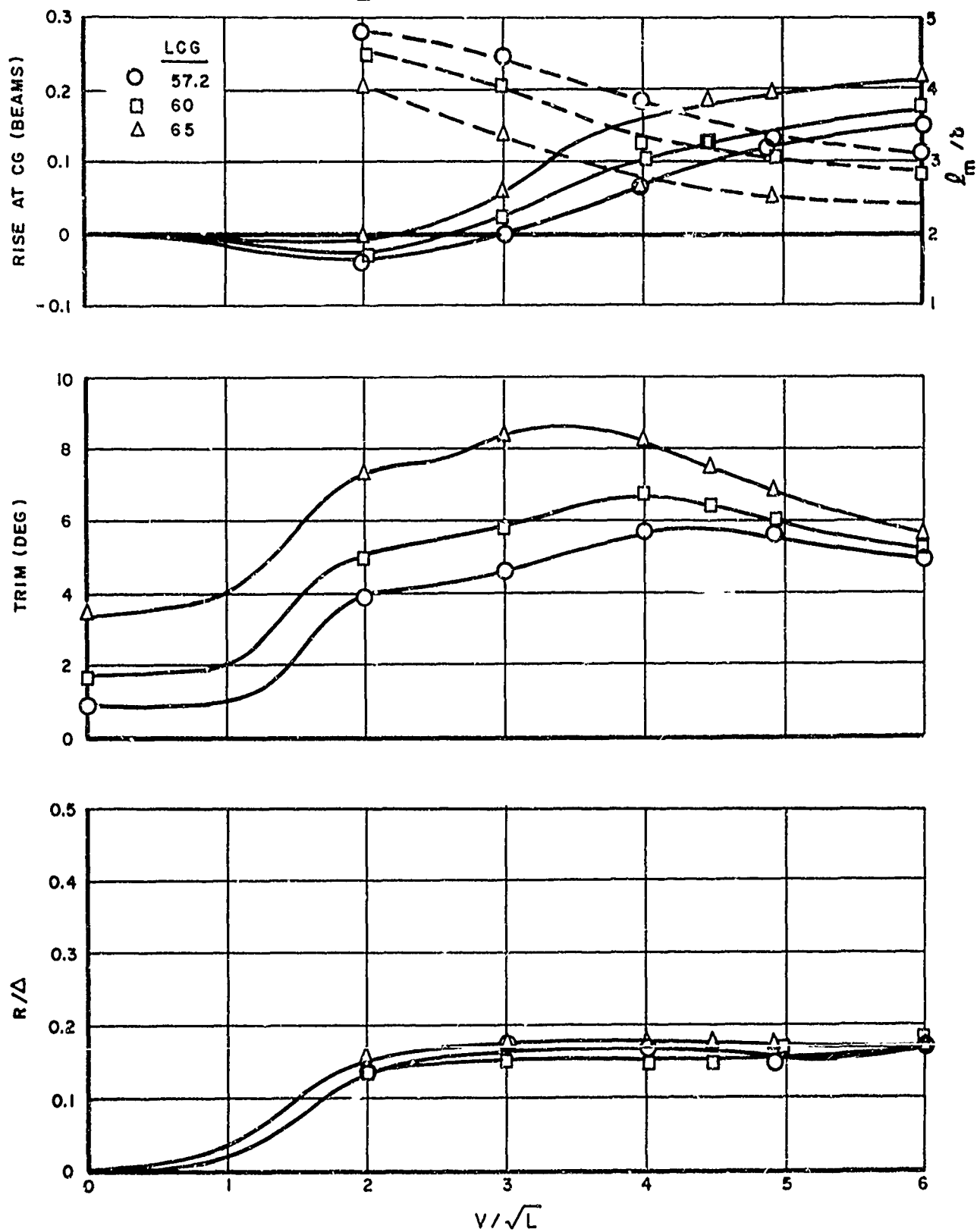


FIG.12. SMOOTH WATER PERFORMANCE

R-1275

PARAMETERS

$C_{\Delta} = 0.608$ $\beta = 20$ $L/b = 6$

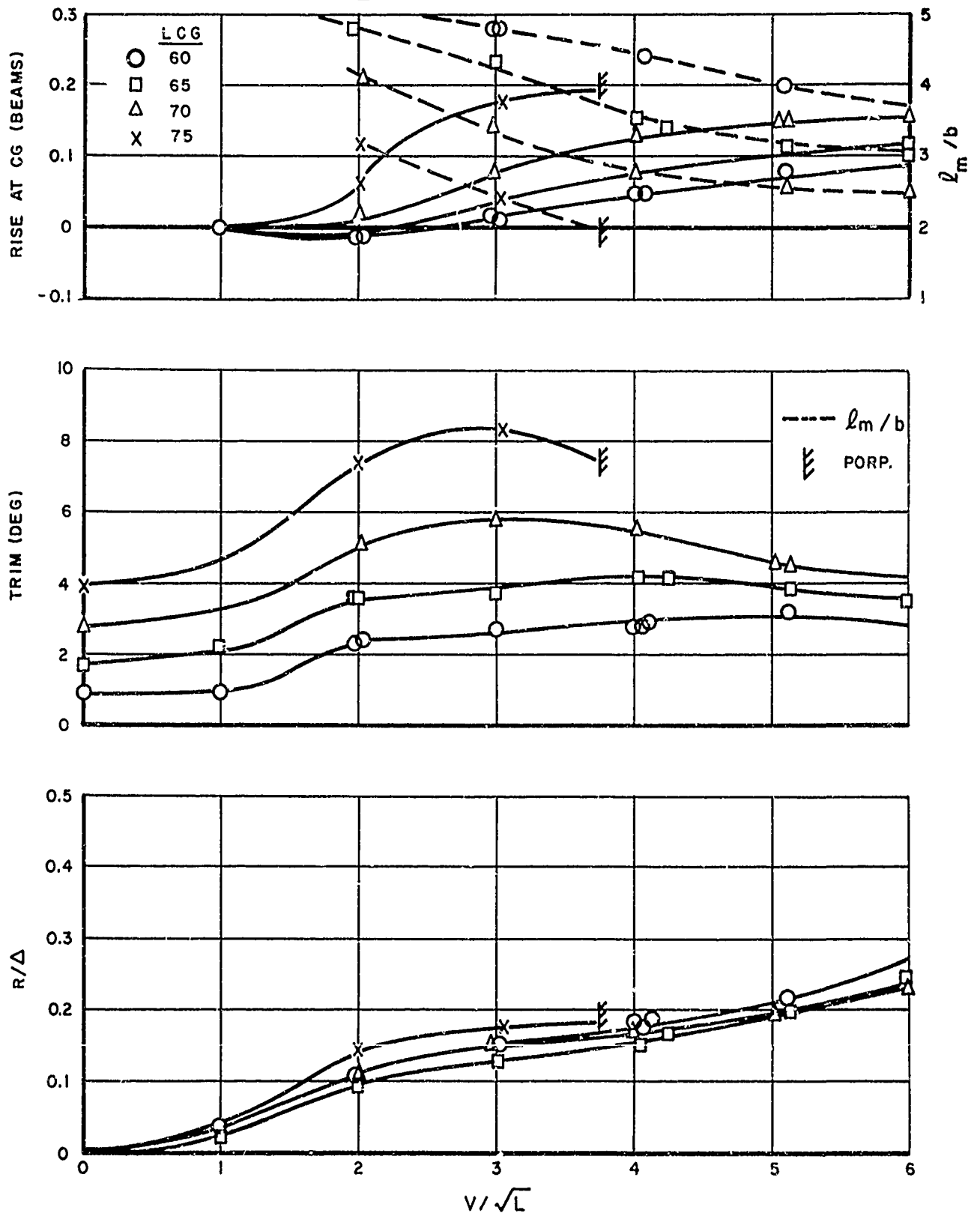


FIG.13. SMOOTH WATER PERFORMANCE

P-1275

PARAMETERS

$C_{\Delta} = 0.912$ $\beta = 20$ $L/b = 6$

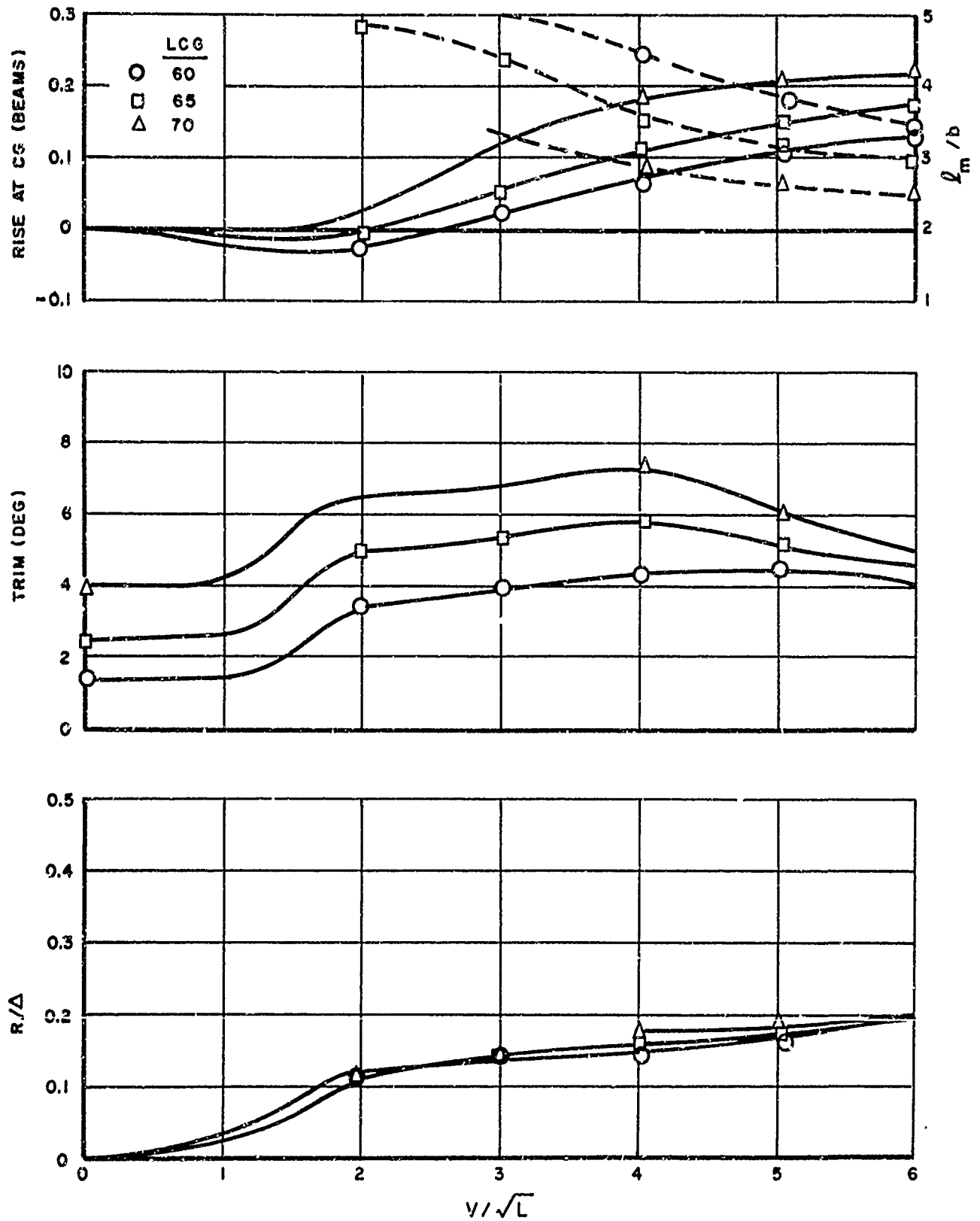


FIG. 14. SMOOTH WATER PERFORMANCE

R-1275

PARAMETERS

$C_{\Delta} = 0.304$ $\beta = 30$ $L/b = 5$

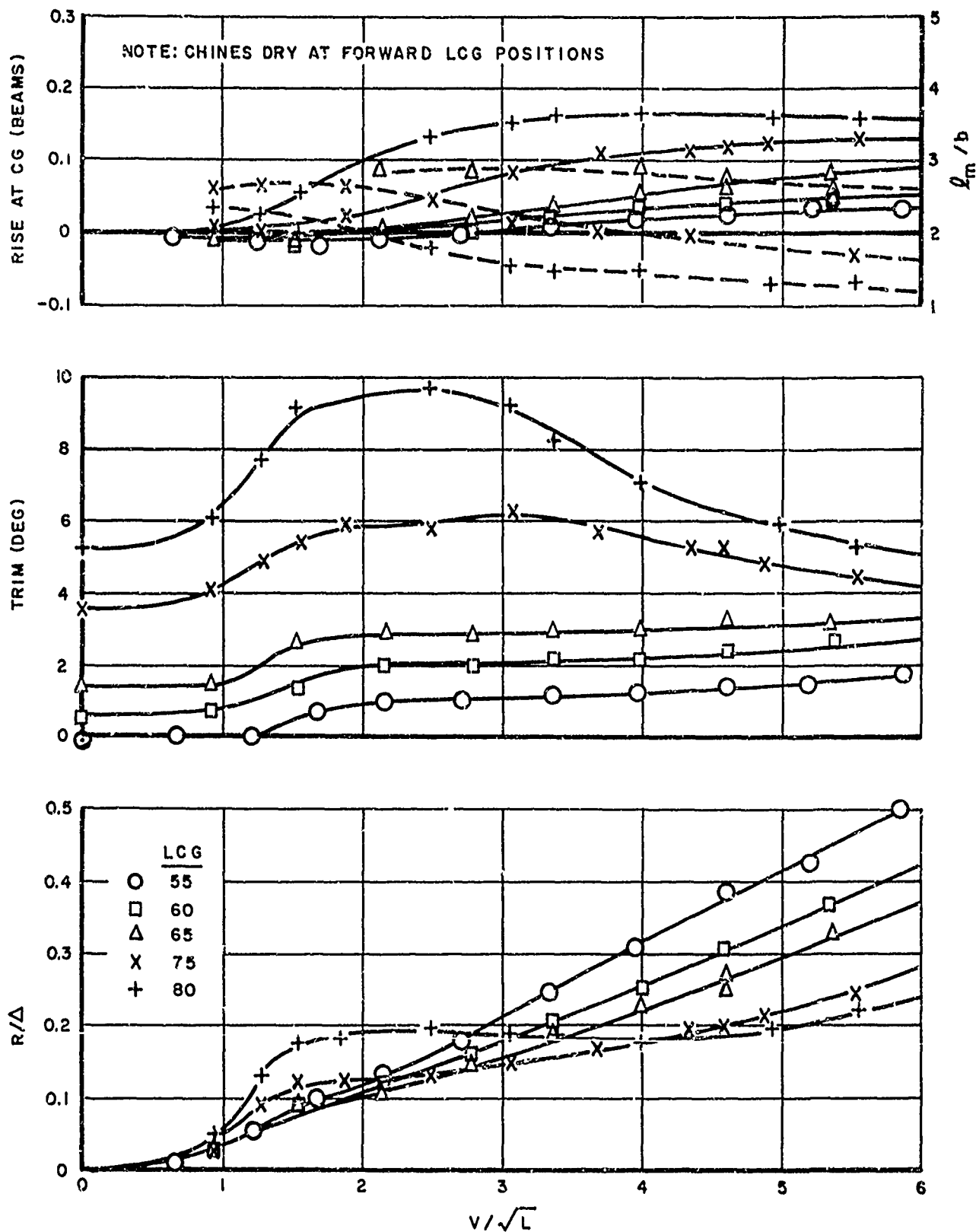


FIG.15. SMOOTH WATER PERFORMANCE

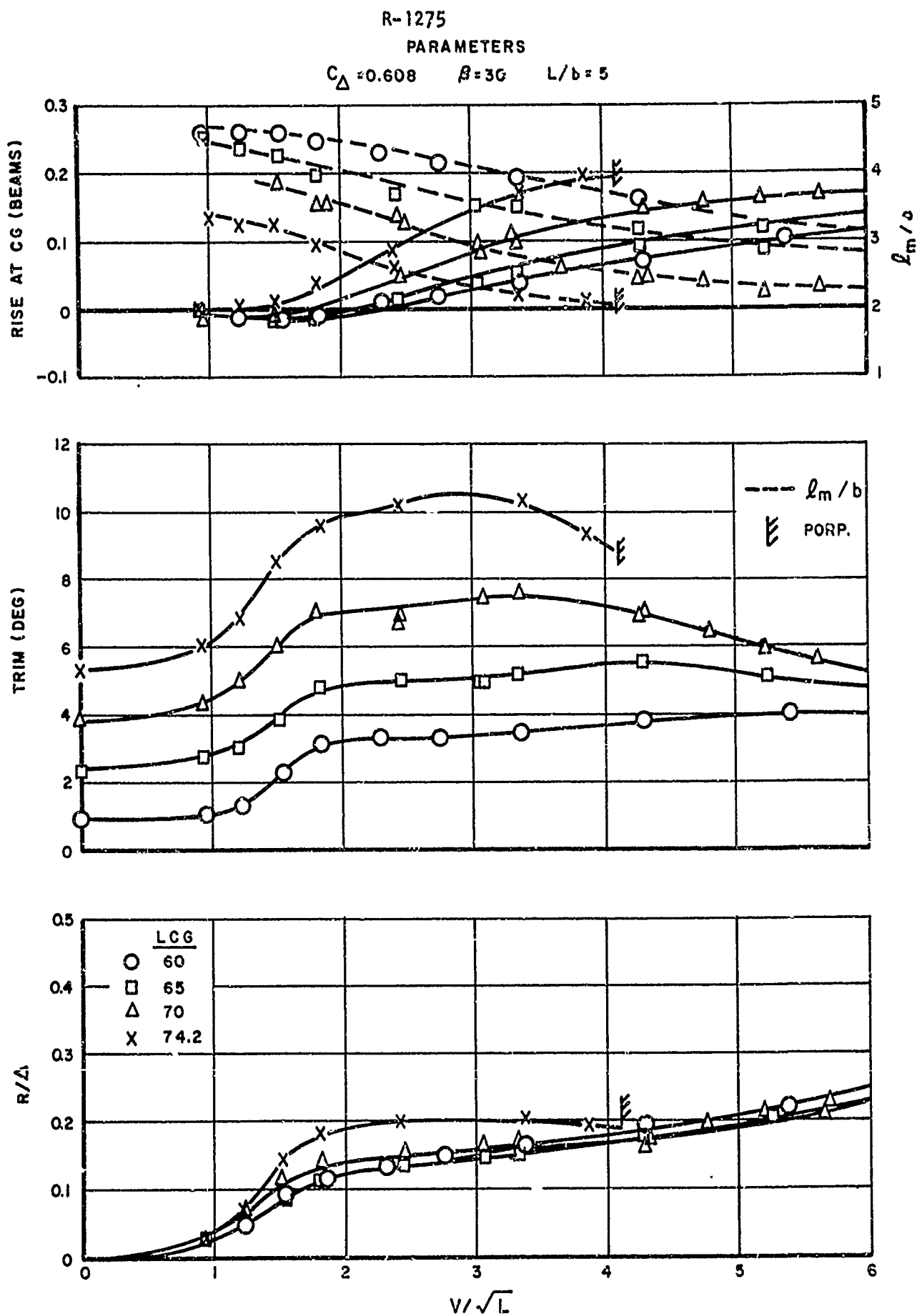


FIG. 16. SMOOTH-WATER PERFORMANCE

R-1275

PARAMETERS

$C_{\Delta} = 0.912$ $\beta = 30$ $L/b = 5$

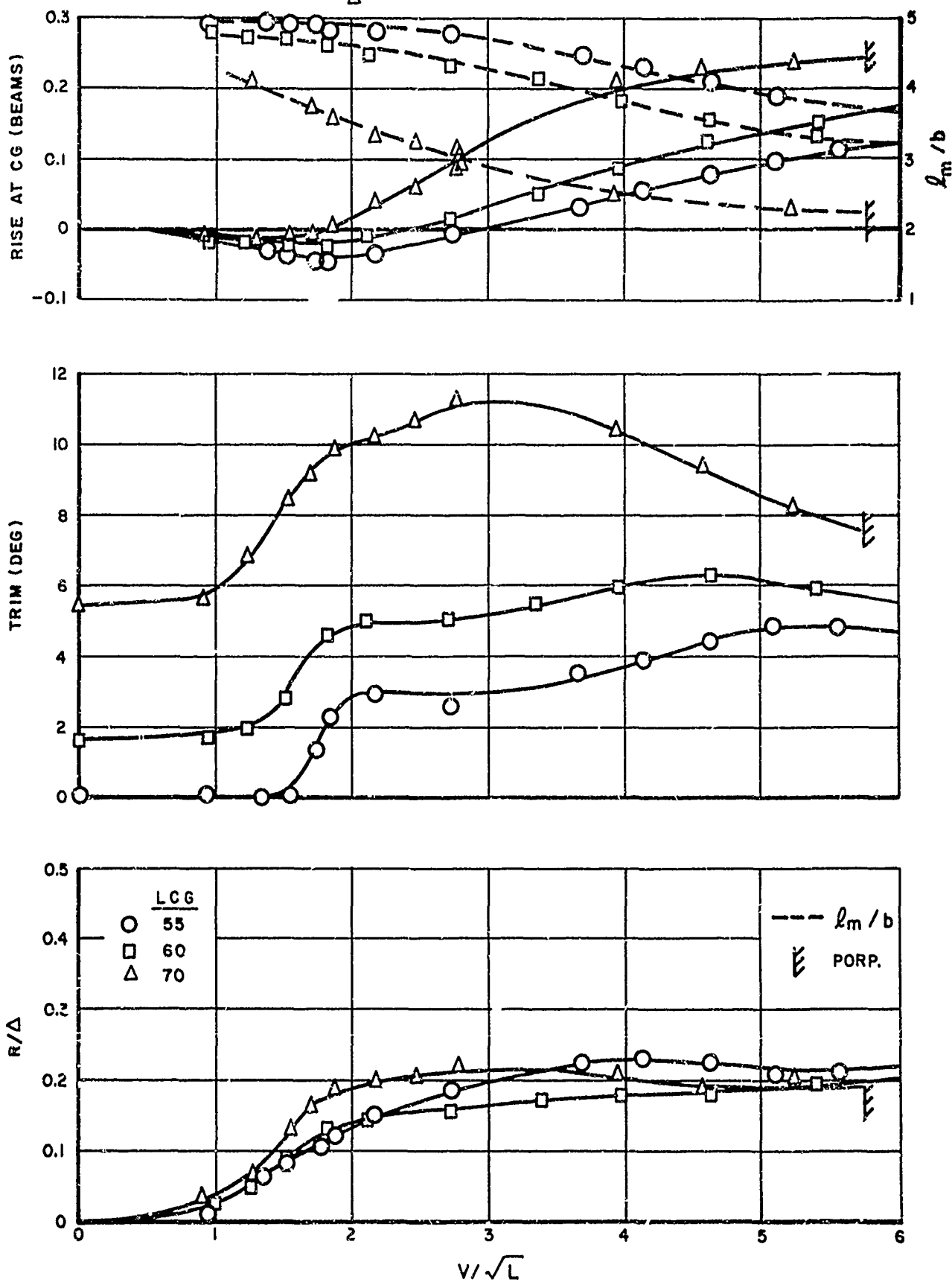


FIG.17. SMOOTH WATER PERFORMANCE

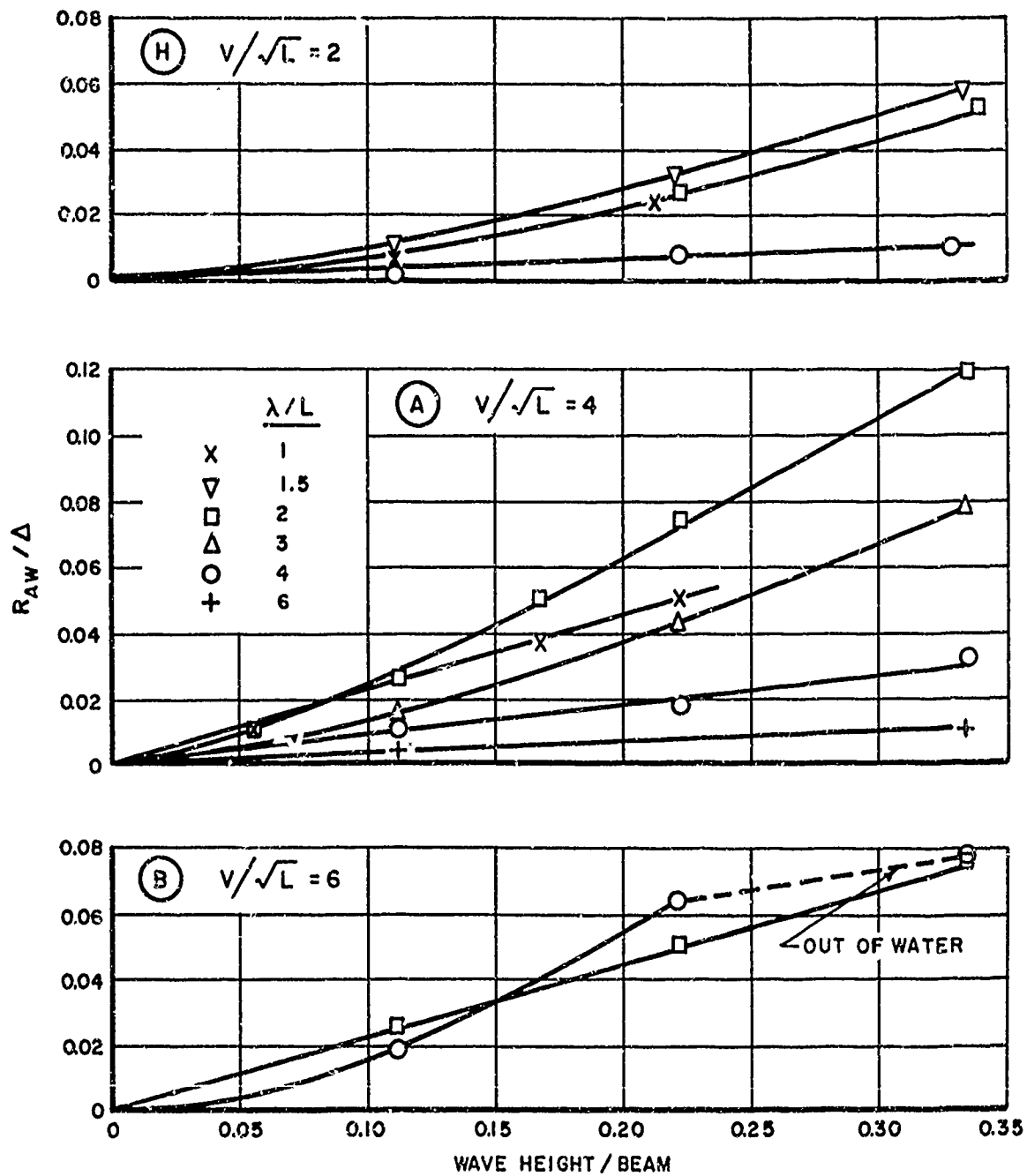


FIG. 18. LINEARITY - ADDED RESISTANCE VERSUS WAVE HEIGHT

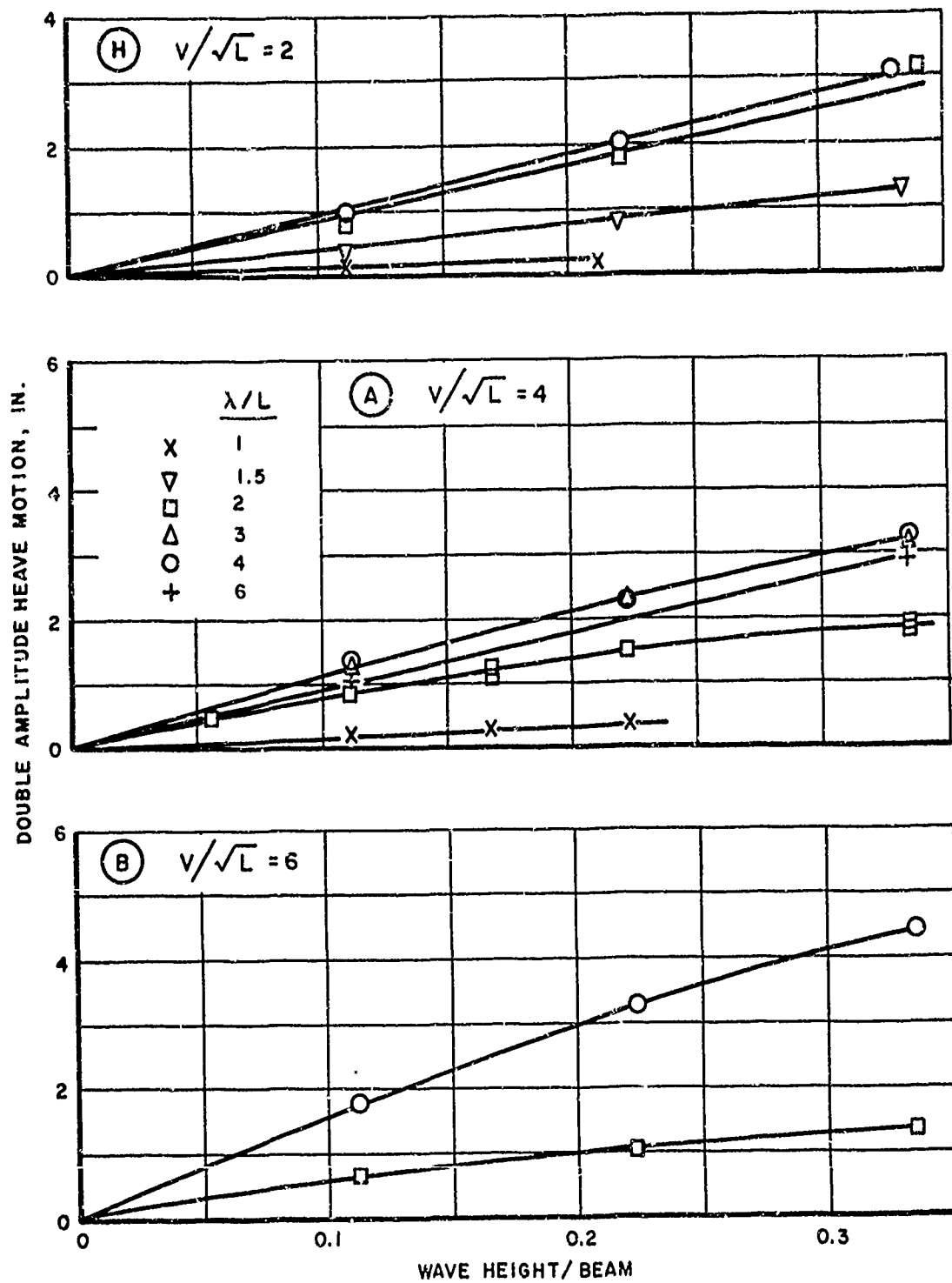


FIG. 19. LINEARITY-HEAVE MOTION VERSUS WAVE HEIGHT

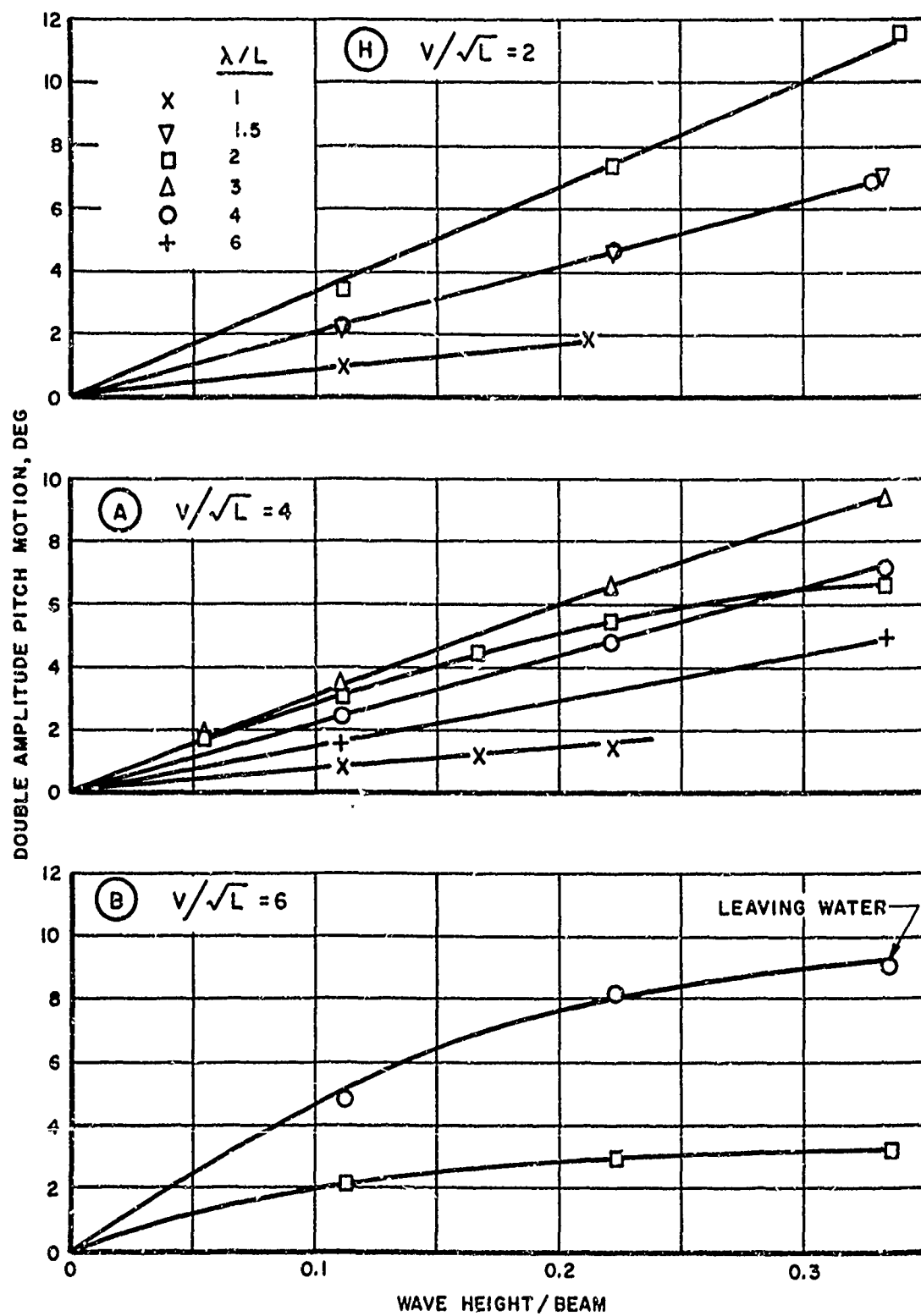


FIG. 20. LINEARITY-PITCH MOTION VERSUS WAVE HEIGHT

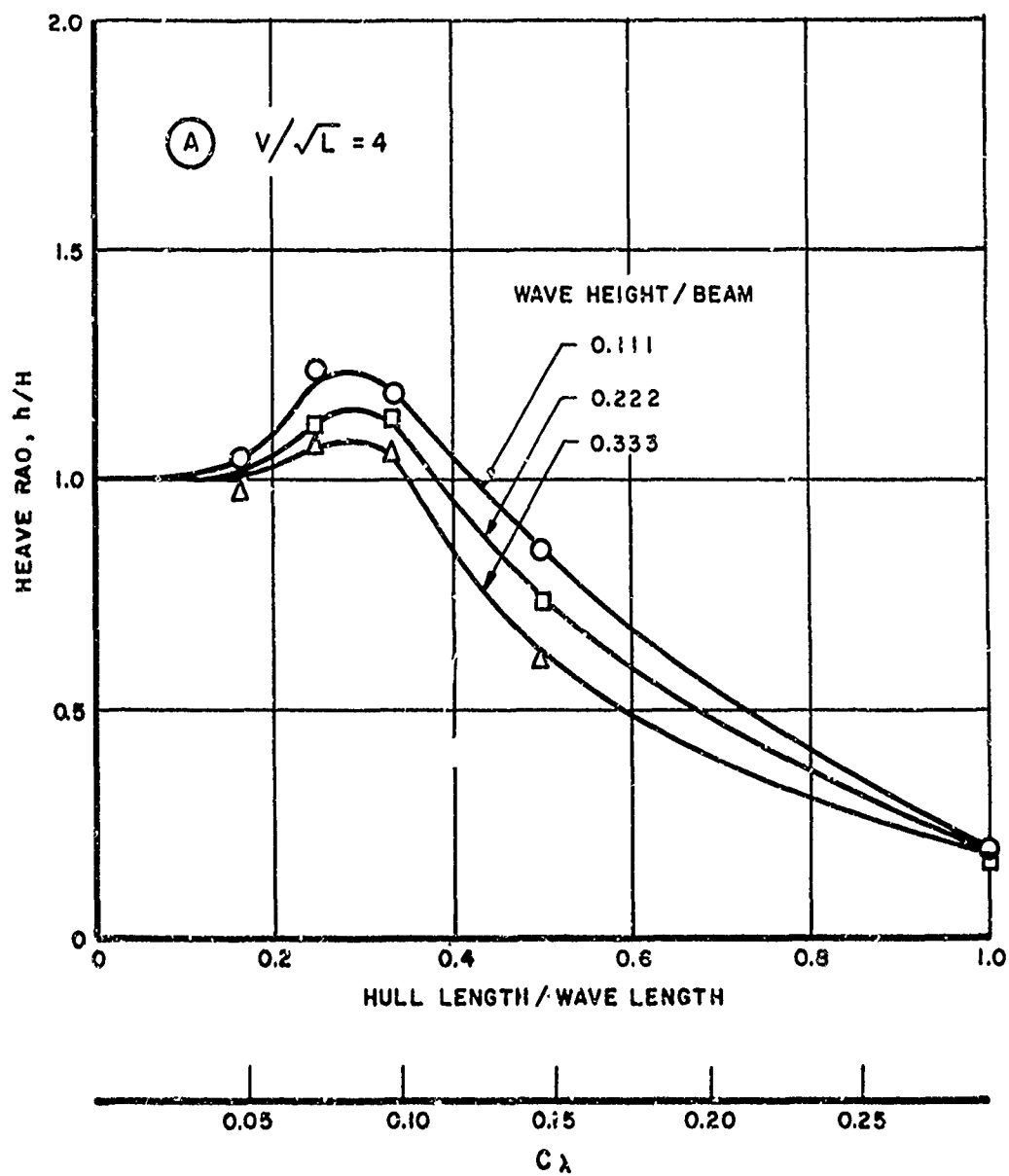


FIG. 21. LINEARITY-HEAVE RESPONSE

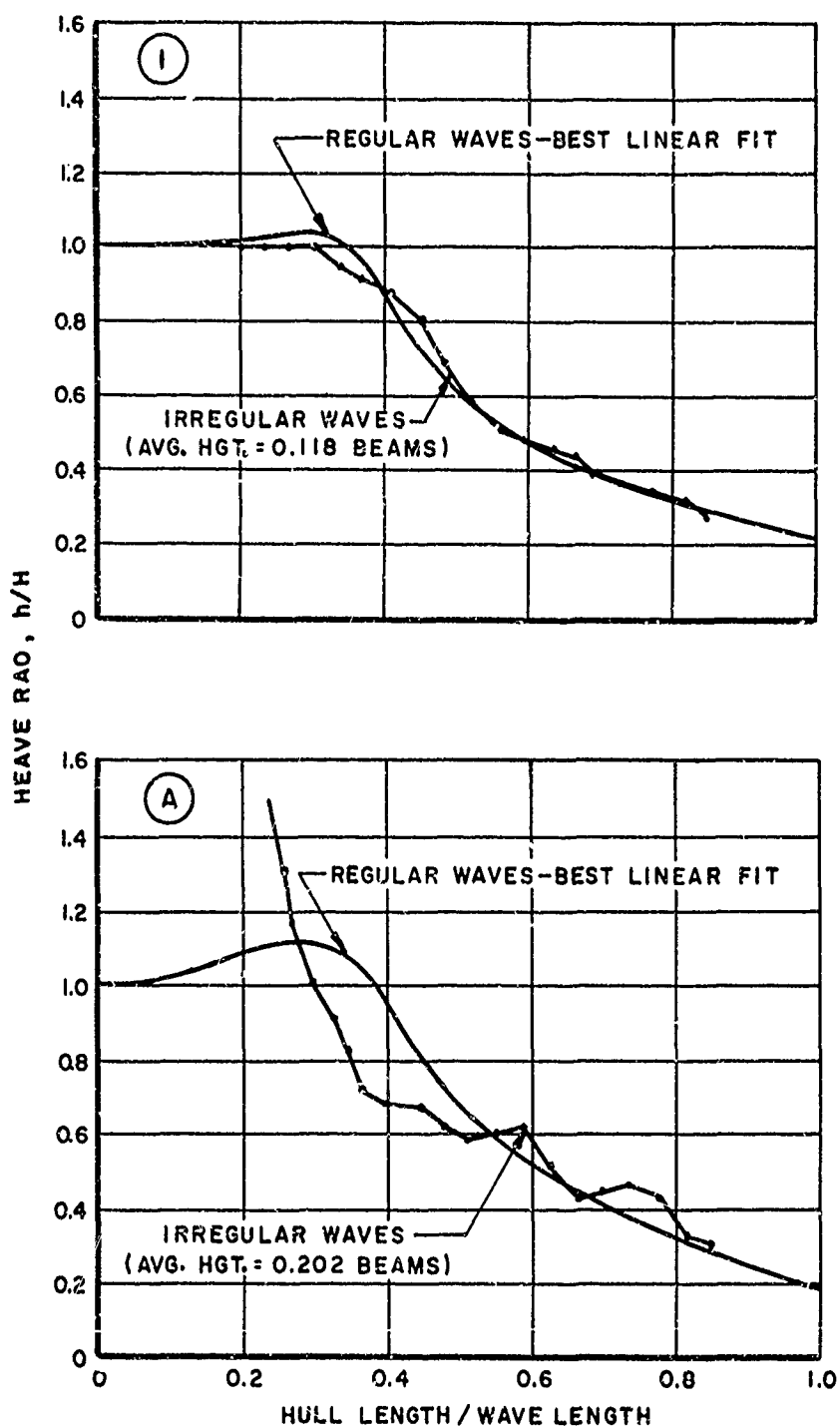


FIG. 22. LINEARITY-CORRELATION BETWEEN REGULAR AND IRREGULAR WAVES FOR HEAVE RESPONSE

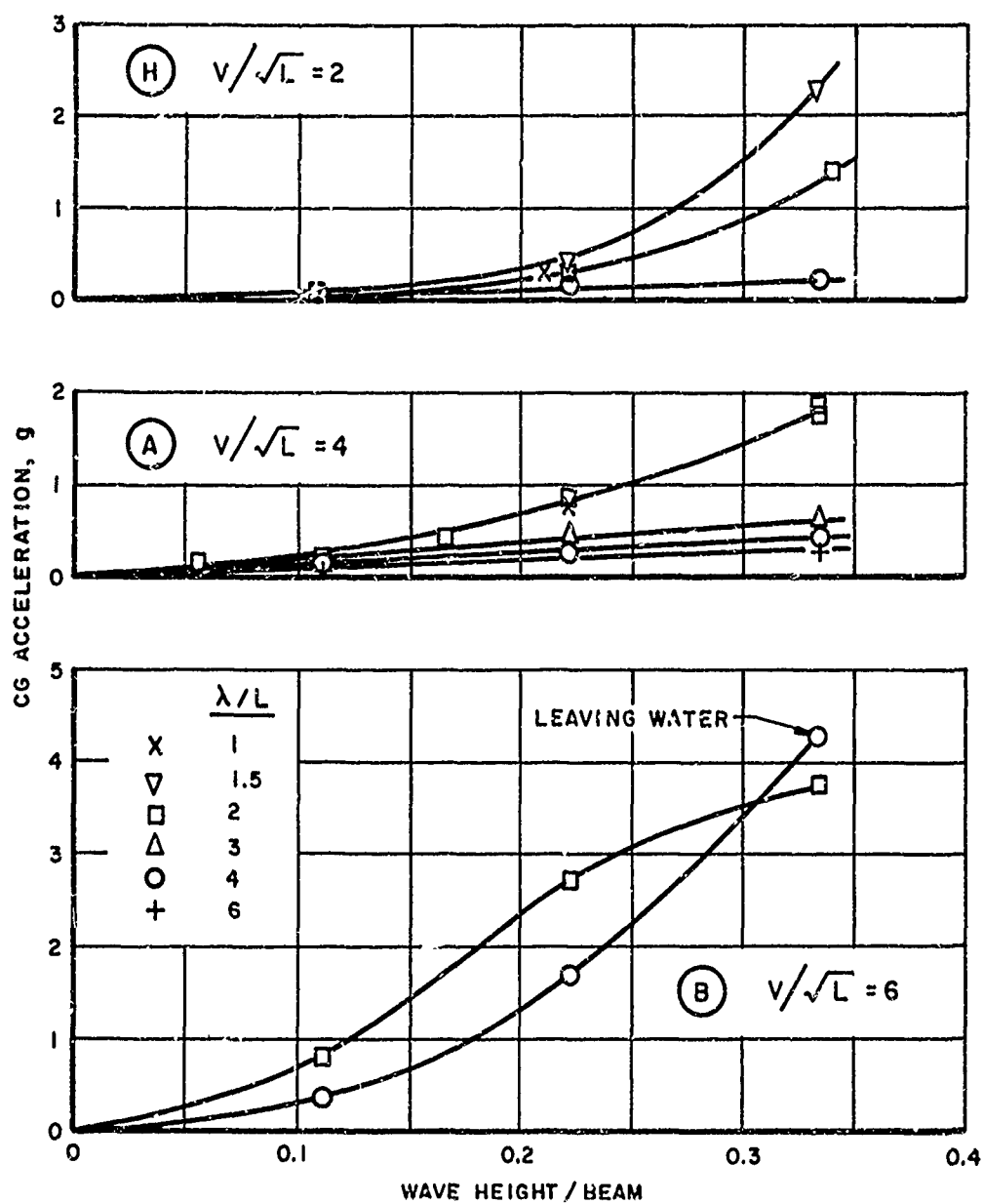


FIG. 23. LINEARITY - CG ACCELERATION VERSUS WAVE HEIGHT

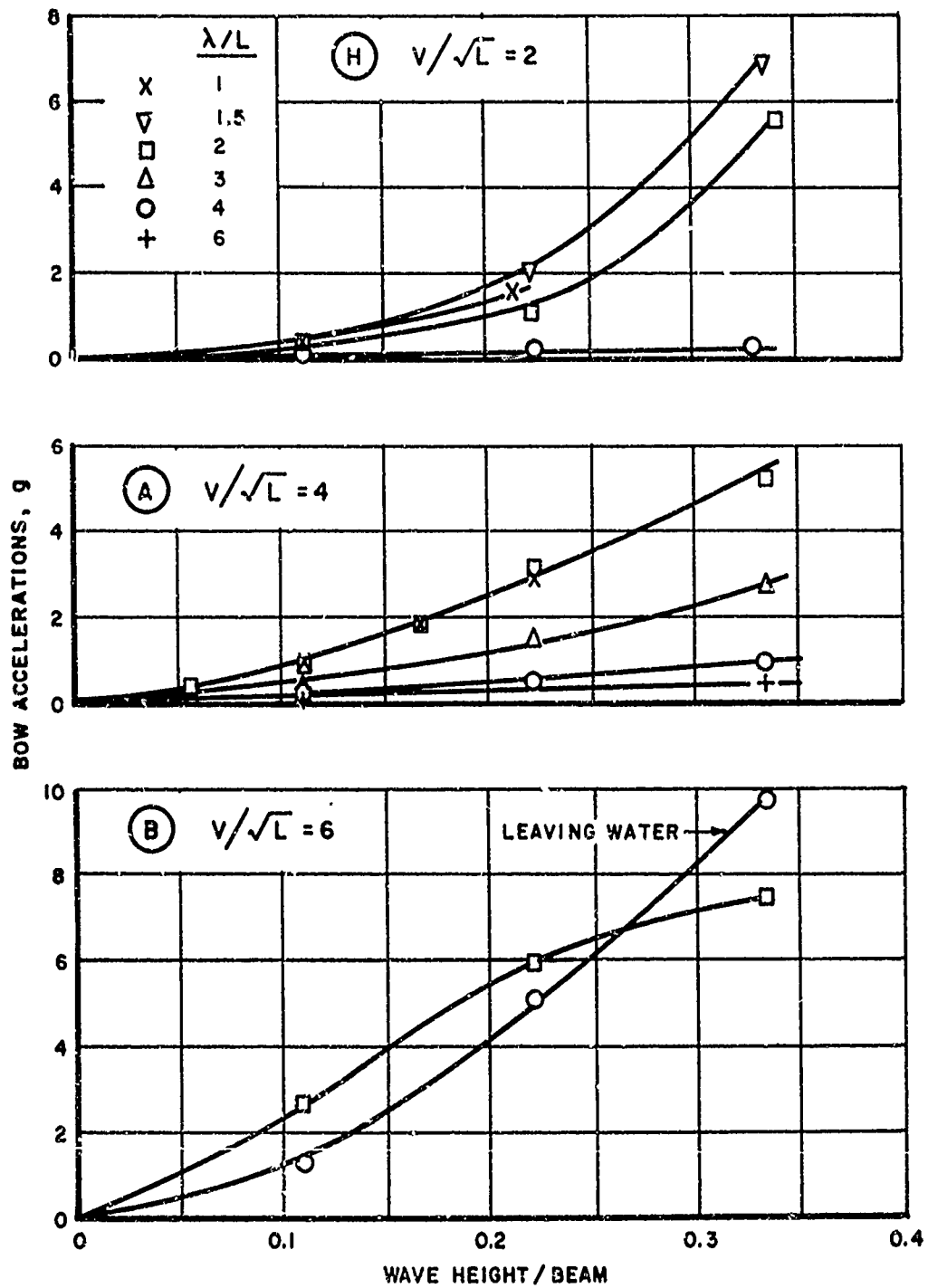


FIG. 24. LINEARITY-BOW ACCELERATION VERSUS WAVE HEIGHT

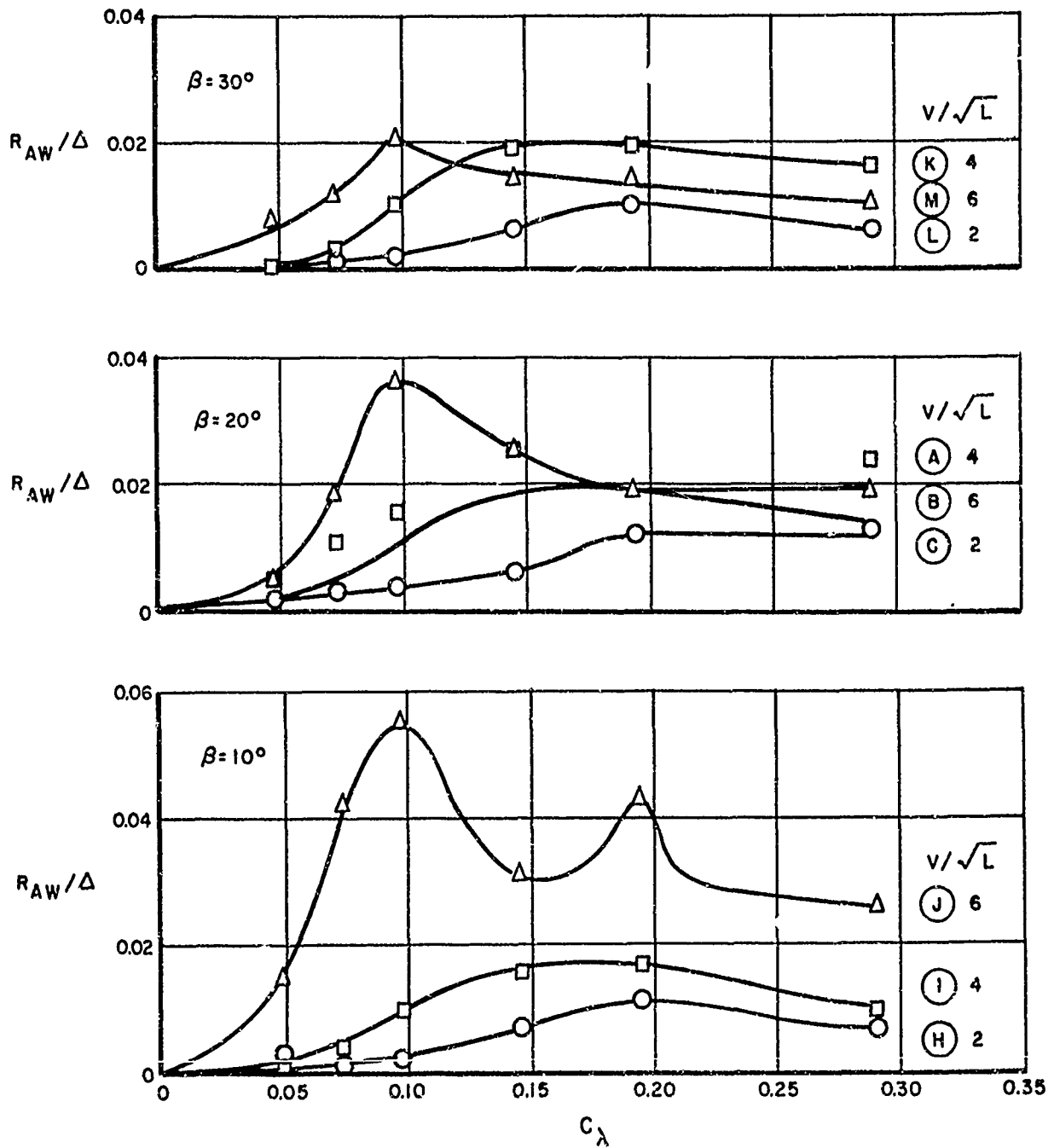


FIG. 25. EFFECT OF SPEED ON ADDED RESISTANCE
($L/b = 5$, $C_\Delta = 0.608$, $\tau = 4^\circ$, $H/b = 0.111$)

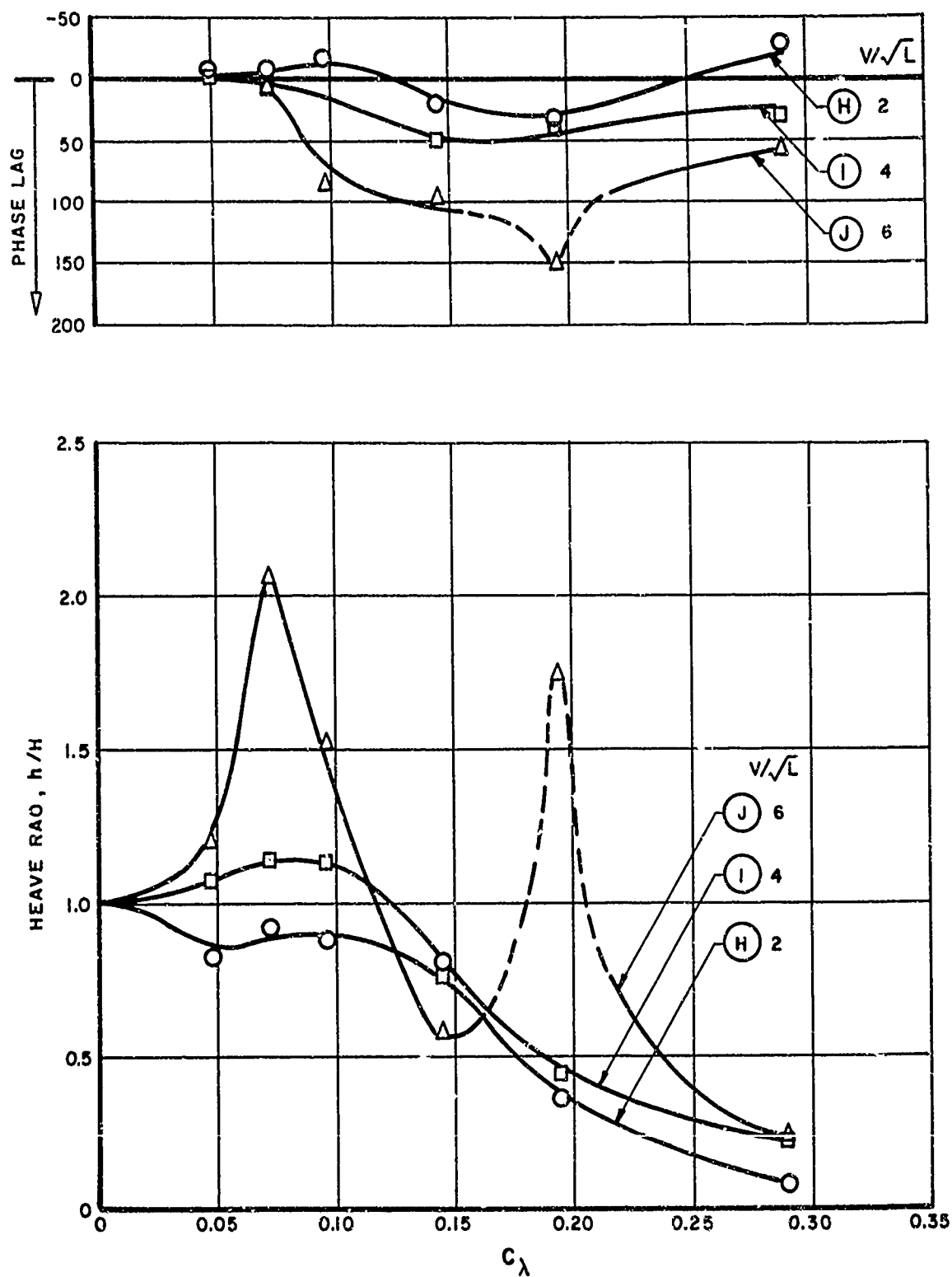


FIG. 26. EFFECT OF SPEED ON THE HEAVE RESPONSE OF THE 10° DEADRISE MODEL
 ($L/b=5$, $C_d=0.608$, $\tau=4^\circ$, $H/b=0.111$)

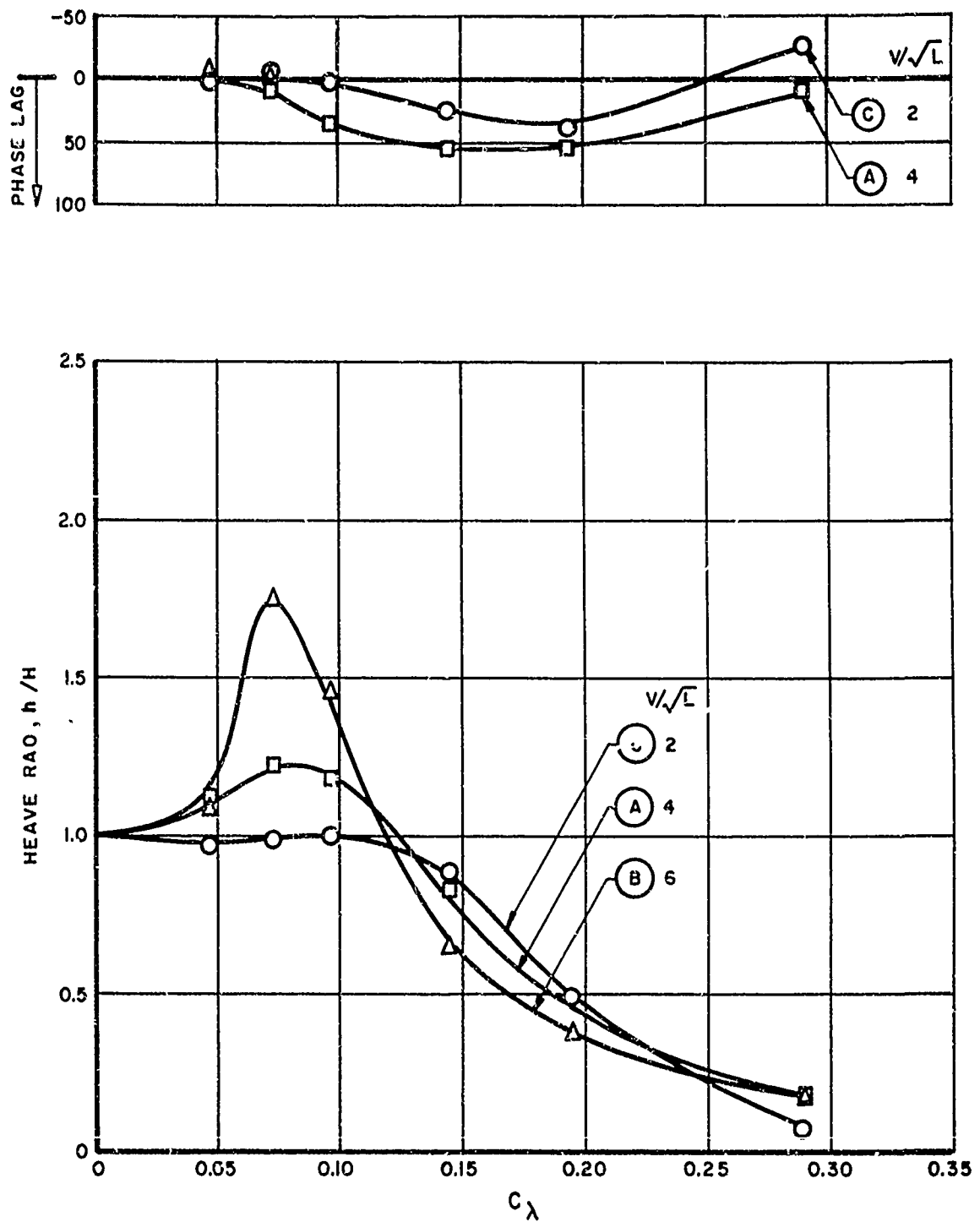


FIG. 27. EFFECT OF SPEED ON THE HEAVE RESPONSE OF THE 20° DEADRISE MODEL
($L/b = 5$, $C_\Delta = 0.608$, $\tau = 4^\circ$, $H/b = 0.111$)

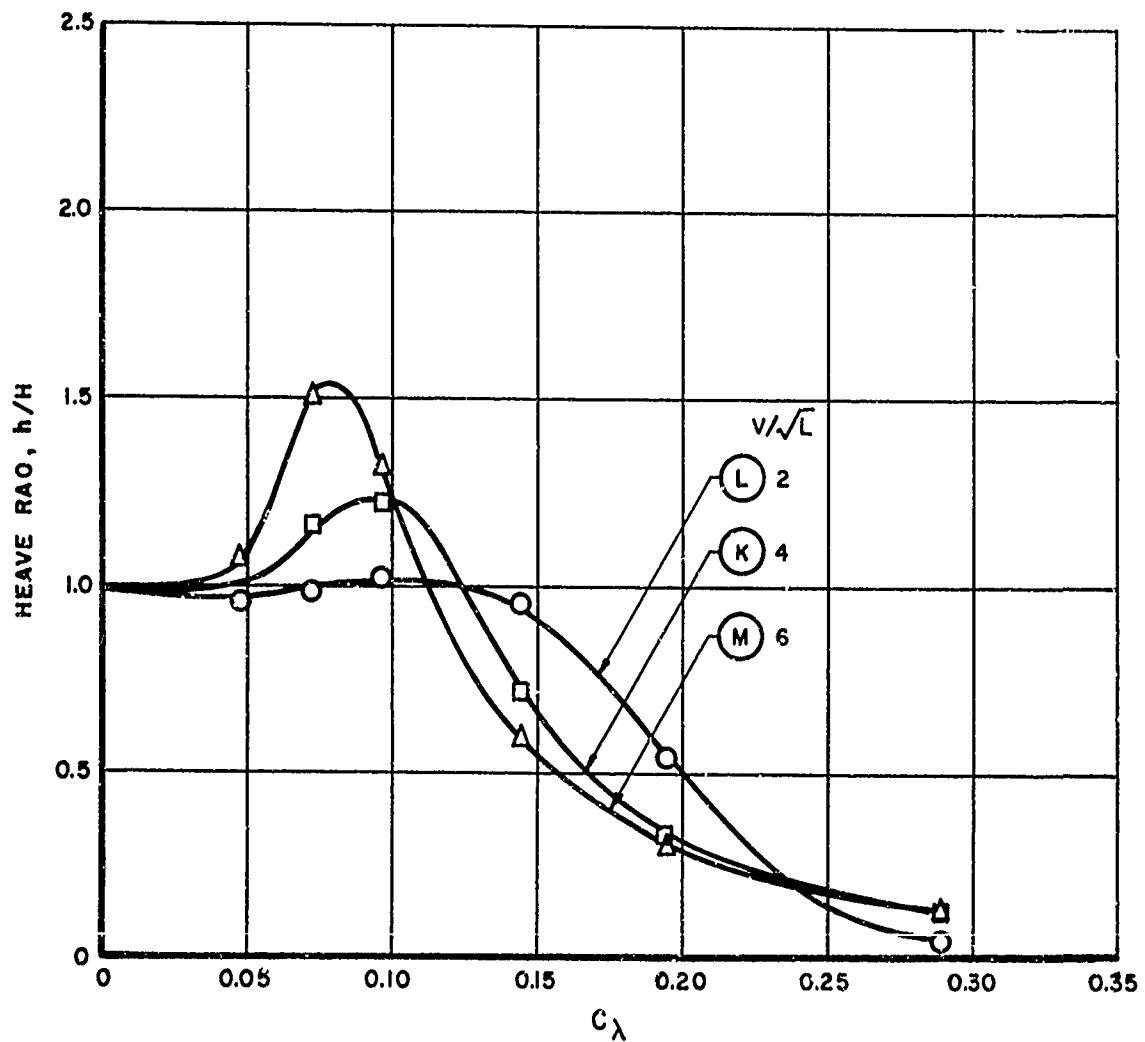
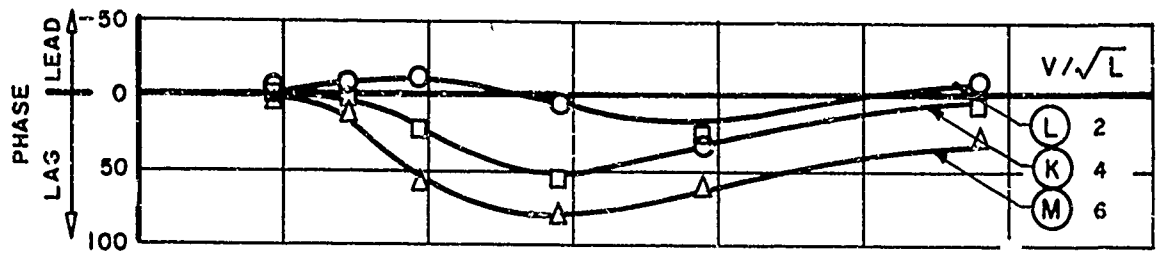


FIG. 28. EFFECT OF SPEED ON THE HEAVE RESPONSE OF THE 30° DEADRISE MODEL.
 $(L/b=5, C_d=0.608, \tau=4^\circ, H/b=0.111)$

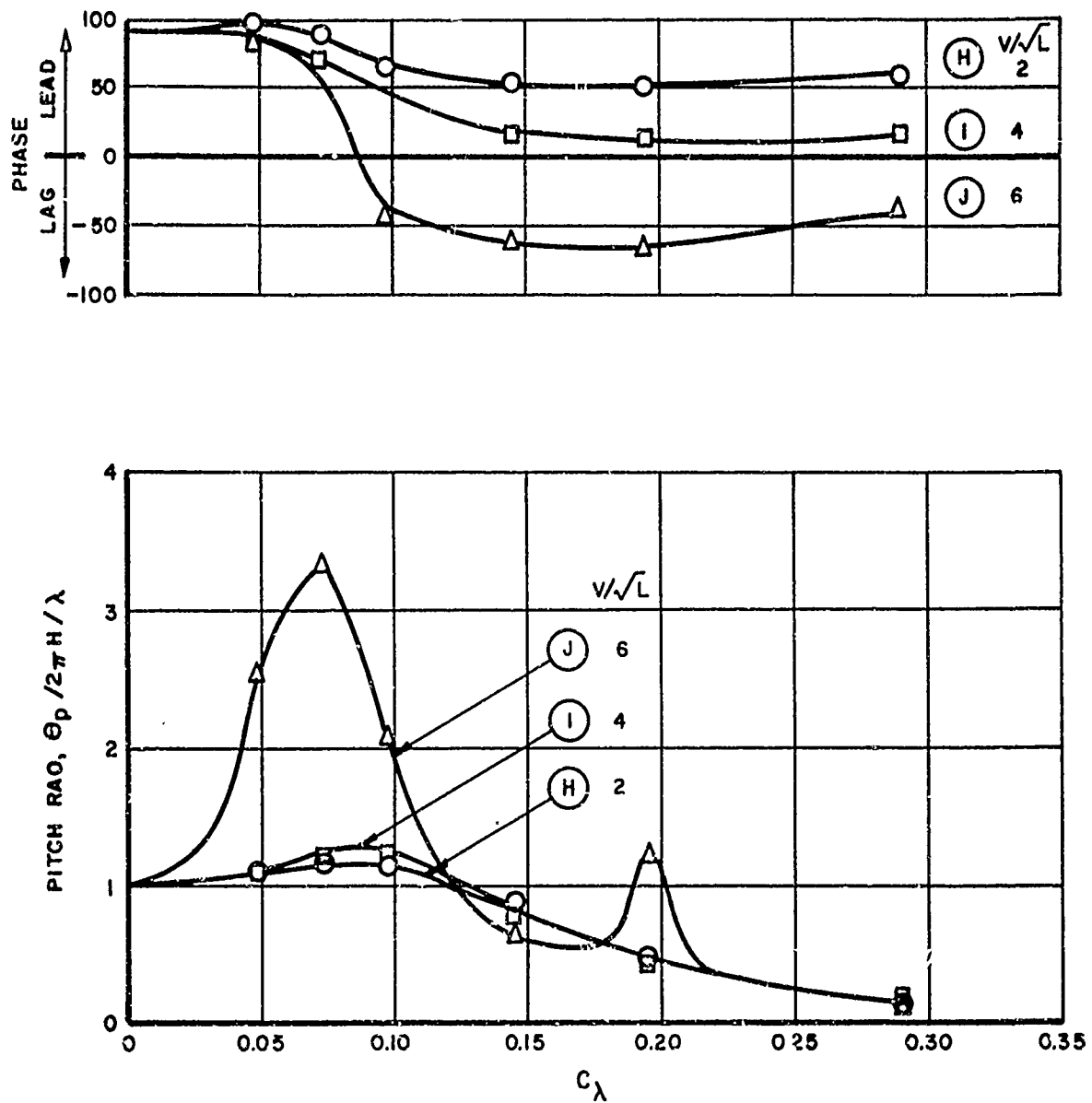


FIG. 29. EFFECT OF SPEED ON THE PITCH RESPONSE OF THE 10° DEADRISE MODEL
 ($L/b=5$, $C_\Delta=0.608$, $\tau=4^\circ$, $H/b=0.111$)

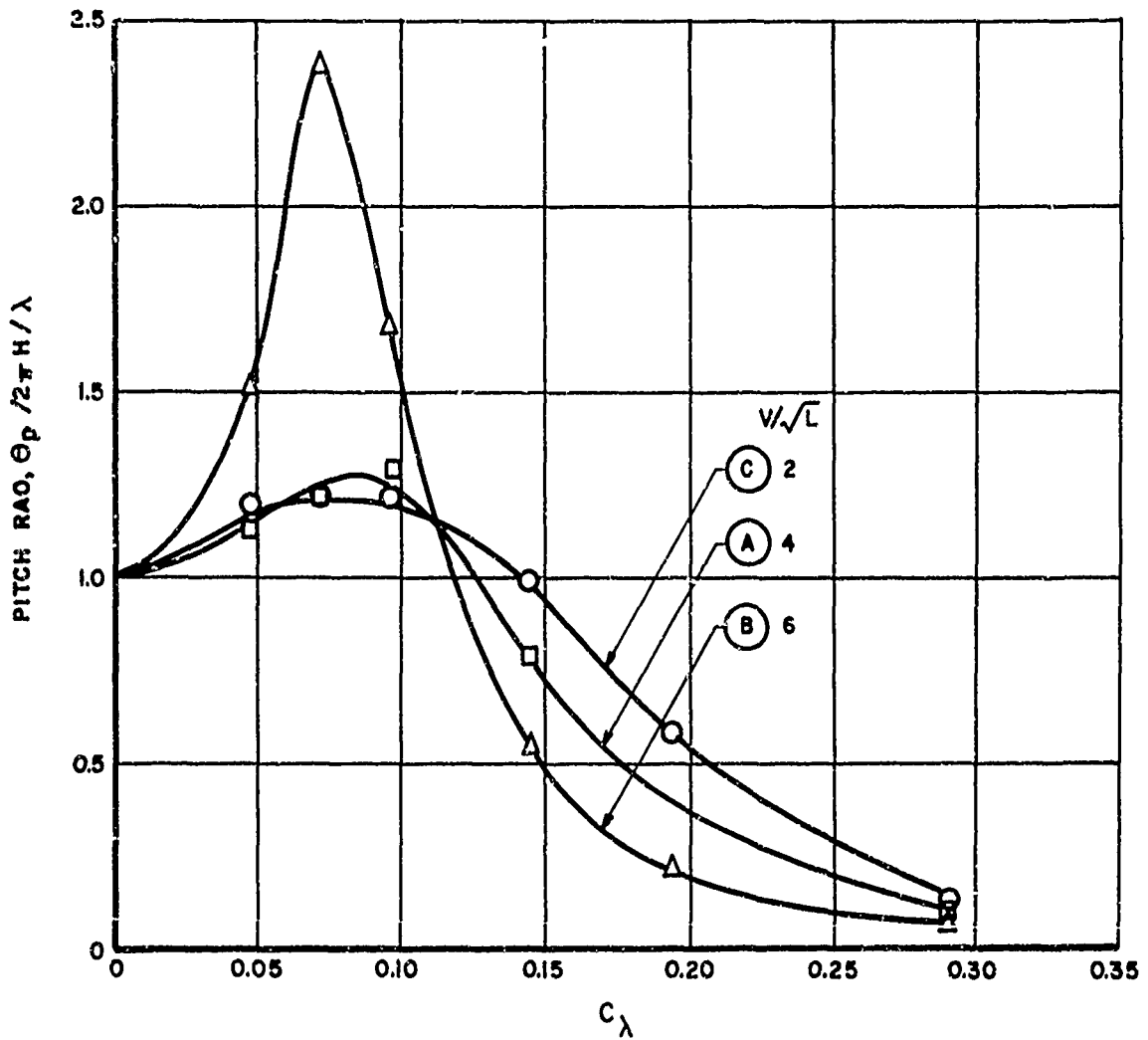
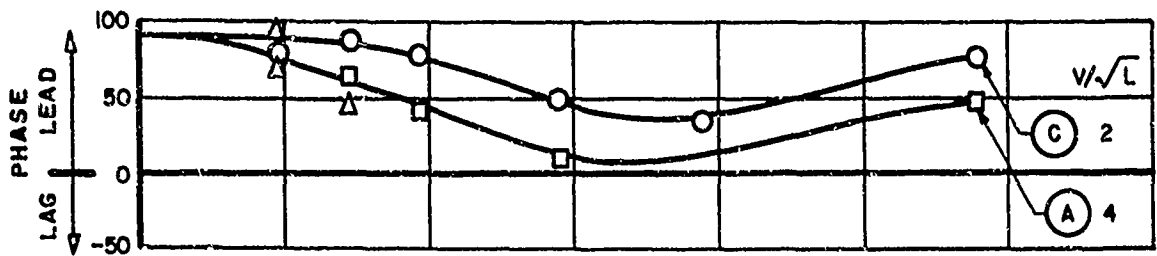


FIG. 30. EFFECT OF SPEED ON THE PITCH RESPONSE OF THE 20° DEADRISE MODEL
($L/b = 5$, $C_A = 0.608$, $\tau = 4^\circ$, $H/b = 0.111$)

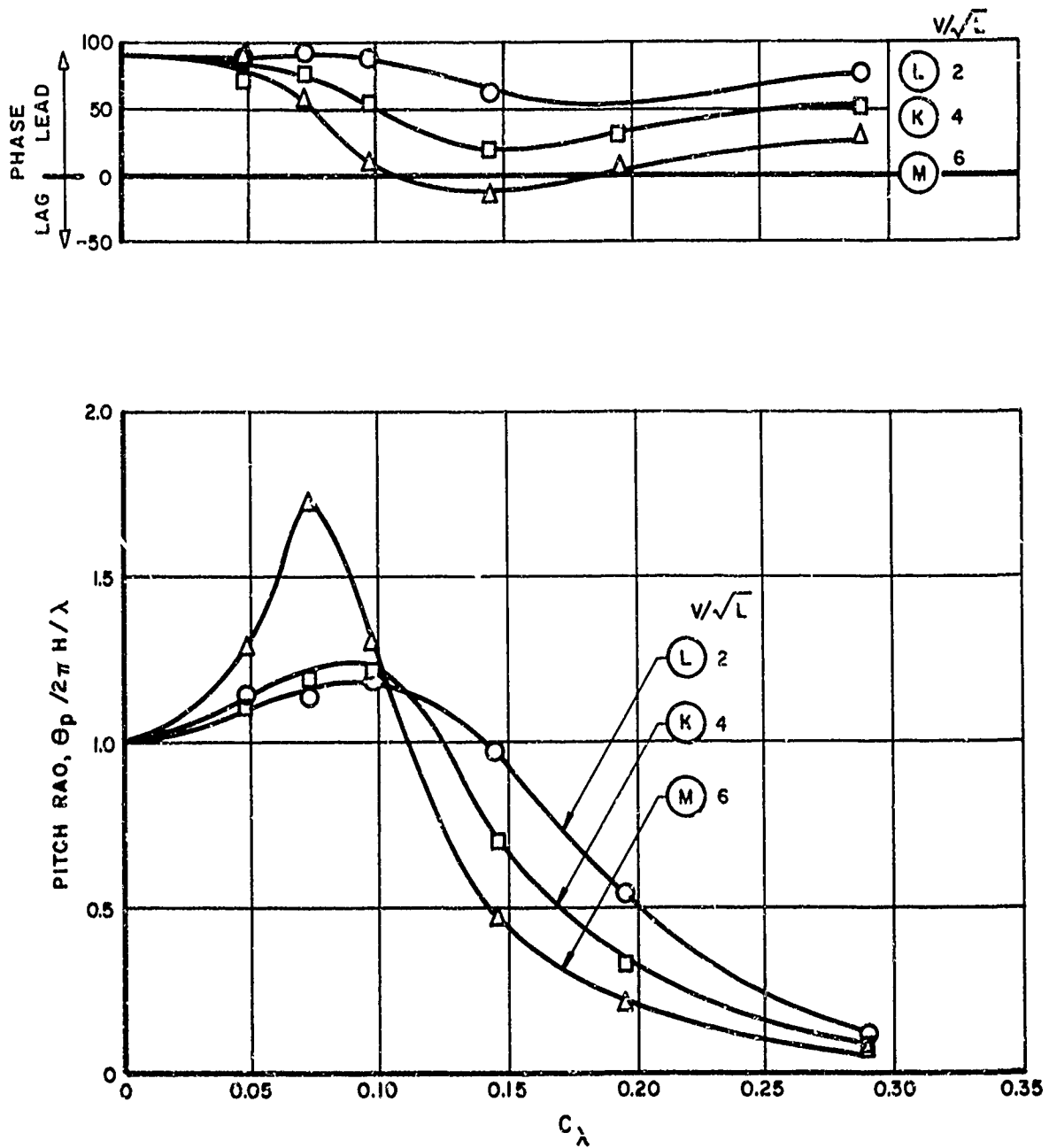


FIG. 31. EFFECT OF SPEED ON THE PITCH RESPONSE OF THE 30° DEADRISE MODEL
 ($L/b = 5$, $C_{\Delta} = 0.608$, $\tau = 4^\circ$, $H/b = 0.111$)

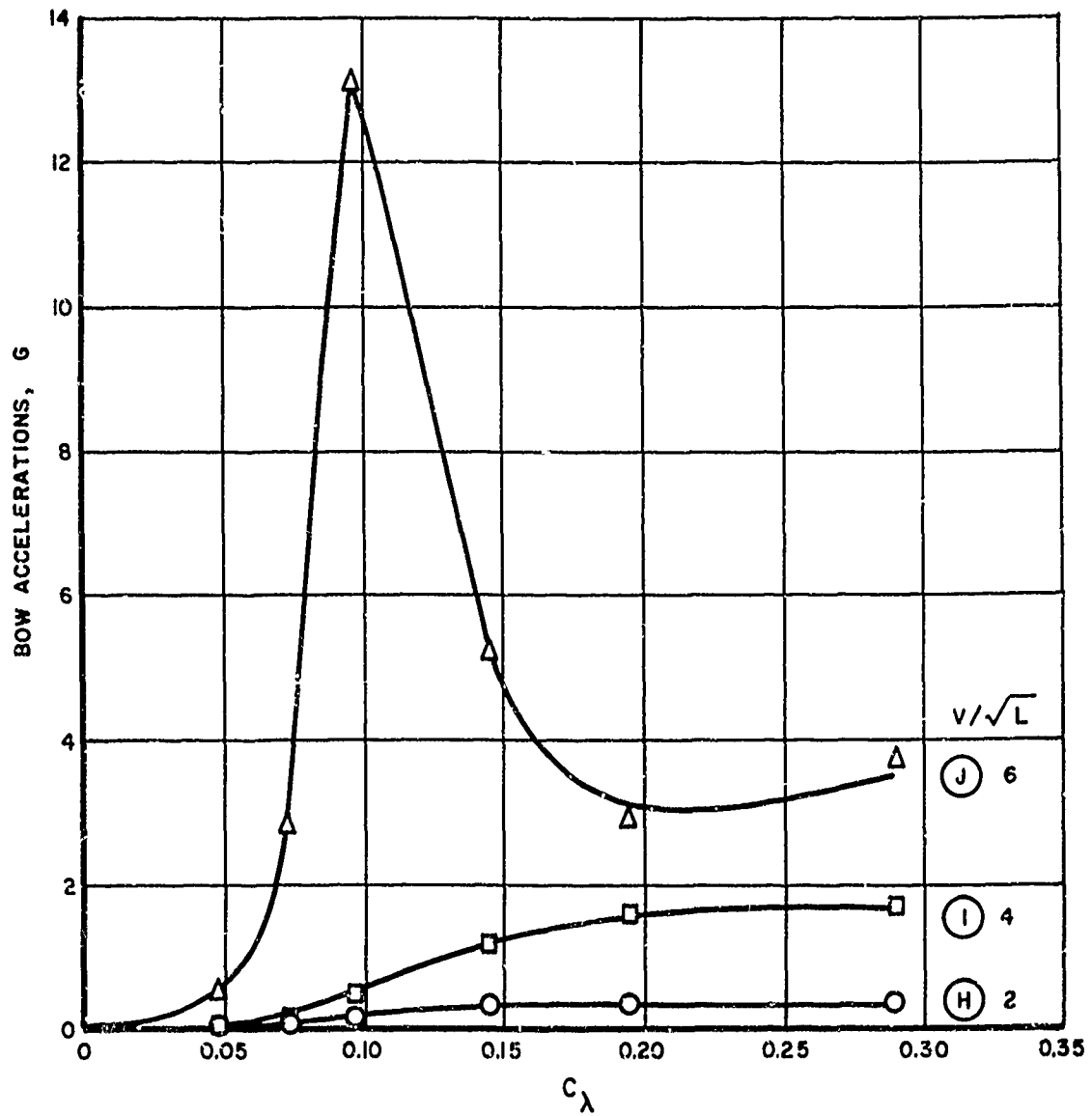


FIG. 32. EFFECT OF SPEED ON THE BOW ACCELERATIONS FOR THE 10° DEADRISE MODEL
($L/b=5$, $C_\Delta=0.608$, $\tau=4^\circ$, $H/b=0.111$)

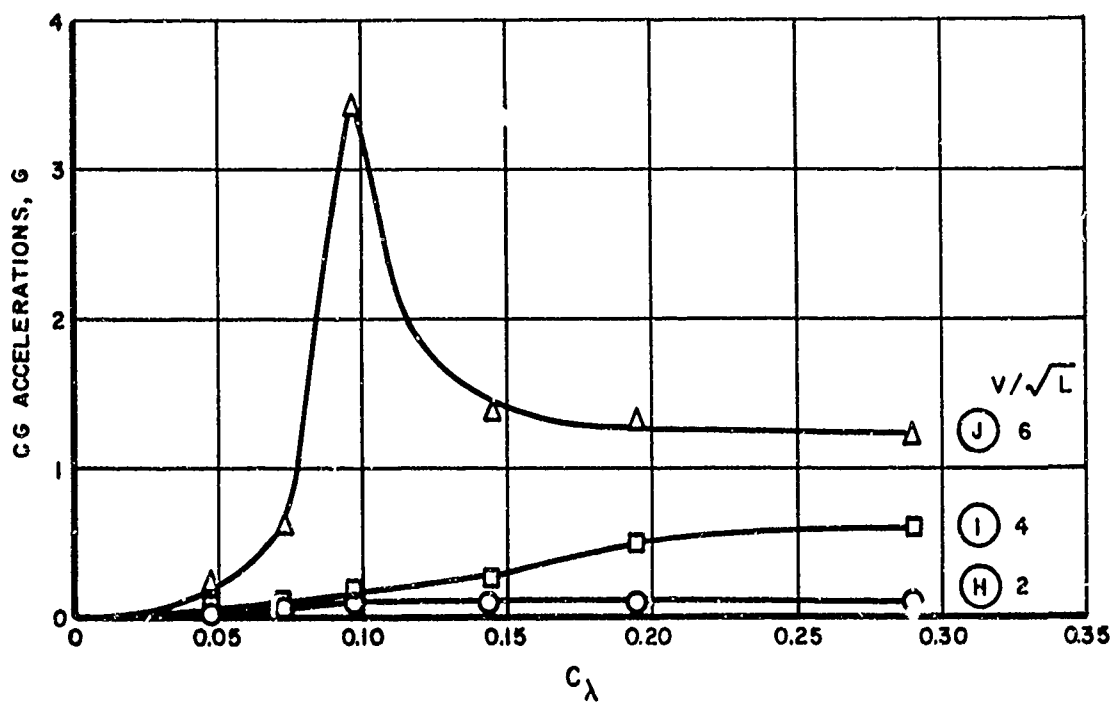


FIG.33. EFFECT OF SPEED ON CG ACCELERATIONS FOR THE
 10° DEADRISE MODEL
 ($L/b = 5$, $C_\Delta = 0.608$, $\tau = 4^\circ$, $H/b = 0.111$)

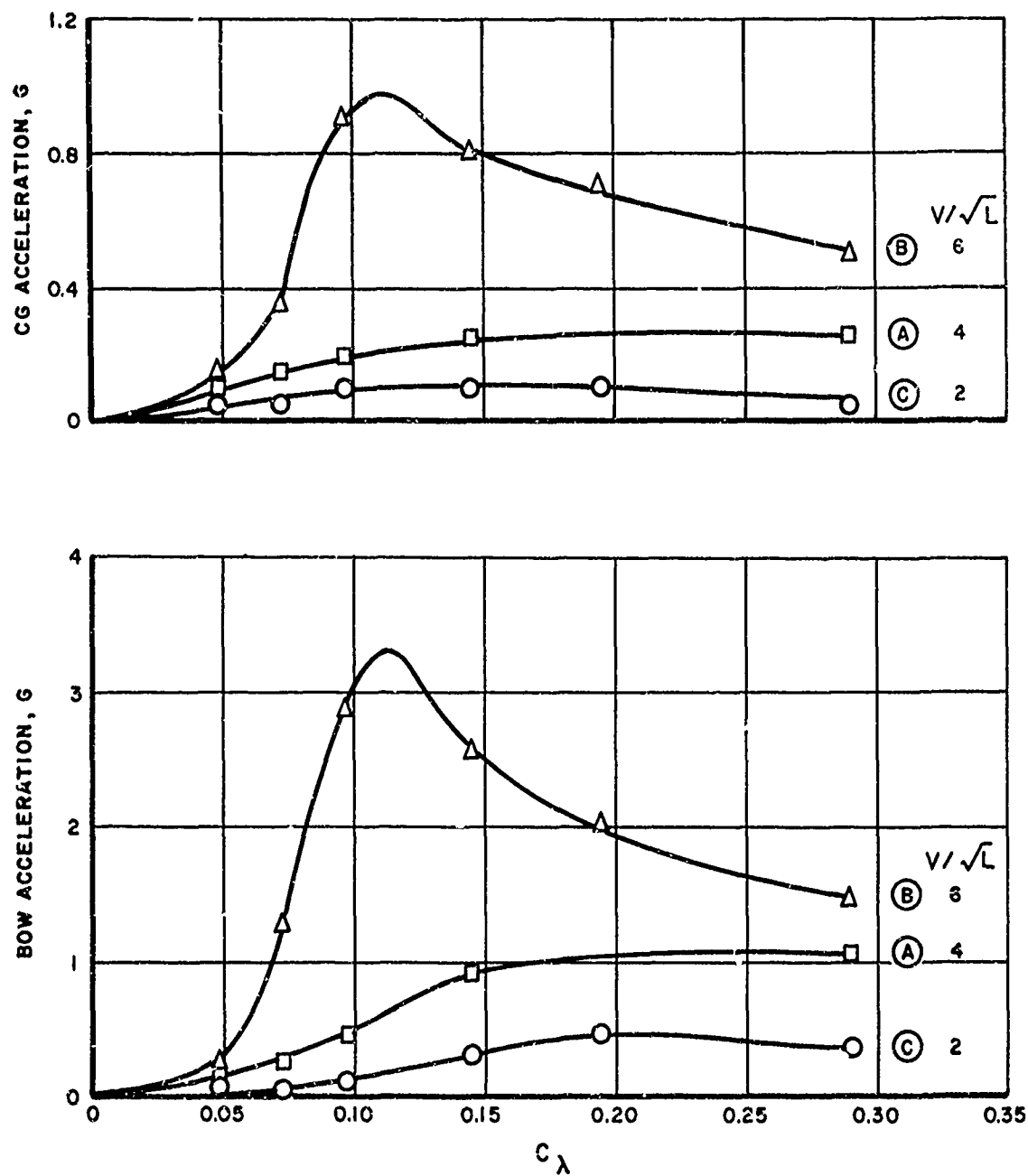


FIG. 34. EFFECT OF SPEED ON ACCELERATIONS FOR THE 20° DEADRISE MODEL
 ($L/b=5$, $C_A=0.608$, $\tau=4^\circ$, $H/b=0.111$)

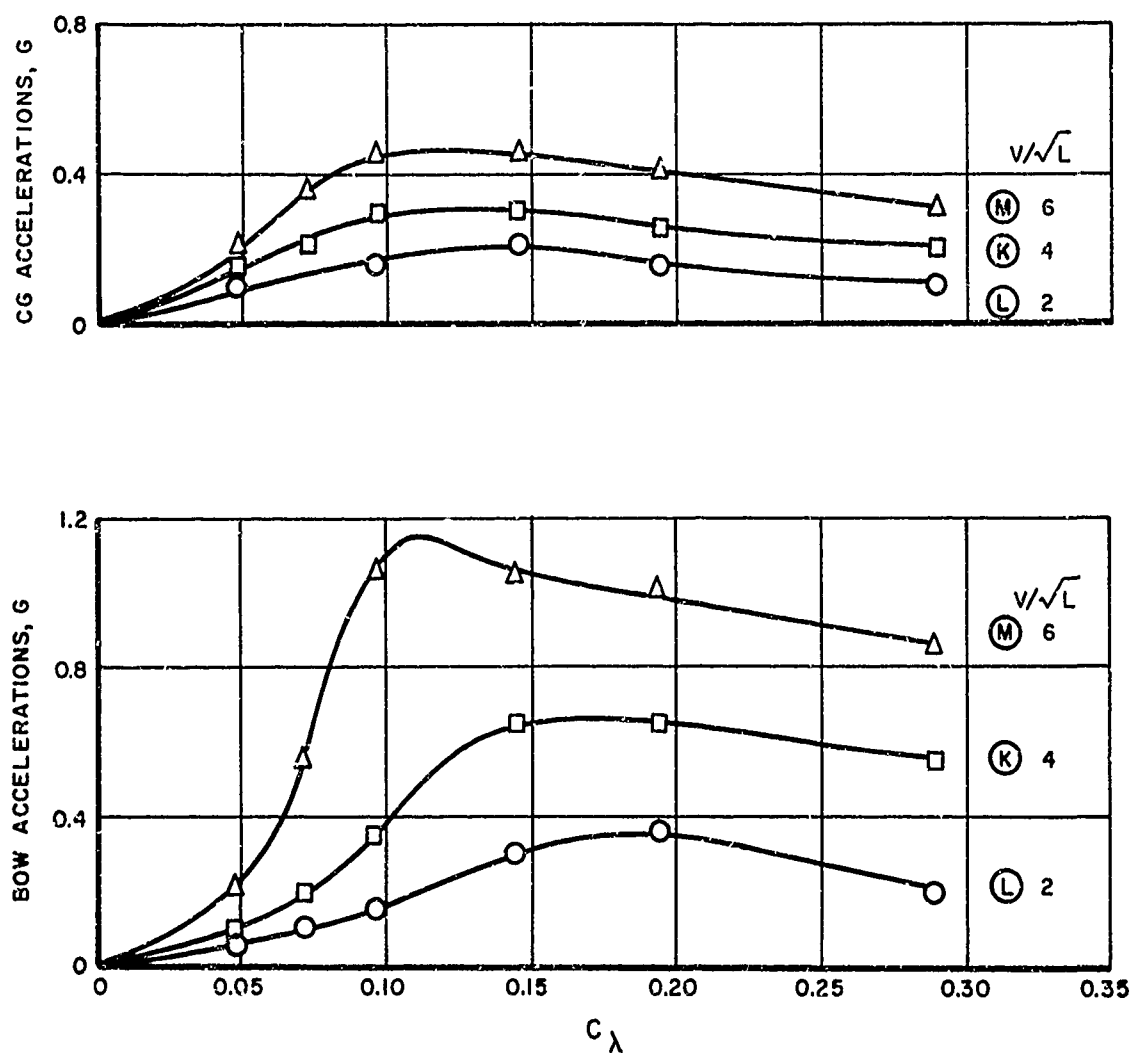


FIG. 35. EFFECT OF SPEED ON ACCELERATIONS FOR THE 30° DEADRISE MODEL
($L/b = 5$, $C_\lambda = 0.608$, $\tau = 4^\circ$, $H/b = 0.111$)

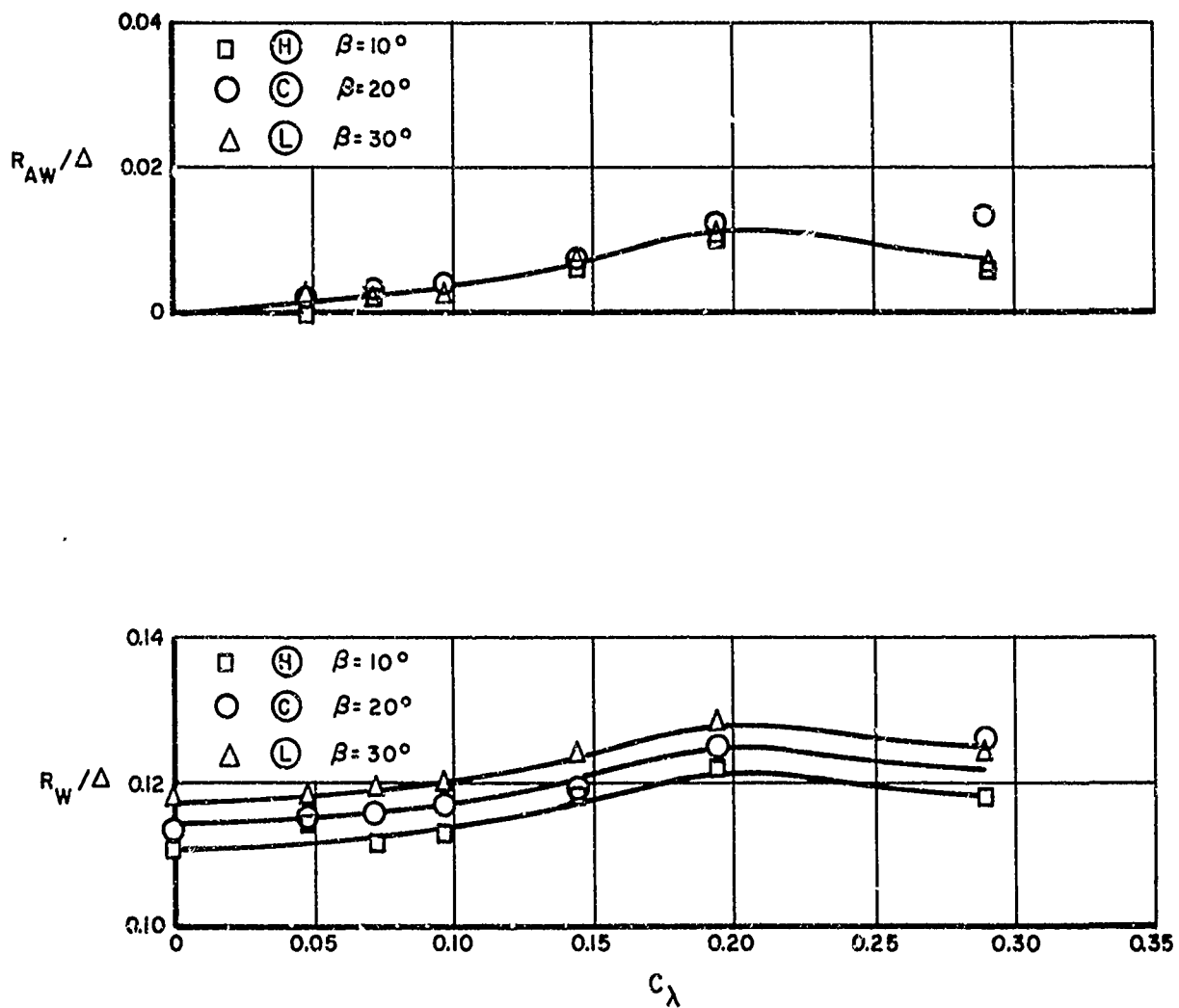


FIG. 36. EFFECT OF DEADRISE ON RESISTANCE AT $V/\sqrt{L}=2$
 ($L/b=5$, $C_\Delta=0.608$, $\tau=4^\circ$, $H/b=0.111$)

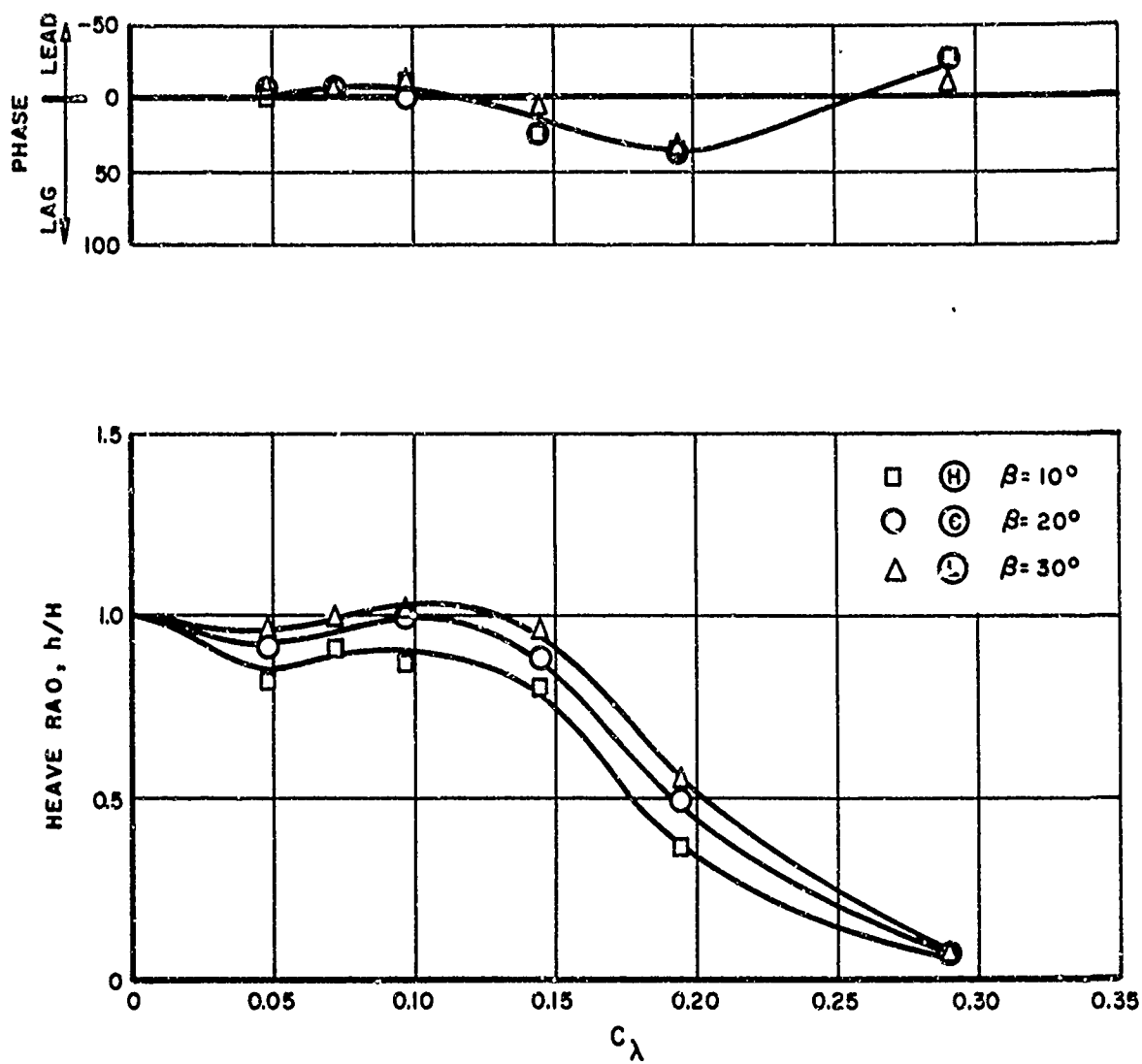


FIG. 37. EFFECT OF DEADRISE ON THE HEAVE RESPONSE AT $V/\sqrt{L} = 2$
 ($L/b = 5$, $C_d = 0.608$, $\tau = 4^\circ$, $H/b = 0.111$)

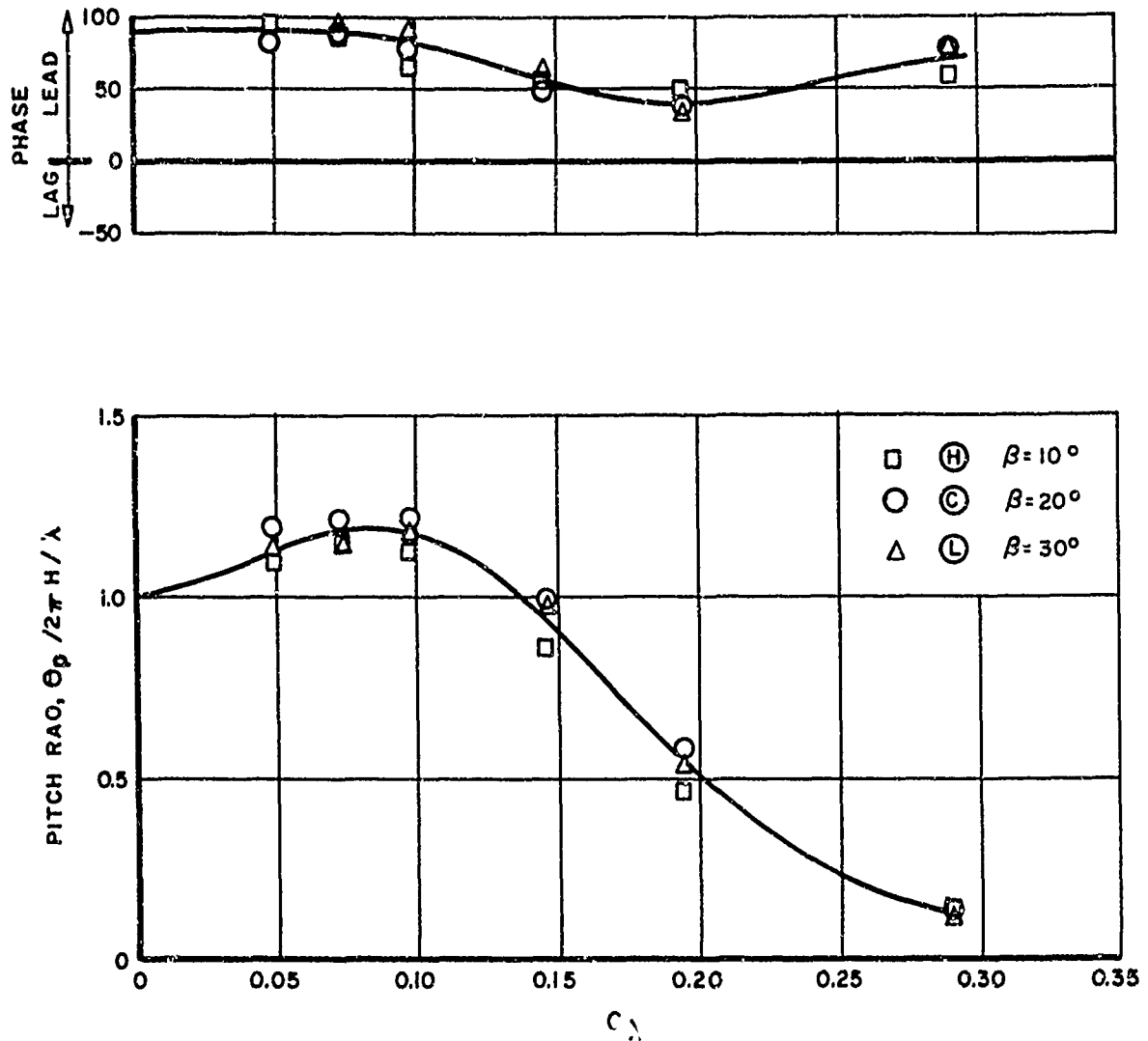


FIG. 38. EFFECT OF DEADRISE ON THE PITCH RESPONSE AT $V/\sqrt{L} = 2$
 ($L/b = 5$, $C_d = 0.608$, $\tau = 4^\circ$, $H/b = 0.111$)

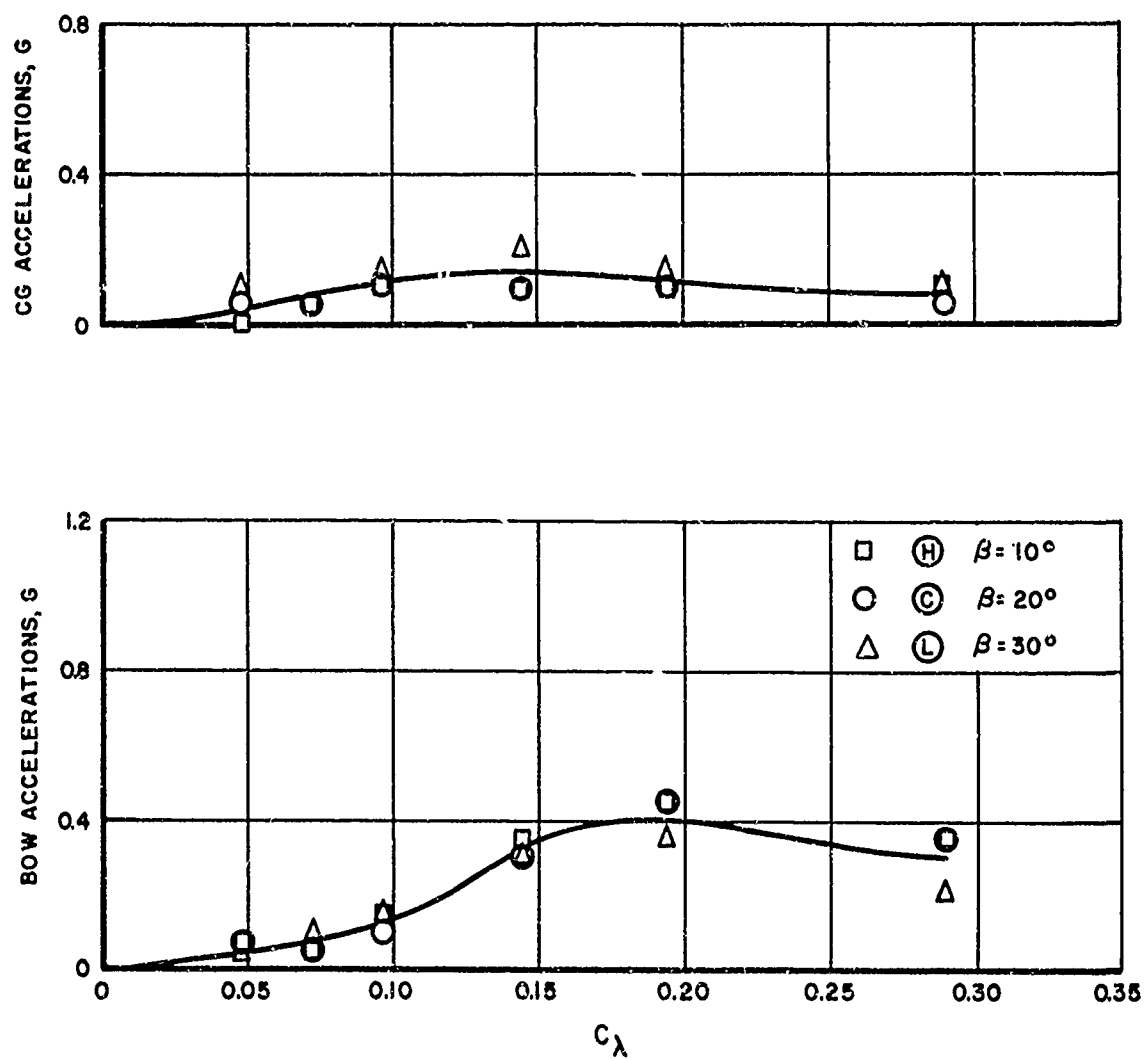


FIG. 39. EFFECT OF DEADRISE ON ACCELERATIONS AT $V/\sqrt{L} = 2$
 ($L/b = 5$, $C_\Delta = 0.608$, $\tau = 4^\circ$, $H/b = 0.111$)

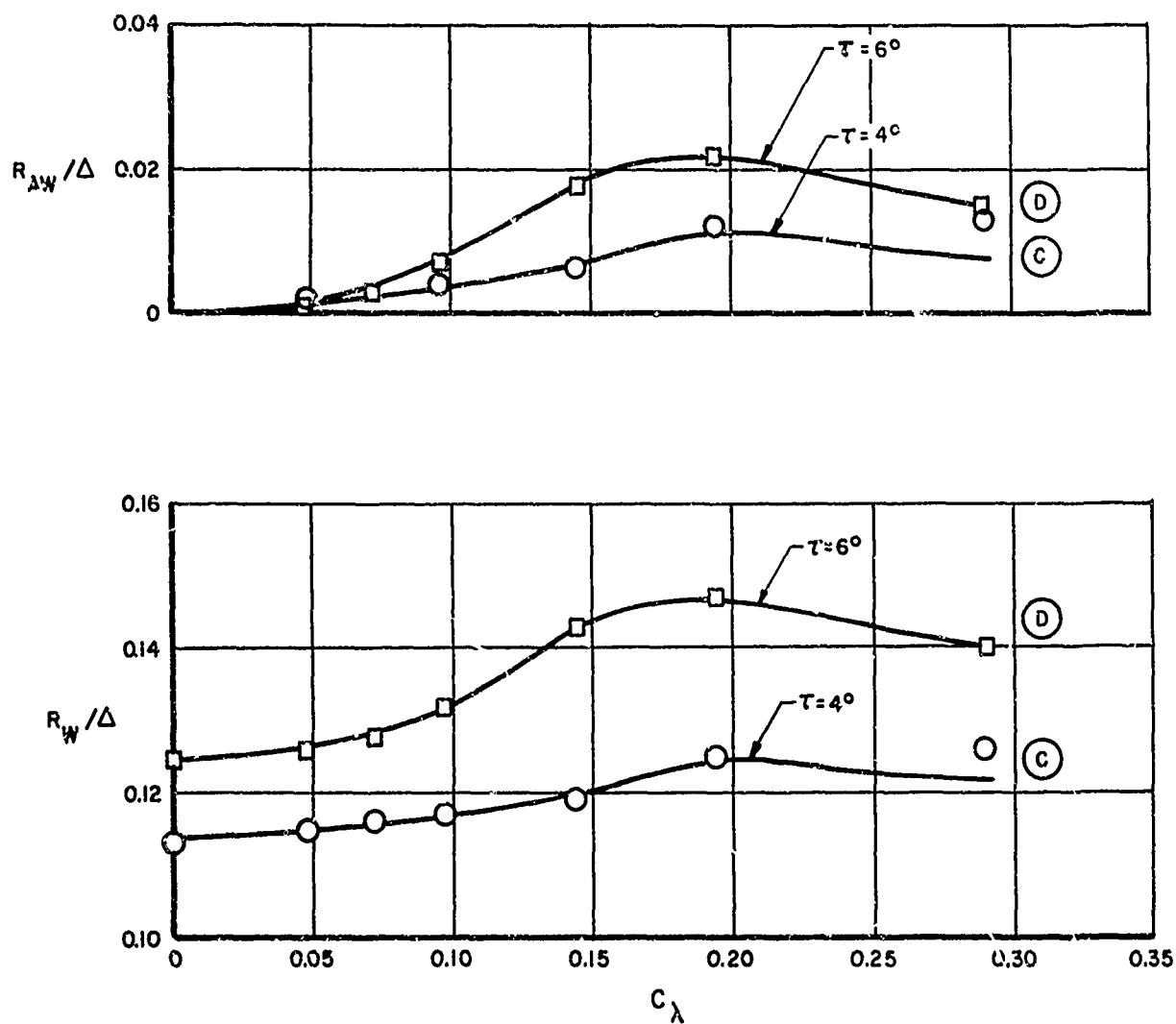


FIG. 40. EFFECT OF TRIM ON RESISTANCE AT $V/\sqrt{L} = 2$
 ($L/b = 5$, $C_\Delta = 0.608$, $\beta = 20^\circ$, $H/b = 0.111$)

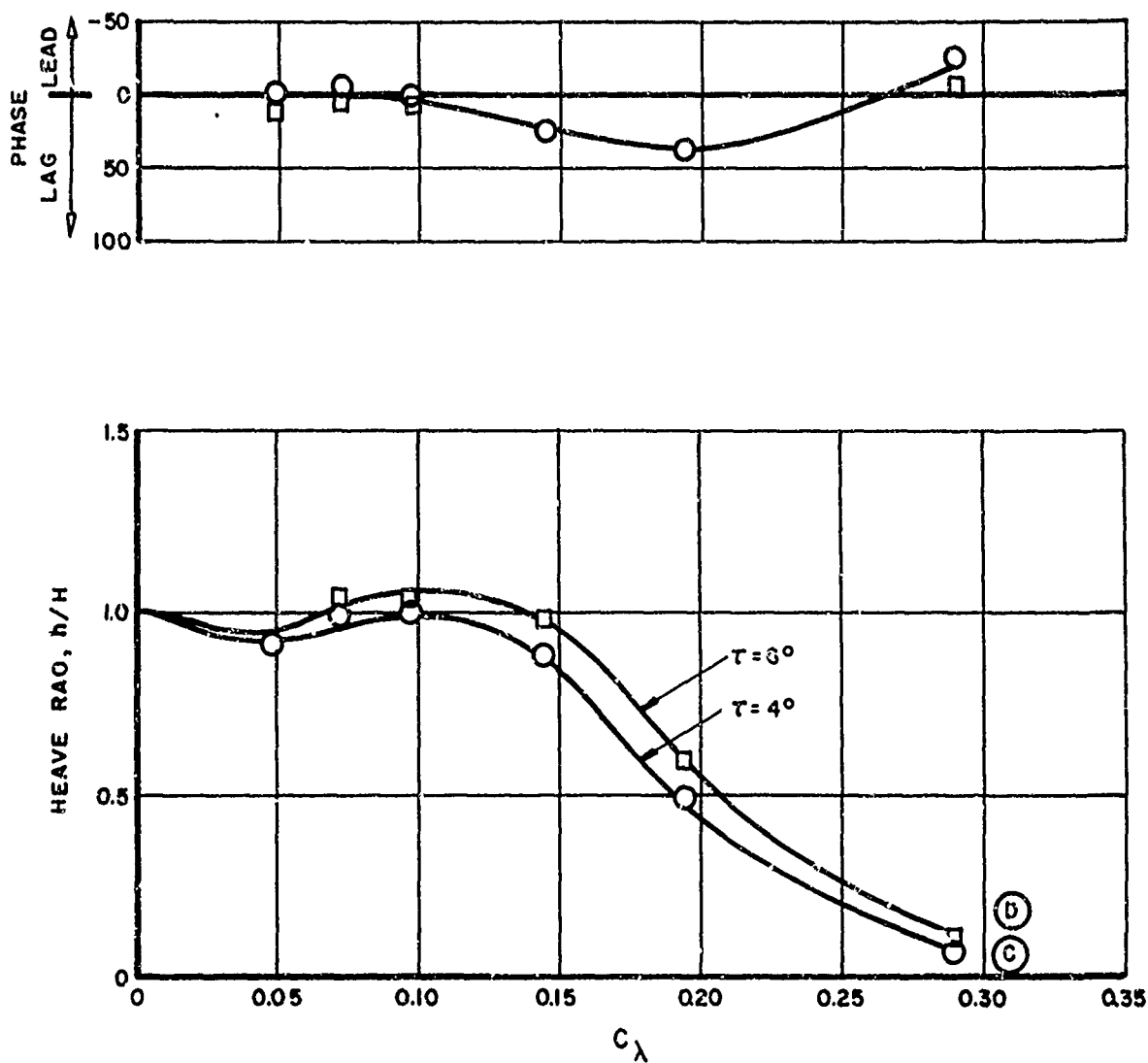


FIG. 41. EFFECT OF TRIM ON THE HEAVE RESPONSE AT $V/\sqrt{L}=2$
 ($L/b=5$, $C_\Delta=0.608$, $\beta=20^\circ$, $H/b=0.111$)

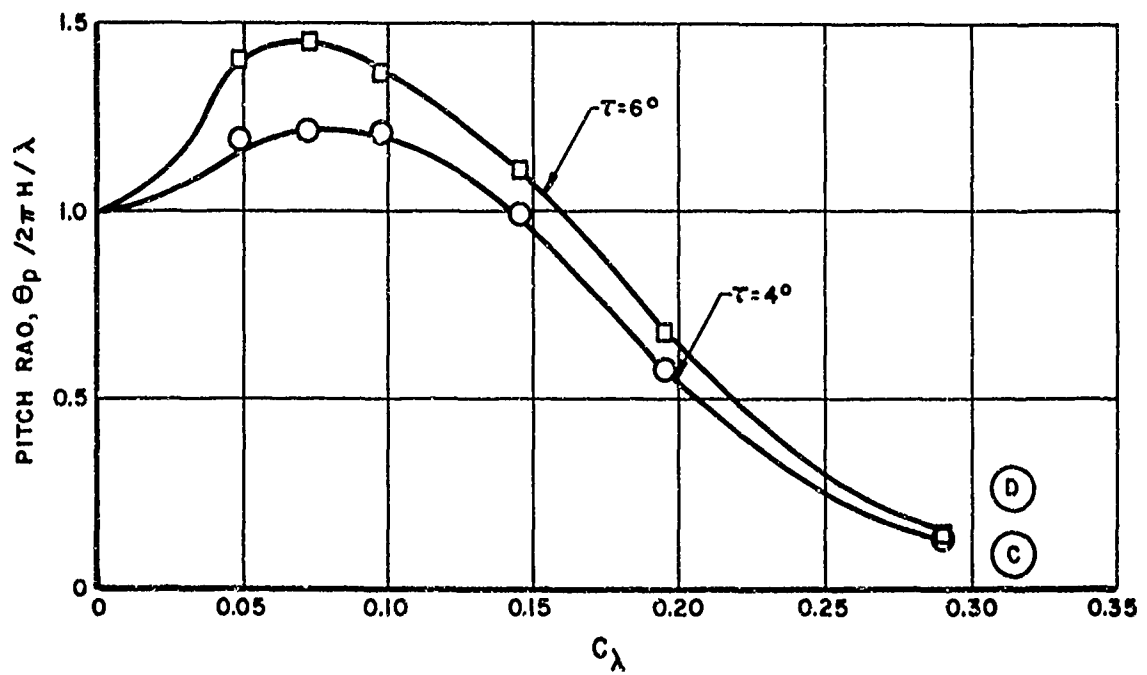
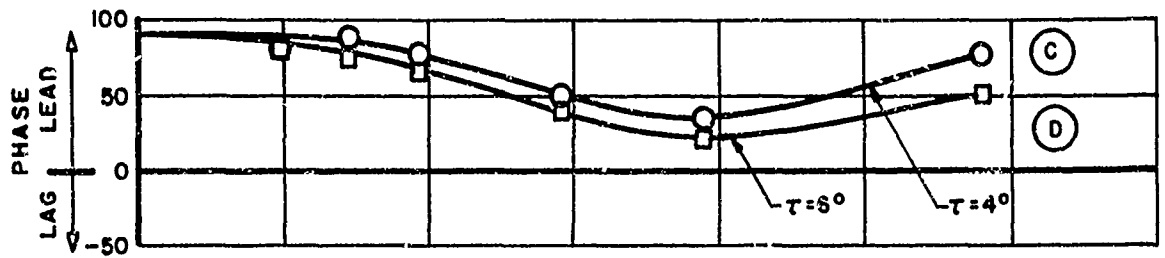


FIG. 42. EFFECT OF TRIM ON THE PITCH RESPONSE AT $V/\sqrt{L}=2$
 ($L/b=5$, $C_\Delta=0.608$, $\beta=20^\circ$, $H/b=0.111$)

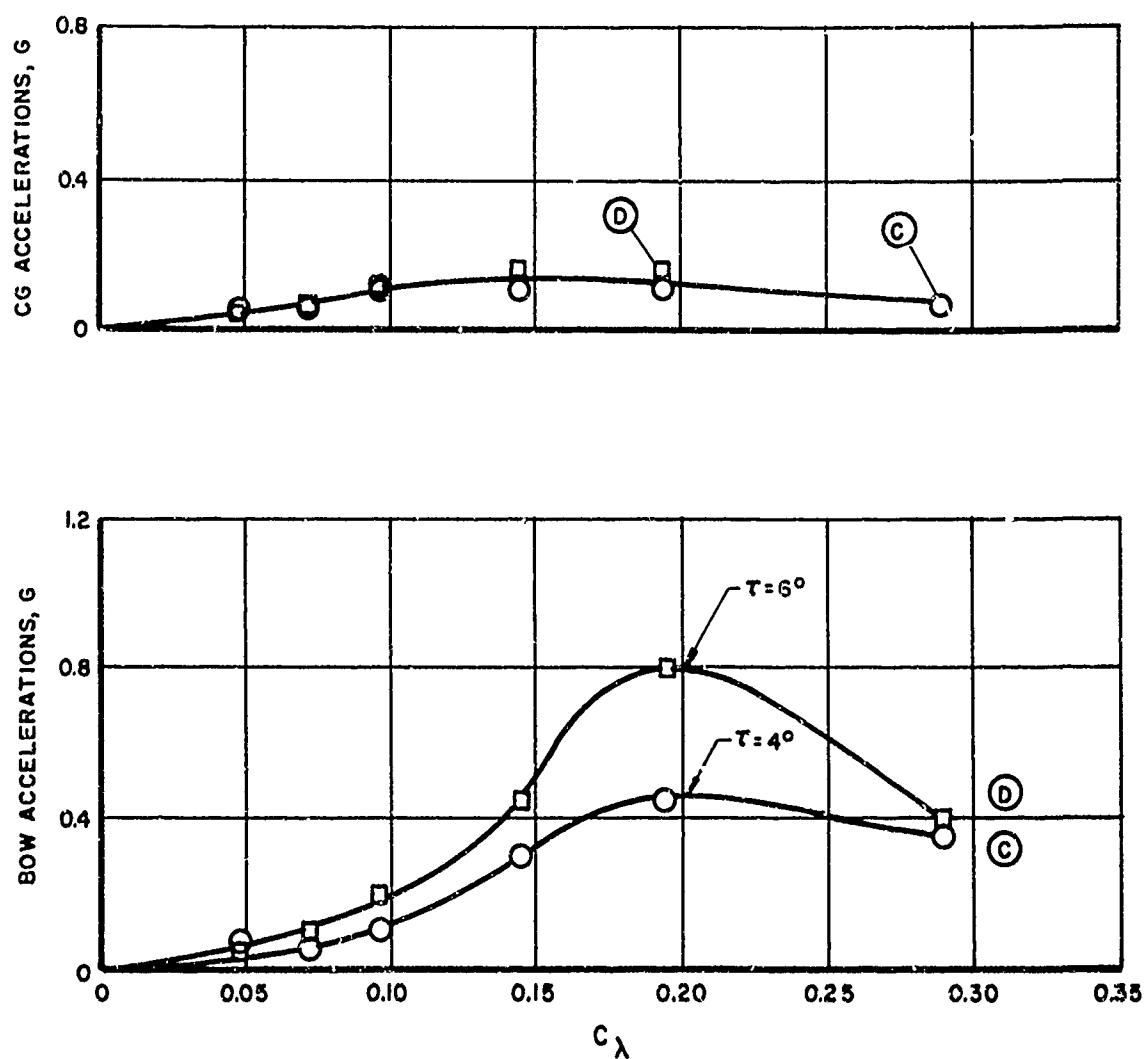


FIG.43. EFFECT OF TRIM ON ACCELERATIONS AT $V/\sqrt{L} = 2$
 $(L/b = 5, C_\Delta = 0.608, \beta = 20^\circ, H/b = 0.111)$

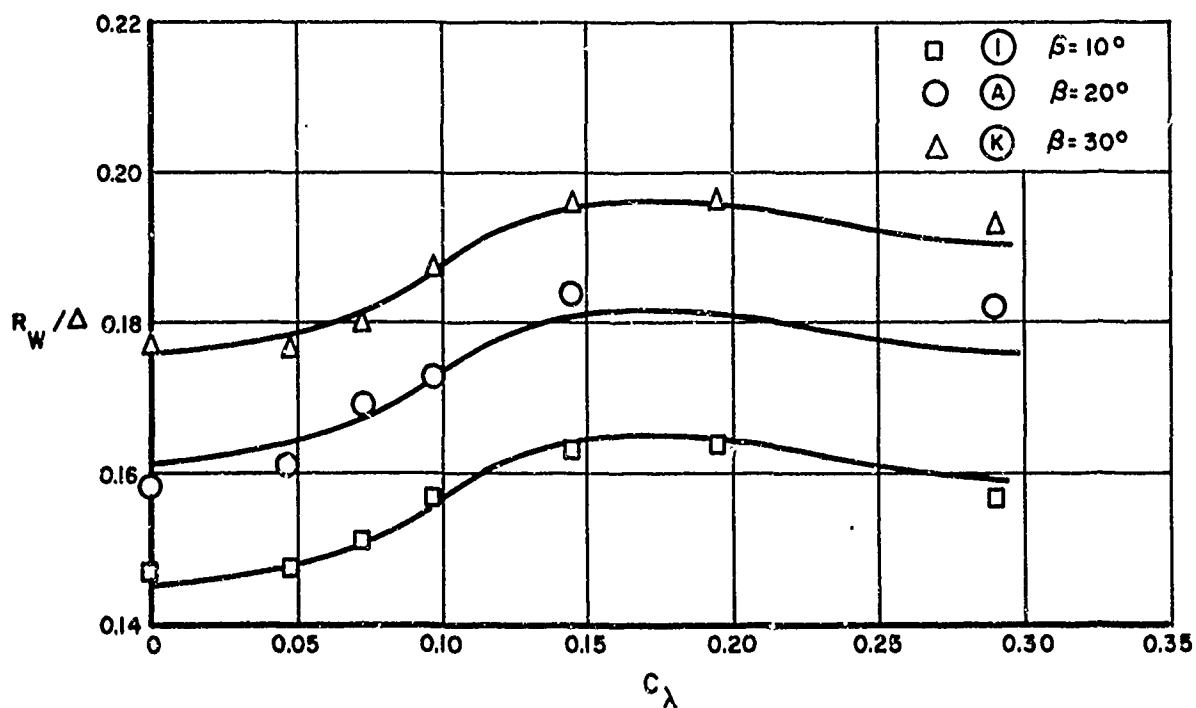
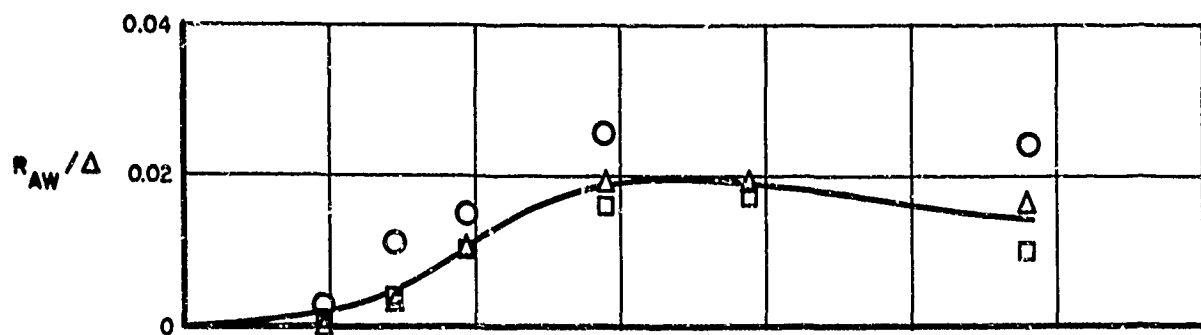


FIG. 44. EFFECT OF DEADRISE ON RESISTANCE AT $V/\sqrt{L} = 4$
 ($L/b = 5$, $C_\Delta = 0.608$, $\tau = 4^\circ$, $H/b = 0.111$)

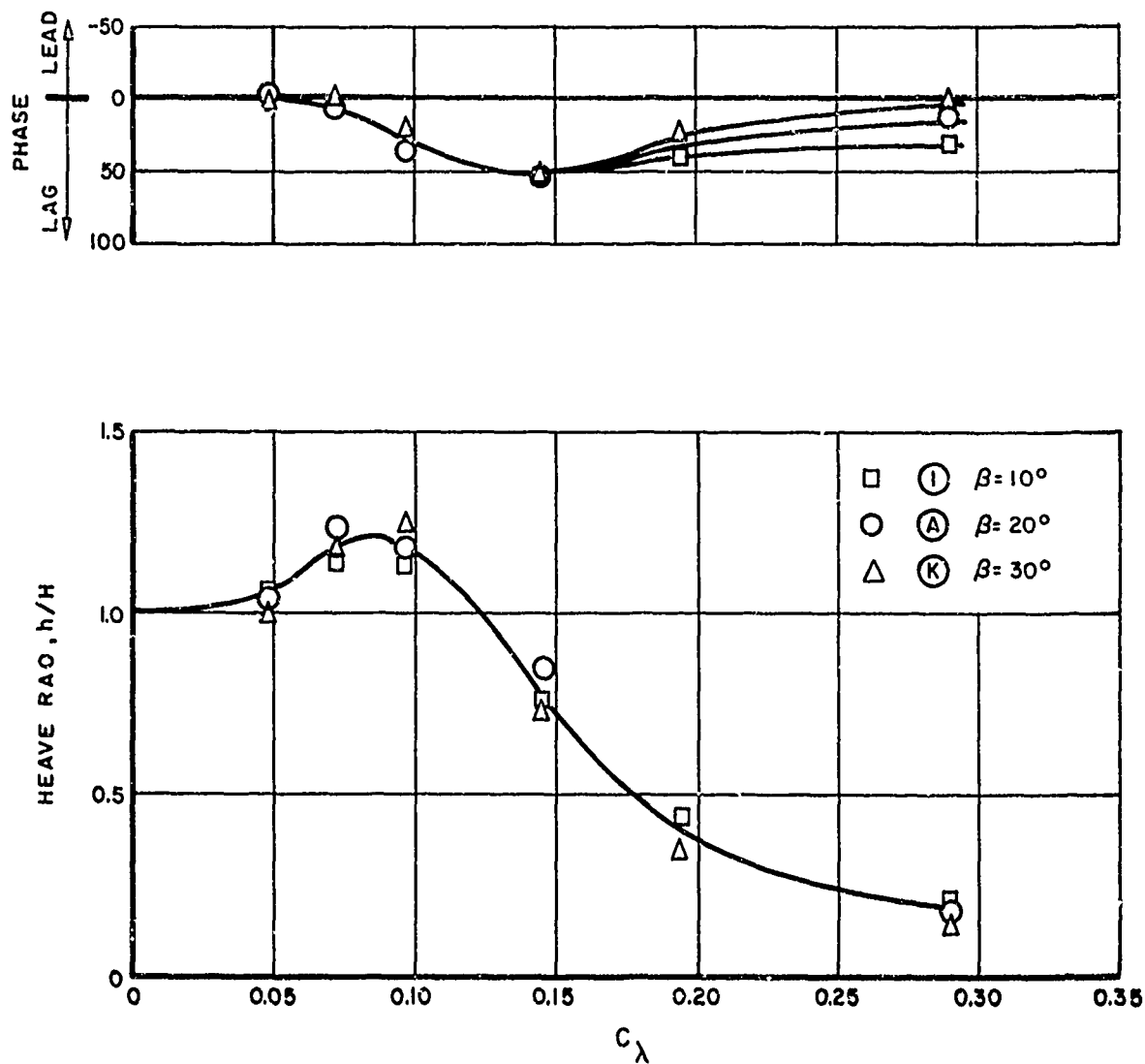


FIG. 45. EFFECT OF DEADRISE ON THE HEAVE RESPONSE AT $V/\sqrt{L} = 4$
 ($L/b = 5$, $C_d = 0.608$, $\tau = 4^\circ$, $H/b = 0.111$)

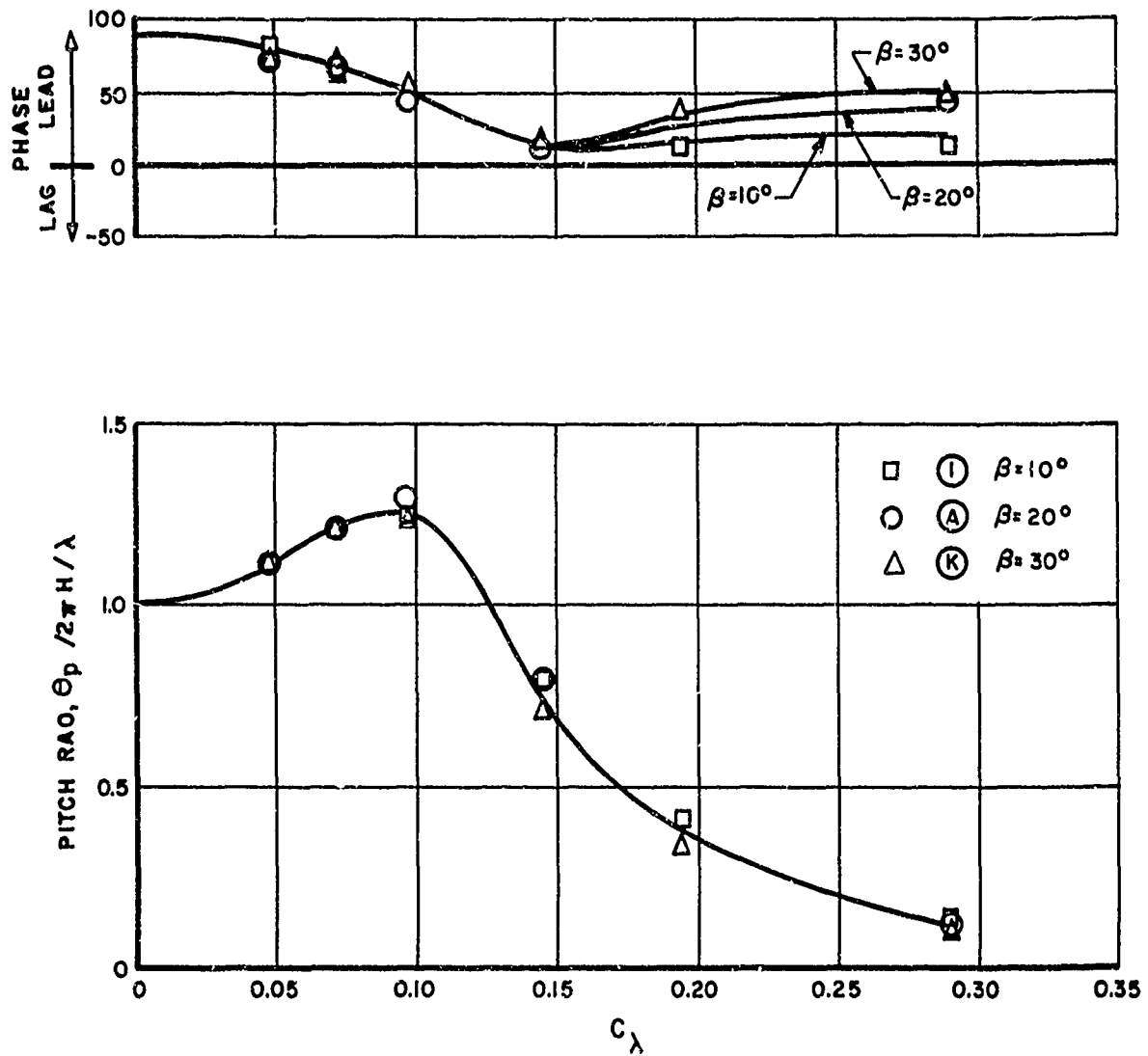


FIG. 46. EFFECT OF DEADRISE ON THE PITCH RESPONSE AT $V/\sqrt{L} = 4$
 ($L/b = 5$, $C_\lambda = 0.608$, $\tau = 4^\circ$, $H/b = 0.111$)

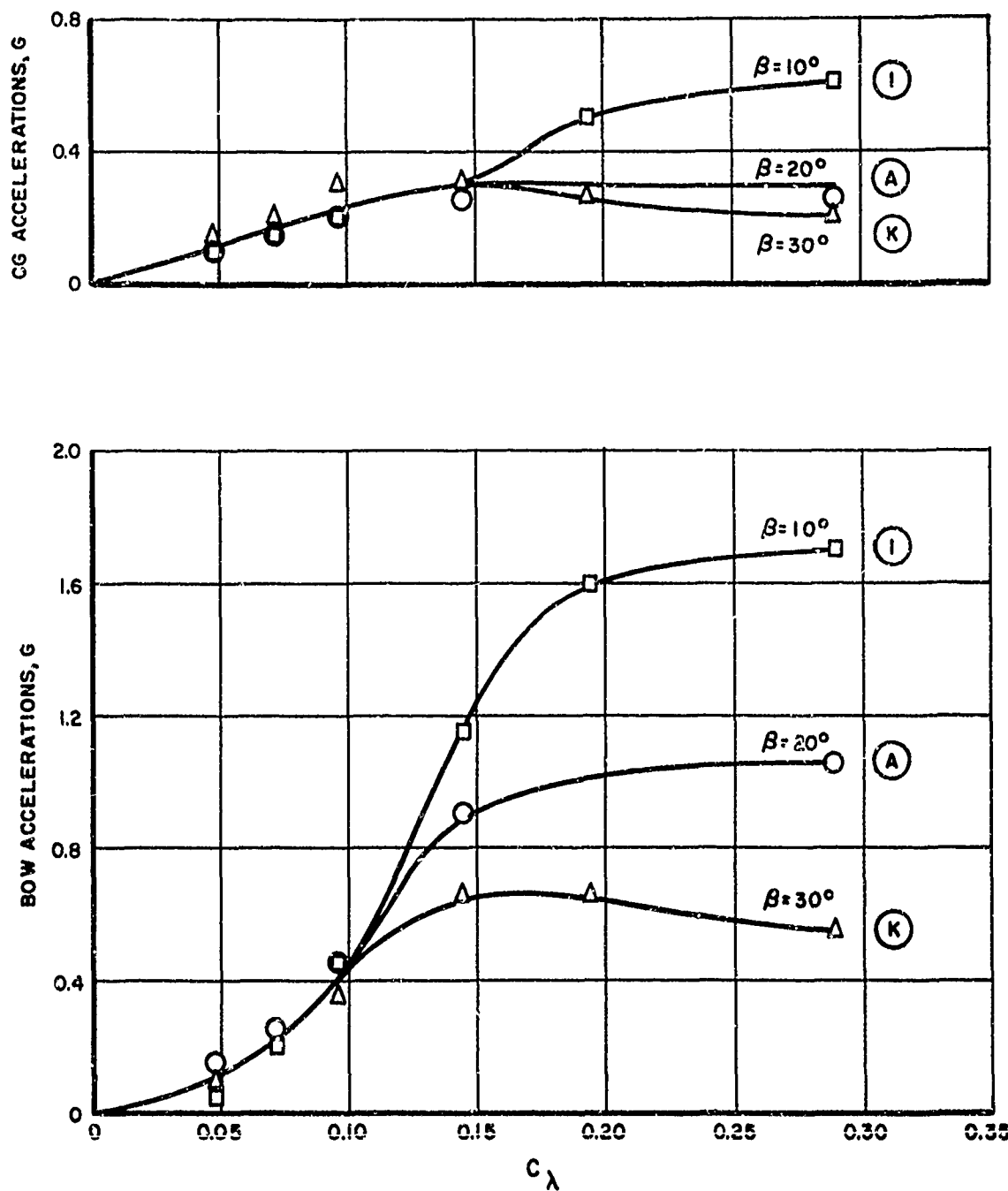


FIG. 47. EFFECT OF DEADRISE ON ACCELERATIONS AT $V/\sqrt{L} = 4$
 ($L/b = 5$, $C_\lambda = 0.608$, $\tau = 4^\circ$, $H/b = 0.111$)

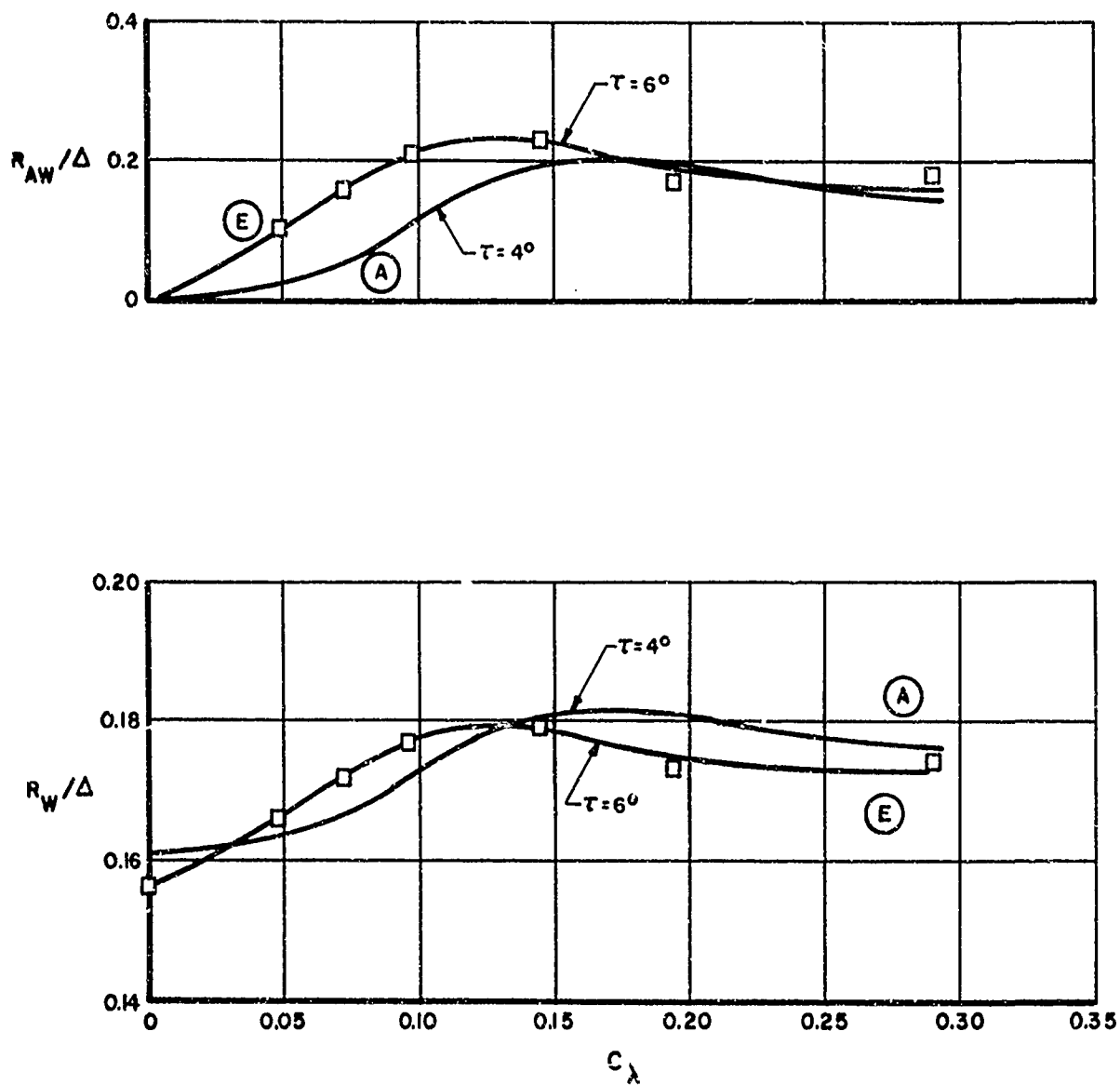


FIG. 48. EFFECT OF TRIM ON RESISTANCE AT $V/\sqrt{L} = 4$
 ($L/b = 5$, $C_A = 0.608$, $\beta = 20^\circ$, $H/b = 0.111$)

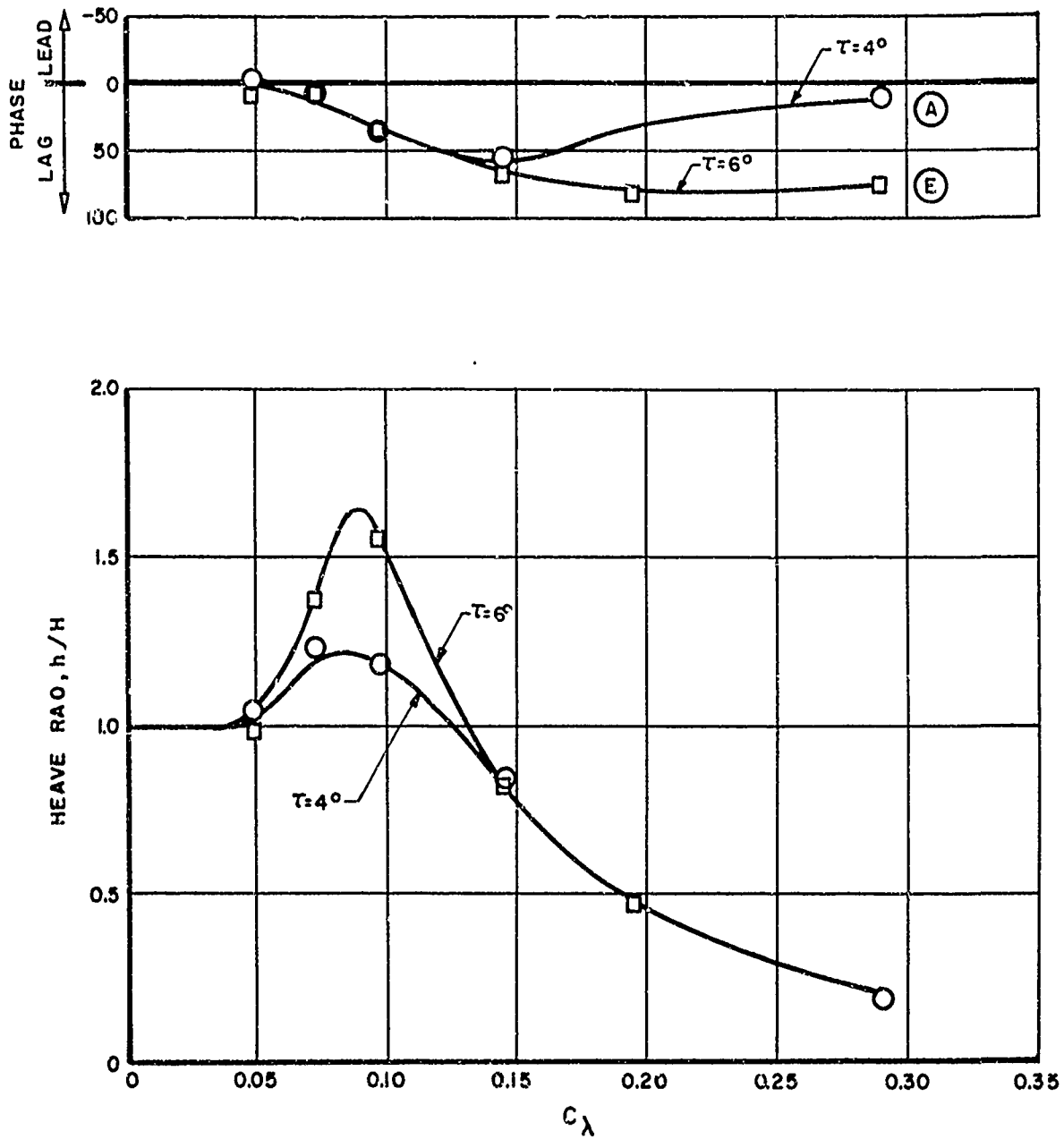


FIG. 49. EFFECT OF TRIM ON HEAVE RESPONSE AT $V/\sqrt{L} = 4$
 ($L/b = 5$, $C_A = 0.608$, $\beta = 20^\circ$, $H/b = 0.111$)

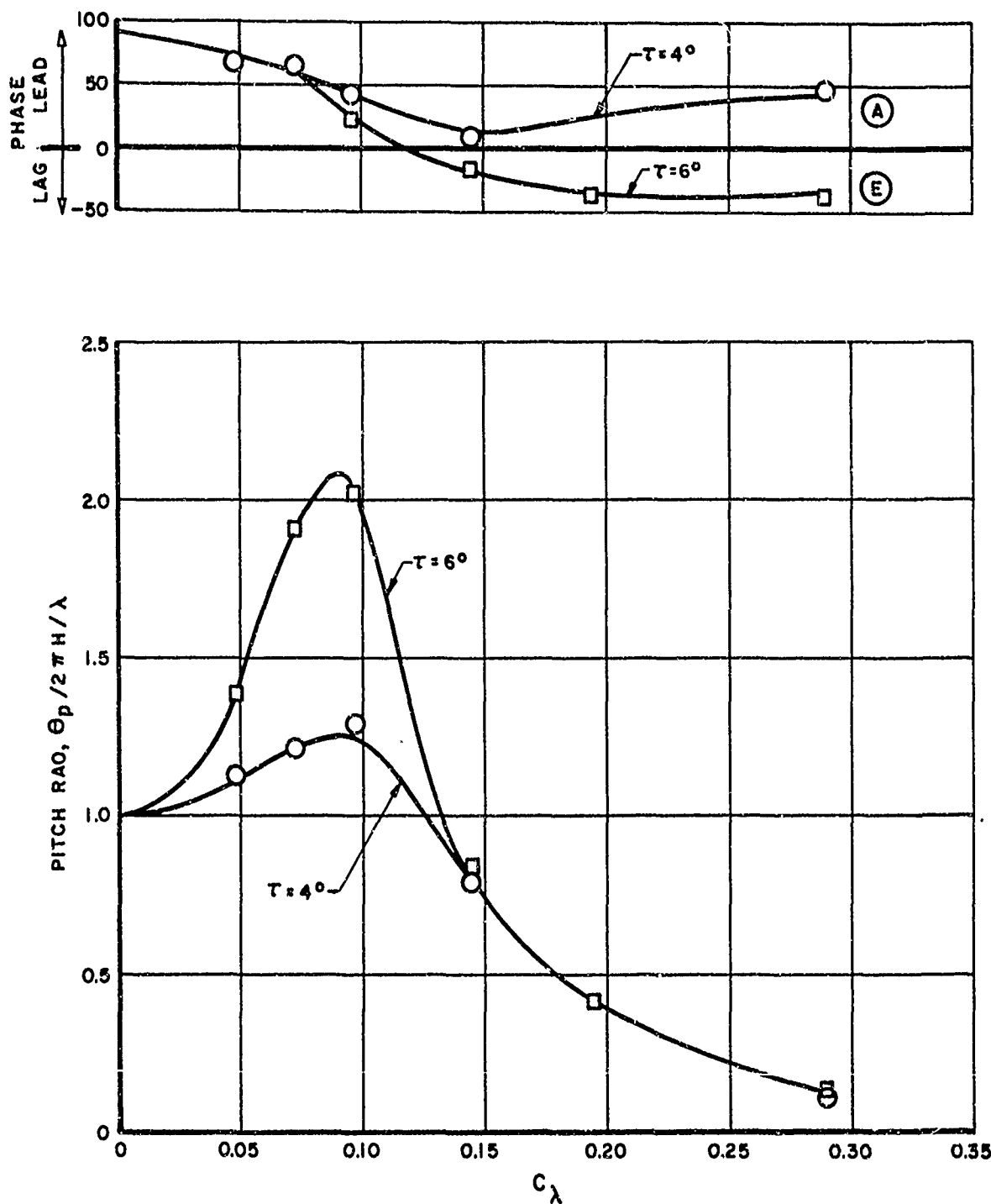


FIG. 50. EFFECT OF TRIM ON PITCH RESPONSE AT $V/\sqrt{L} = 4$
 ($L/b = 5$, $C_A = 0.608$, $\beta = 20^\circ$, $H/b = 0.111$)

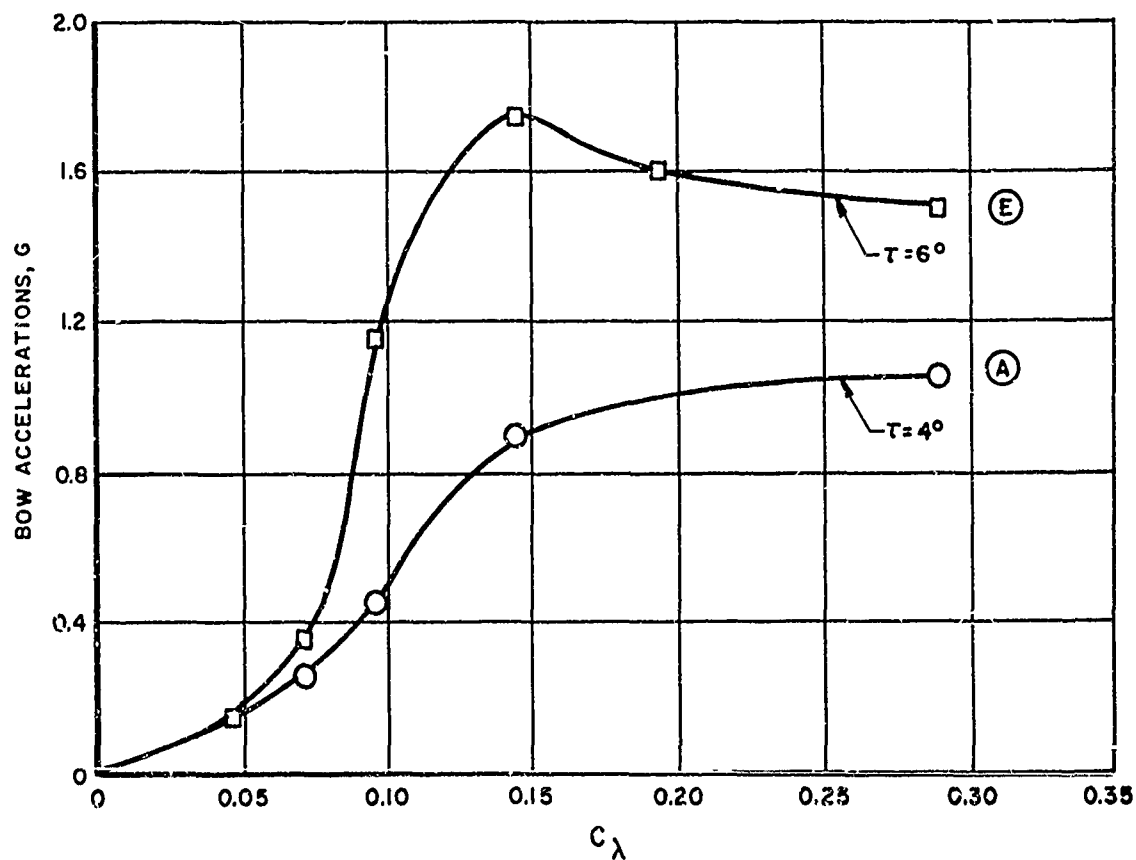
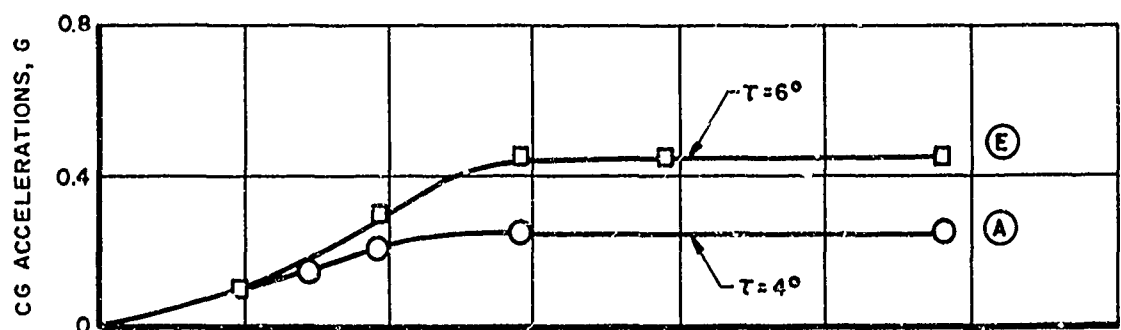


FIG. 51. EFFECT OF TRIM ON ACCELERATIONS AT $V/\sqrt{L} = 4$
 $(L/b = 5, C_d = 0.608, \beta = 20^\circ, H/b = 0.111)$

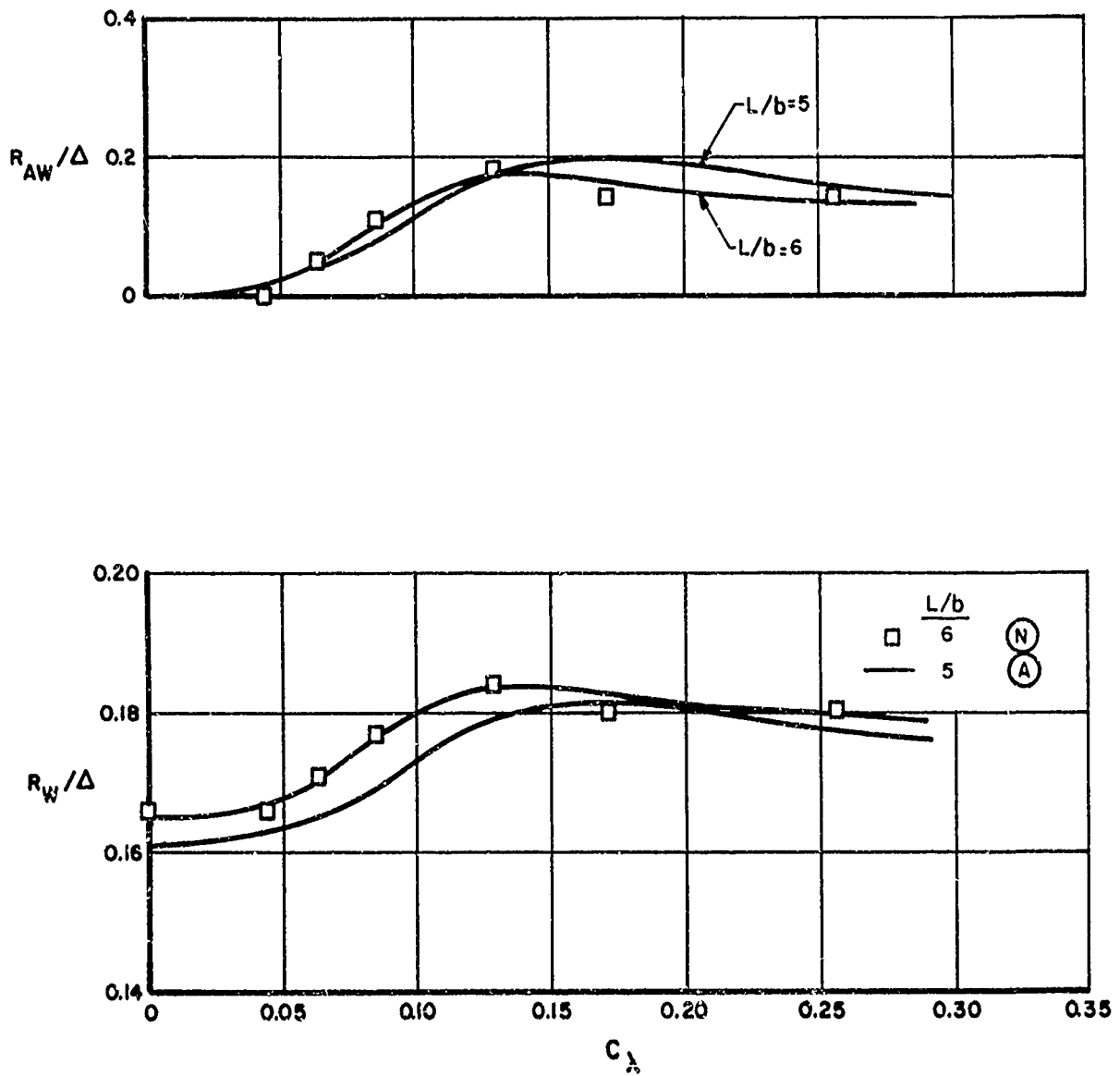


FIG. 52. EFFECT OF LENGTH-BEAM RATIO ON RESISTANCE AT $V/\sqrt{L}=4$
 ($C_A=0.608$, $\tau=4^\circ$, $H/b=0.111$, $\beta=20^\circ$)

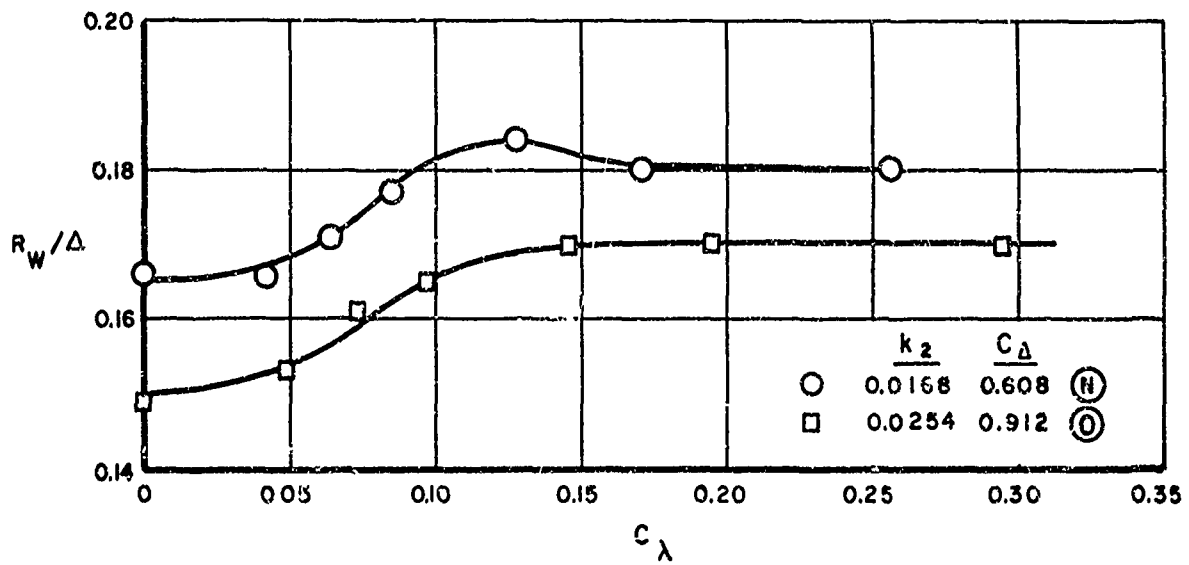
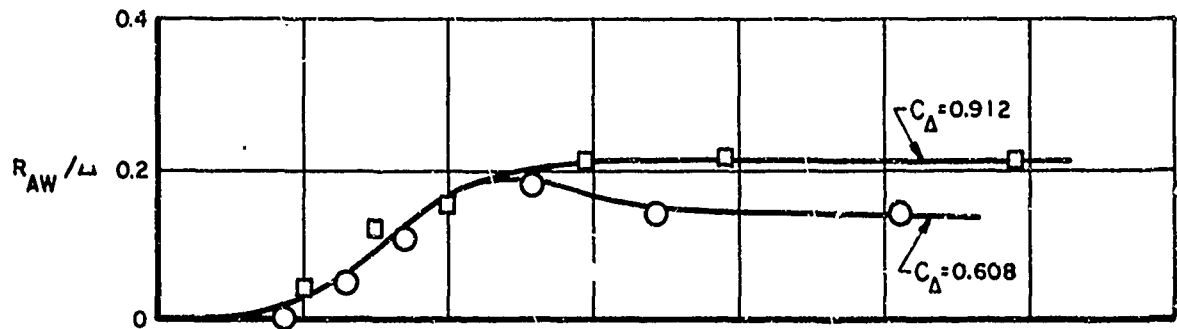


FIG. 53. EFFECT OF LOAD ON RESISTANCE AT $V/\sqrt{L} = 4$
 ($L/b = 6$, $\tau = 4^\circ$, $H/b = 0.111$, $\beta = 20^\circ$)

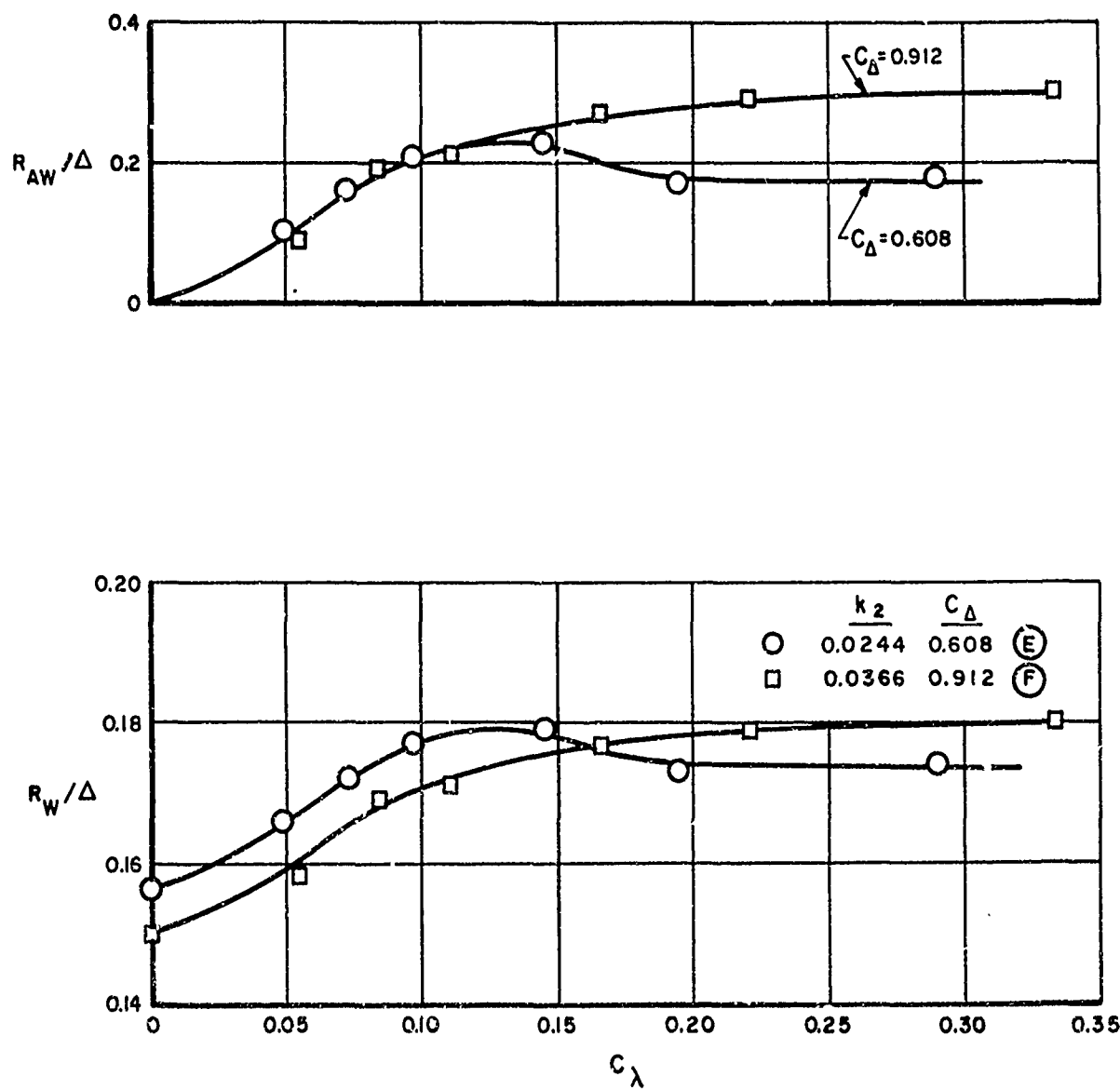


FIG. 54. EFFECT OF LOAD ON RESISTANCE AT $V/\sqrt{L} = 4$
 ($L/b = 5$, $\tau = 6^\circ$, $H/b = 0.111$, $\beta = 20^\circ$)

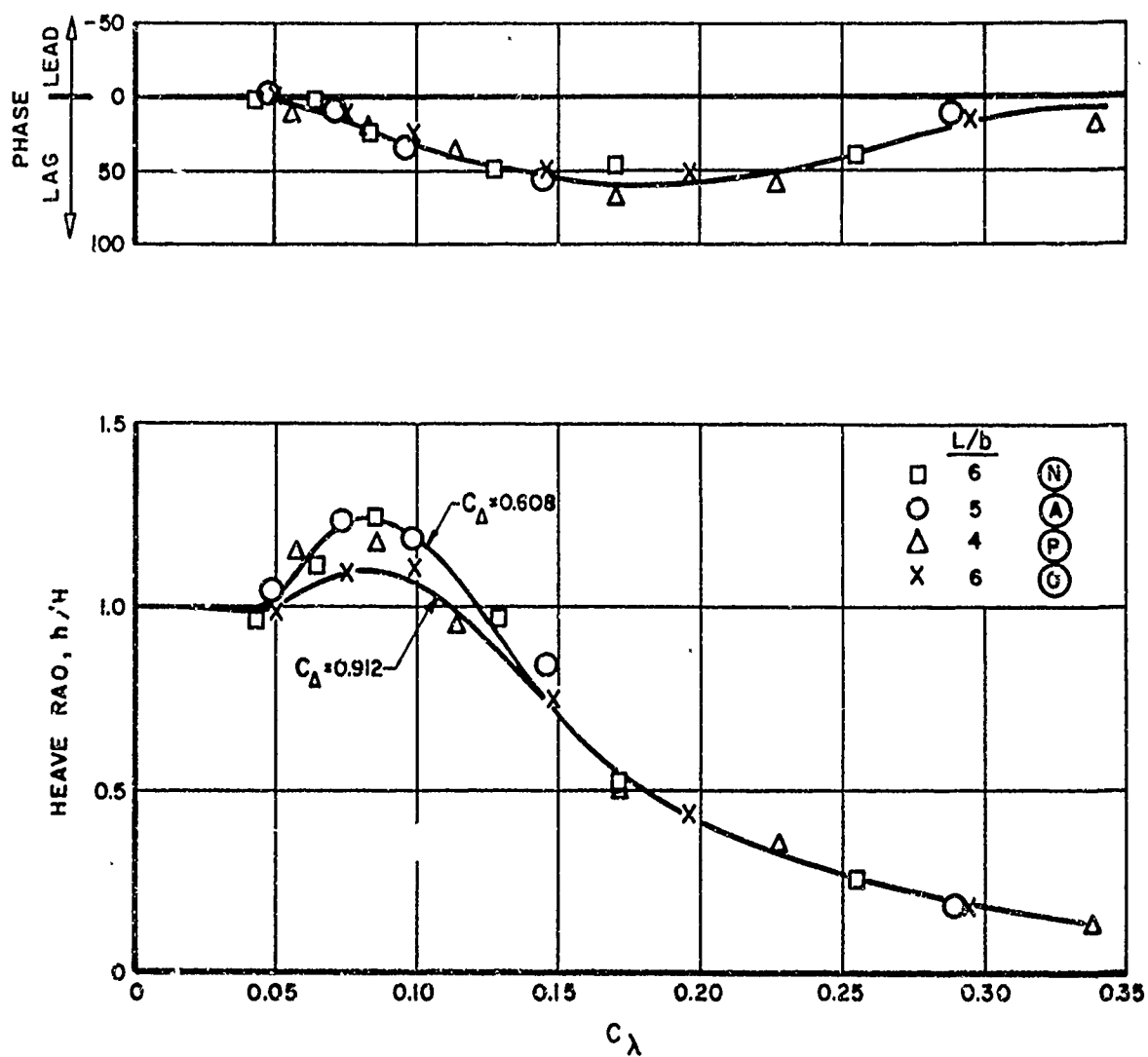


FIG. 55. EFFECT OF LENGTH-BEAM RATIO AND LOAD ON HEAVE RESPONSE AT $V/\sqrt{L} = 4$
 ($\tau = 4^\circ$, $H/b = 0.111$, $\beta = 20^\circ$)

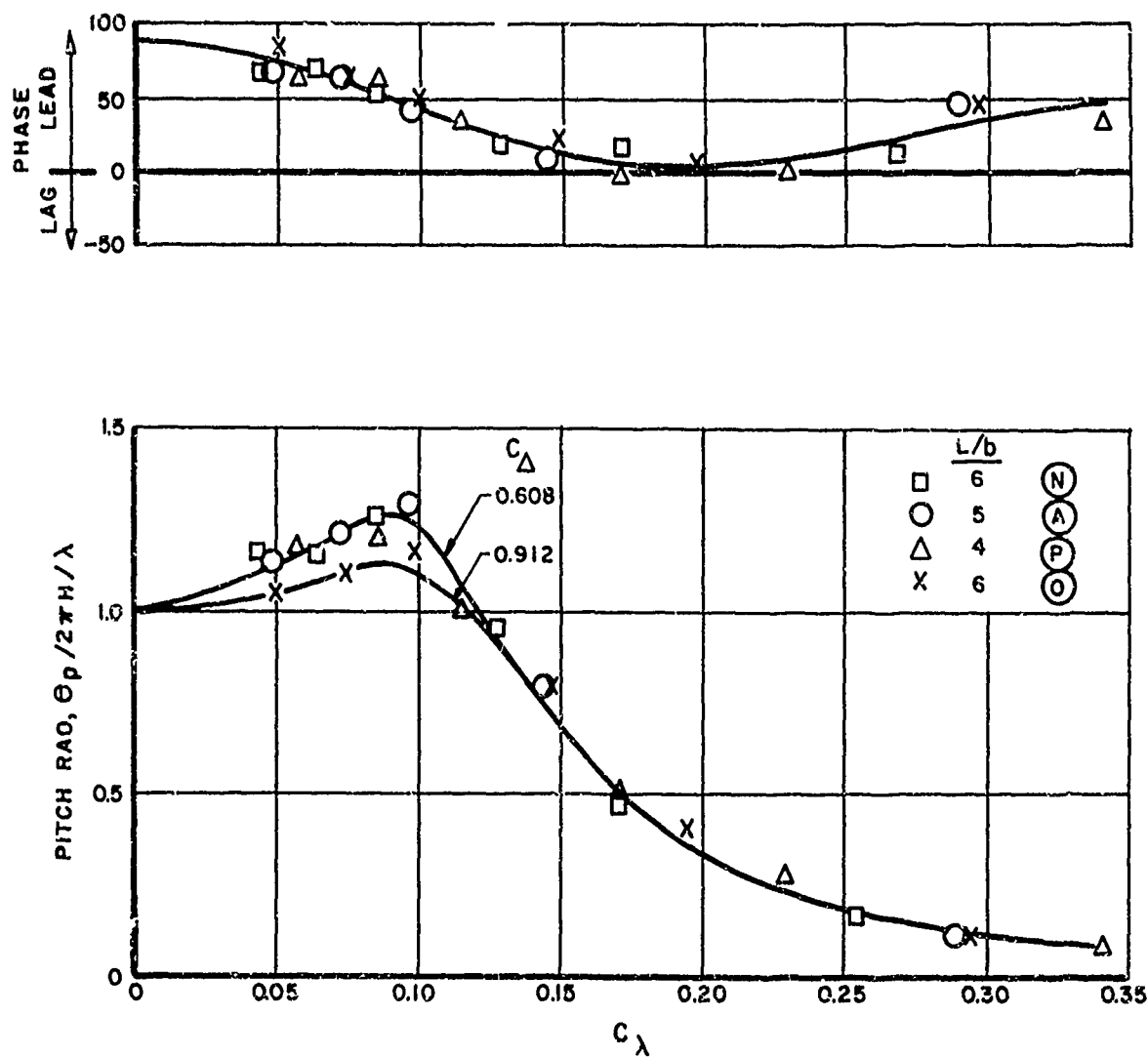


FIG. 56. EFFECT OF LENGTH-BEAM RATIO AND LOAD ON PITCH RESPONSE AT $V/\sqrt{L} = 4$

($C_\Delta = 0.608$, $\tau = 4^\circ$, $H/b = 0.111$, $\beta = 20^\circ$)

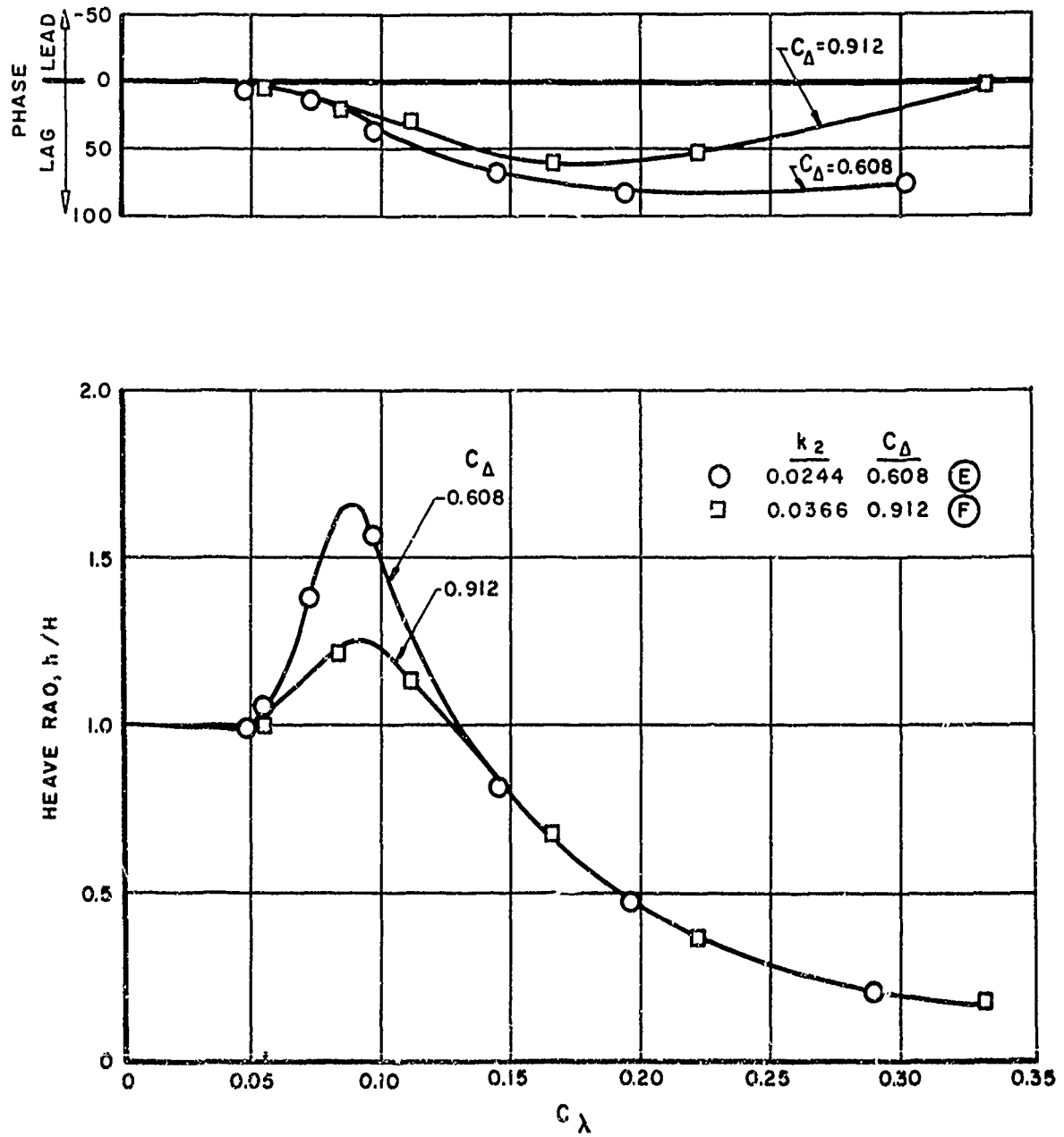


FIG. 57. EFFECT OF LOAD ON THE HEAVE RESPONSE AT $V/\sqrt{L} = 4$
 $(L/b=5, \tau=6^\circ, H/b=0.111, \beta=20^\circ)$

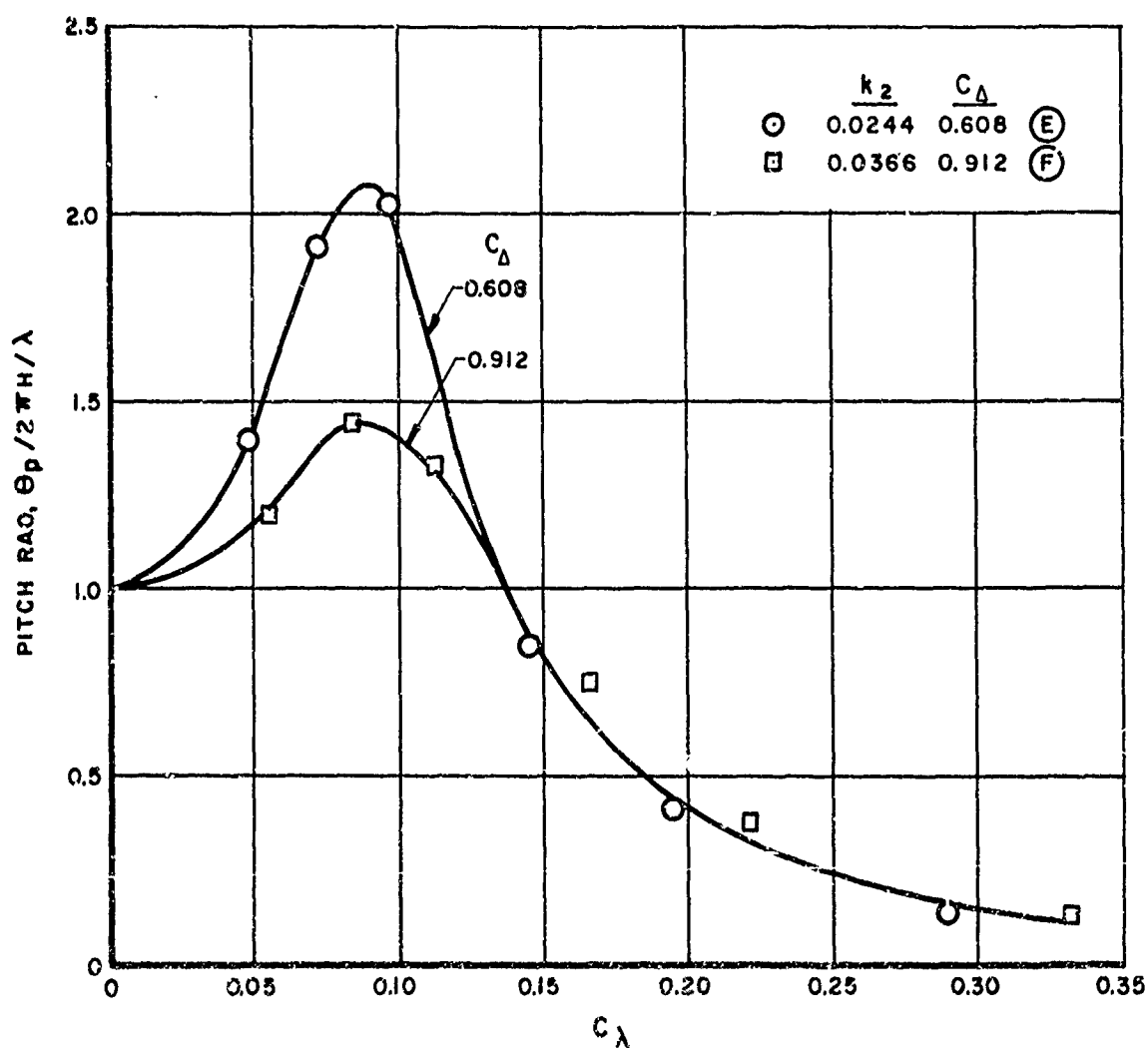
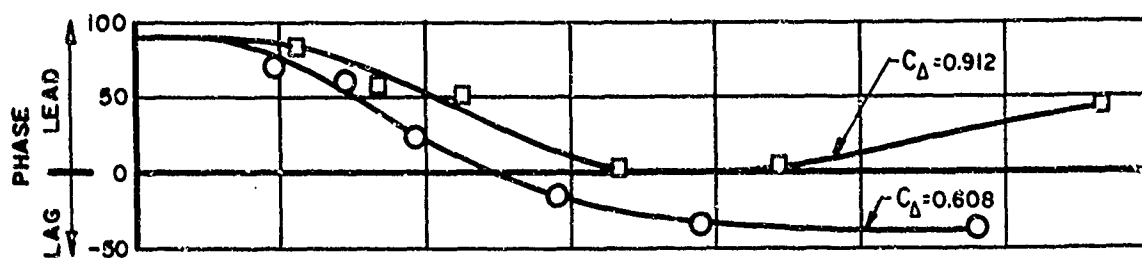


FIG.58. EFFECT OF LOAD ON PITCH RESPONSE AT $V/\sqrt{L} = 4$
 $(L/b = 5, \tau = 6^\circ, H/b = 0.111, \beta = 20^\circ)$

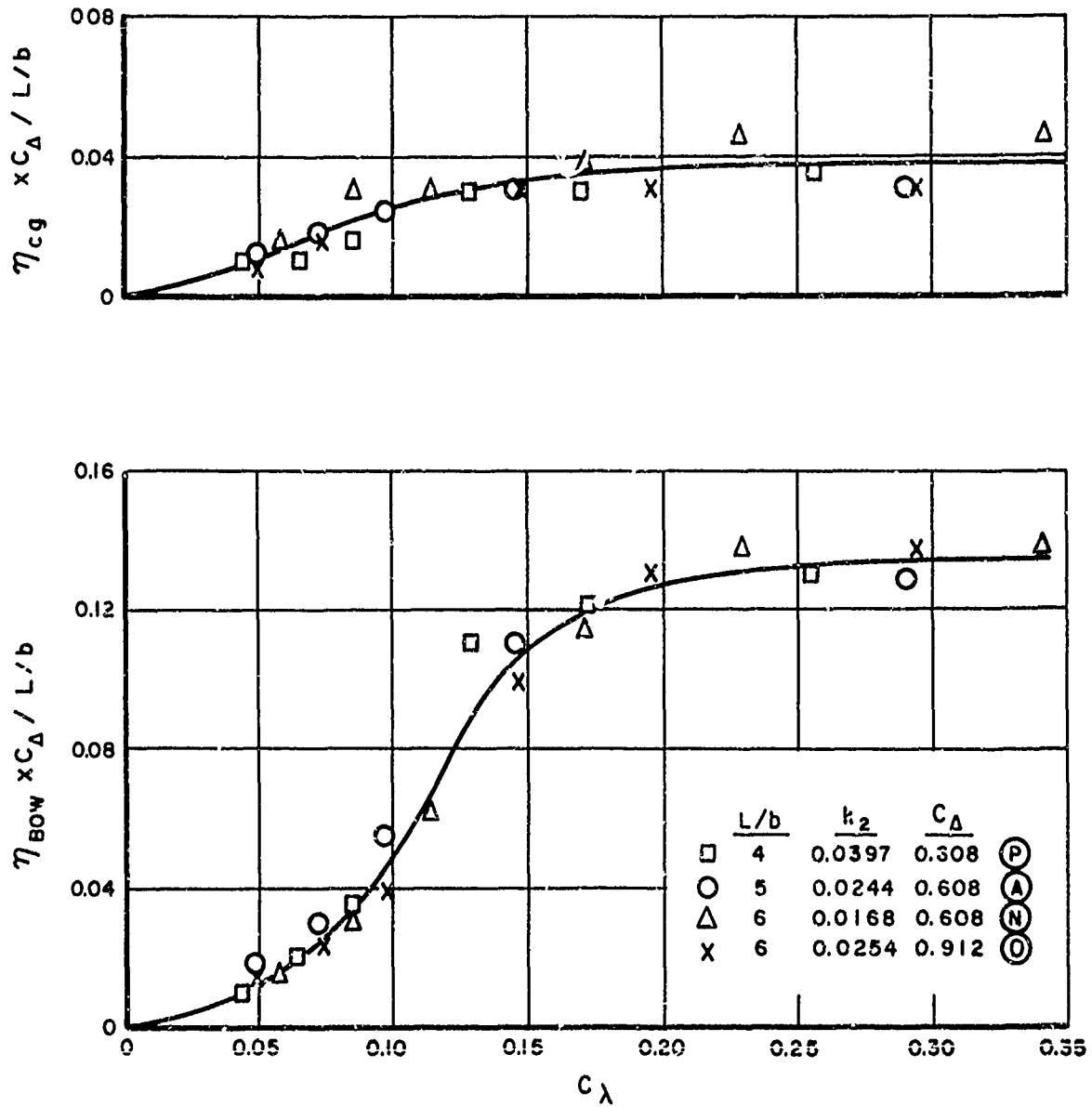


FIG. 59. EFFECT OF LENGTH-BEAM RATIO AND LOAD ON ACCELERATIONS
AT $V/\sqrt{L}=4$ ($\tau=4^\circ$, $H/b=0.111$, $\beta=20^\circ$)

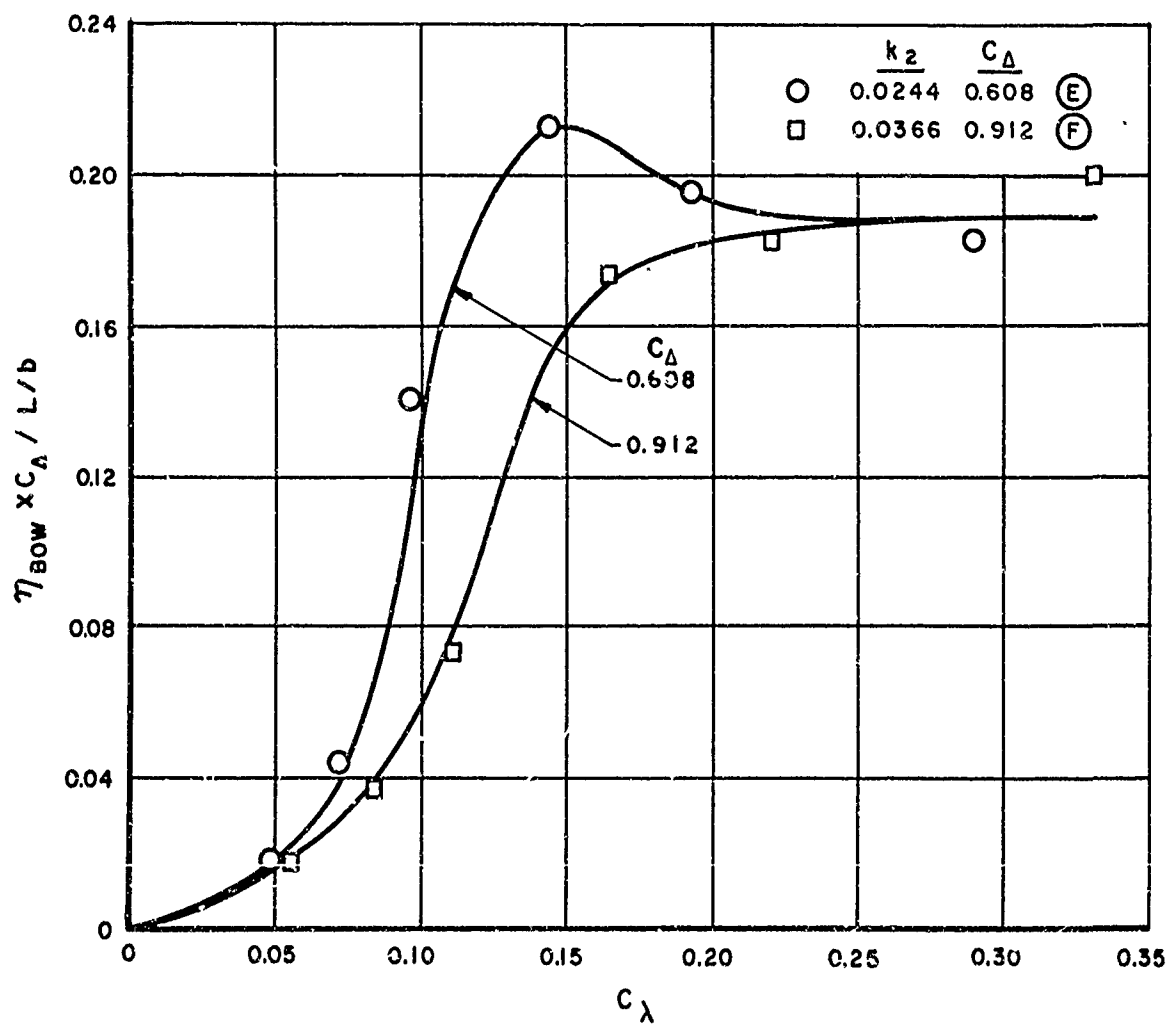
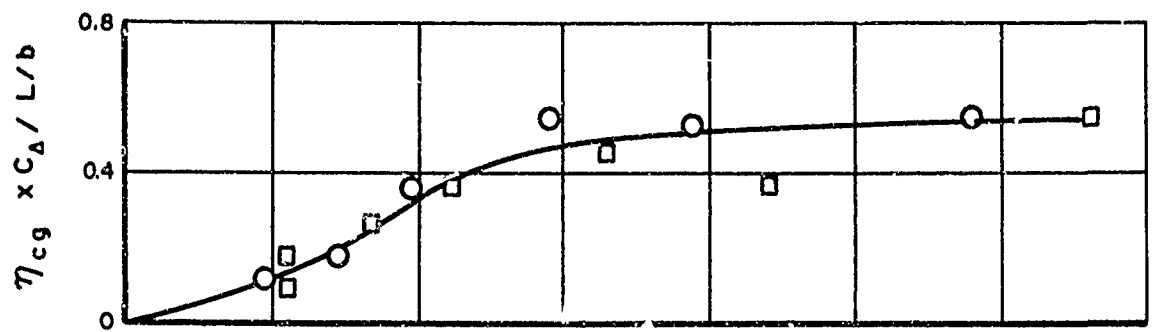


FIG. 60. EFFECT OF LOAD ON ACCELERATIONS AT $V/\sqrt{L} = 4$
 ($L/b = 5$, $\tau = 6^\circ$, $H/b = 0.111$, $\beta = 20^\circ$)

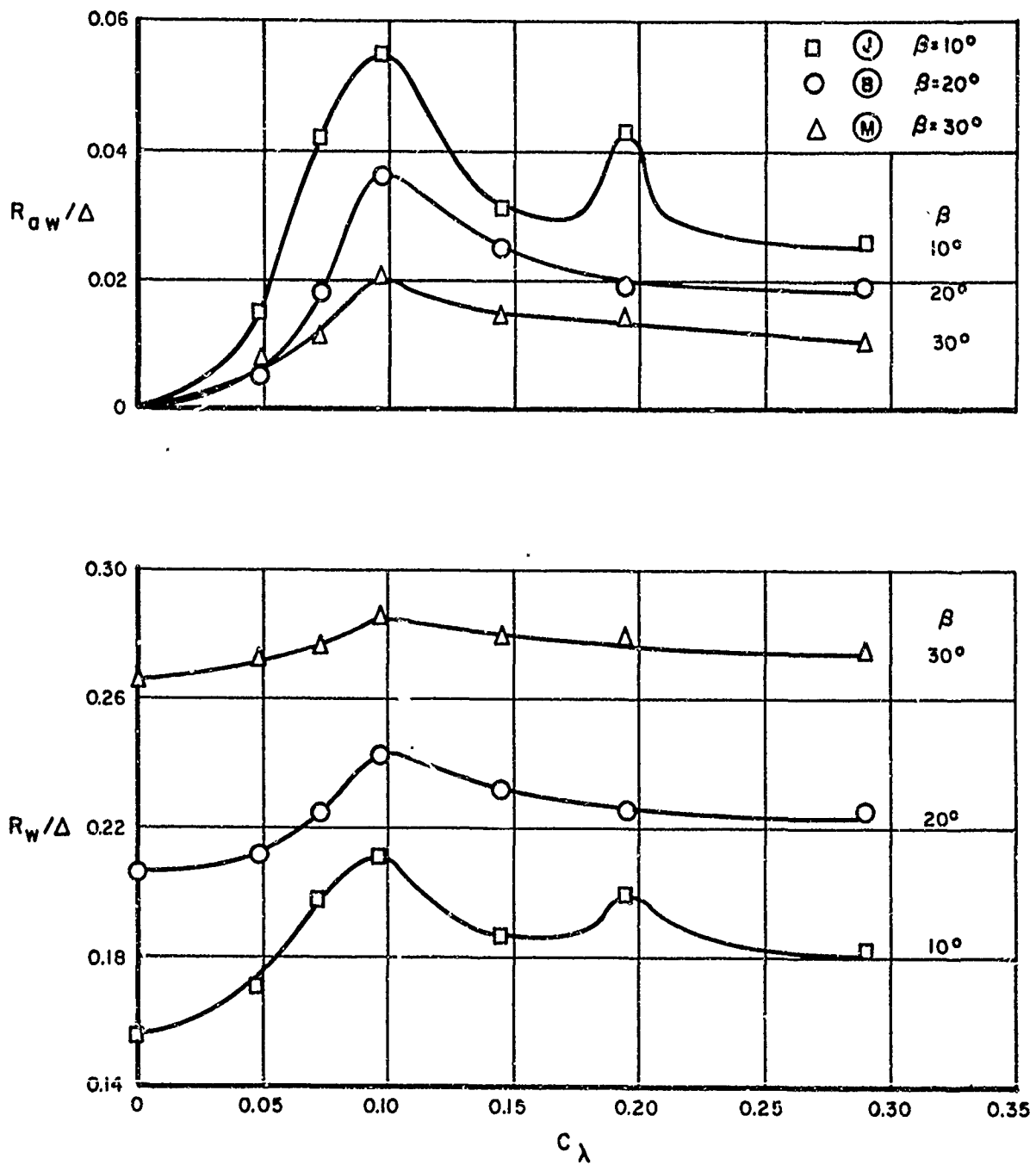


FIG. 6I. EFFECT OF DEADRISE ON RESISTANCE AT $V/\sqrt{L}=6$
 ($L/b=5$, $C_\Delta=0.608$, $\tau=4^\circ$, $H/b=0.111$)

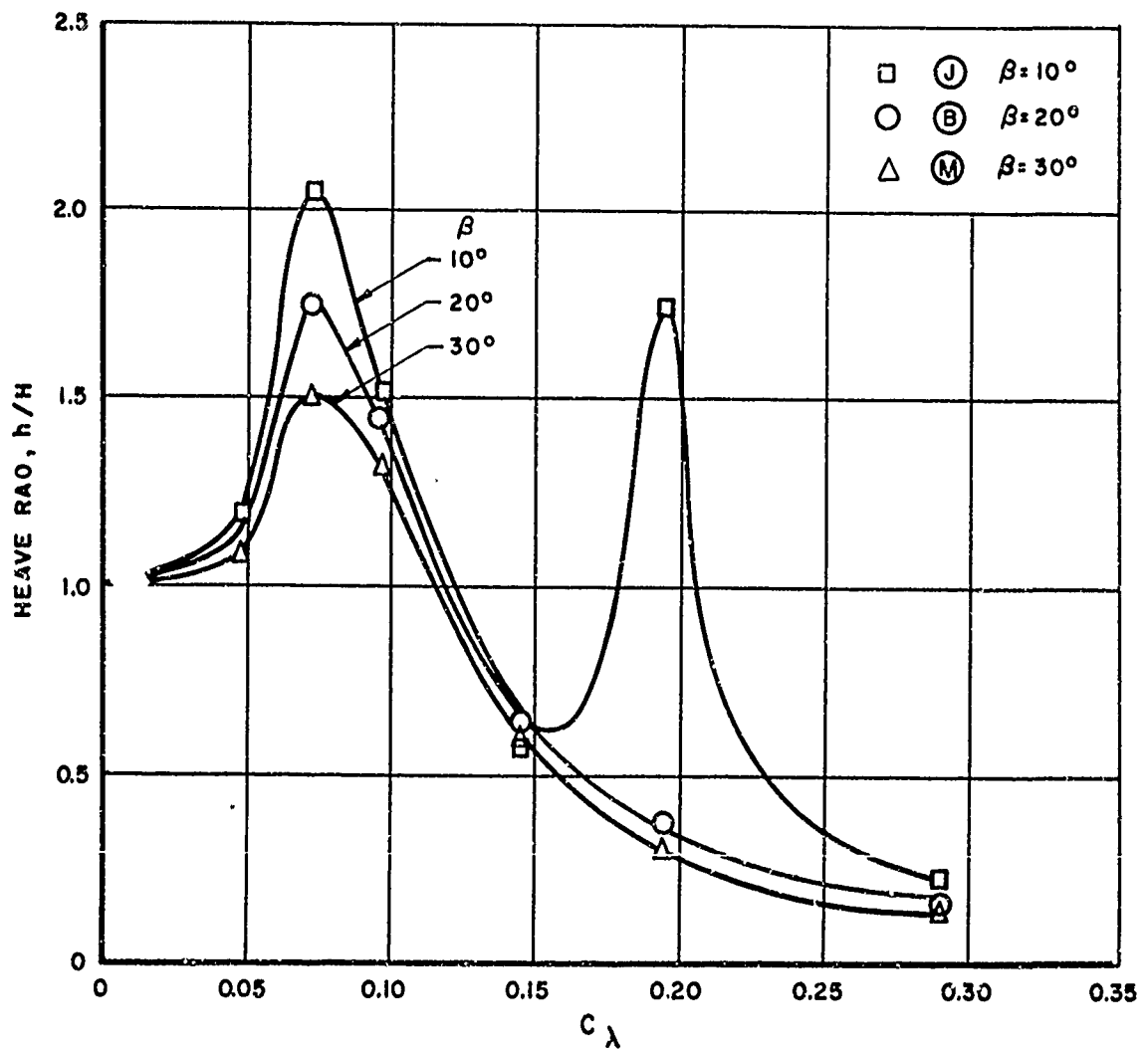
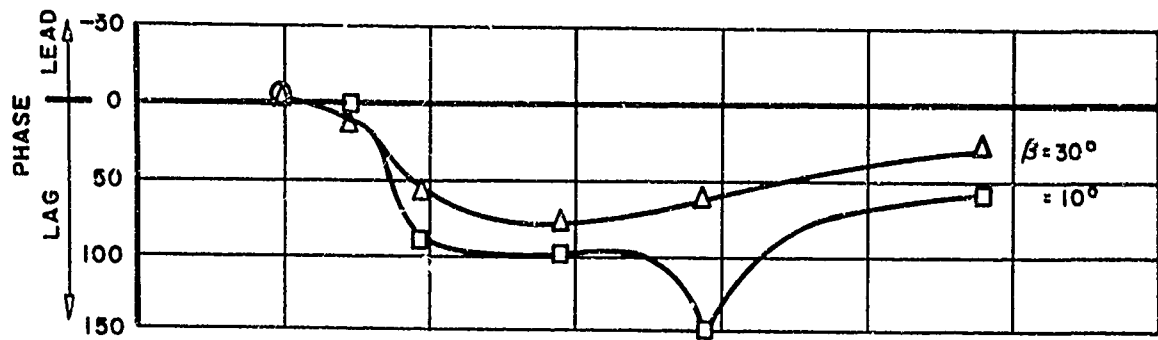


FIG. 62. EFFECT OF DEADRISE ON THE HEAVE RESPONSE AT $V/\sqrt{L} = 6$
 ($L/b = 5$, $C_\Delta = 0.608$, $\tau = 4^\circ$, $H/b = 0.111$)

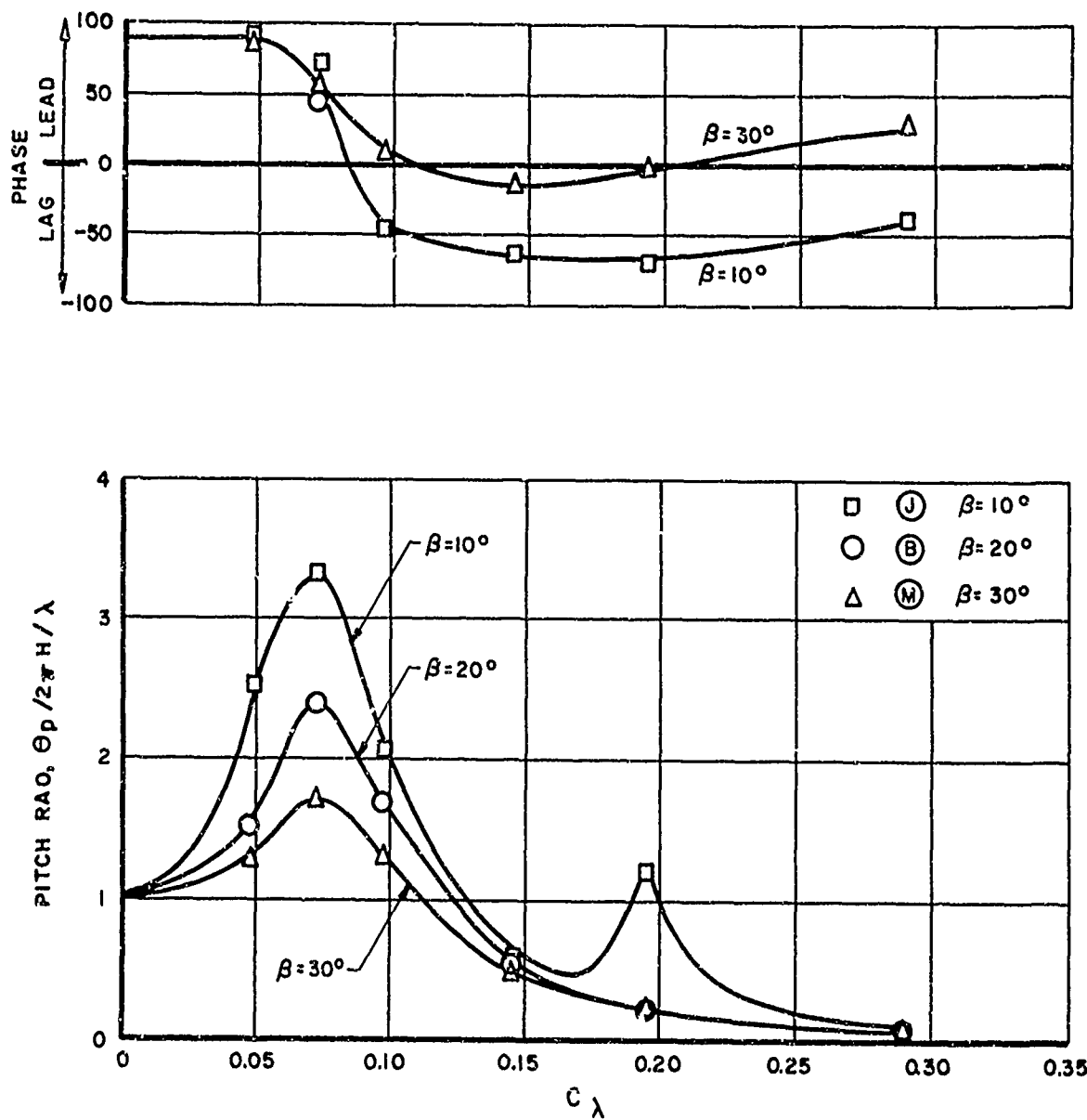


FIG.63. EFFECT OF DEADRISE ON THE PITCH RESPONSE AT $V/\sqrt{L} = 6$
 ($L/b = 5$, $C_d = 0.608$, $\tau = 4^\circ$, $H/b = 0.111$)

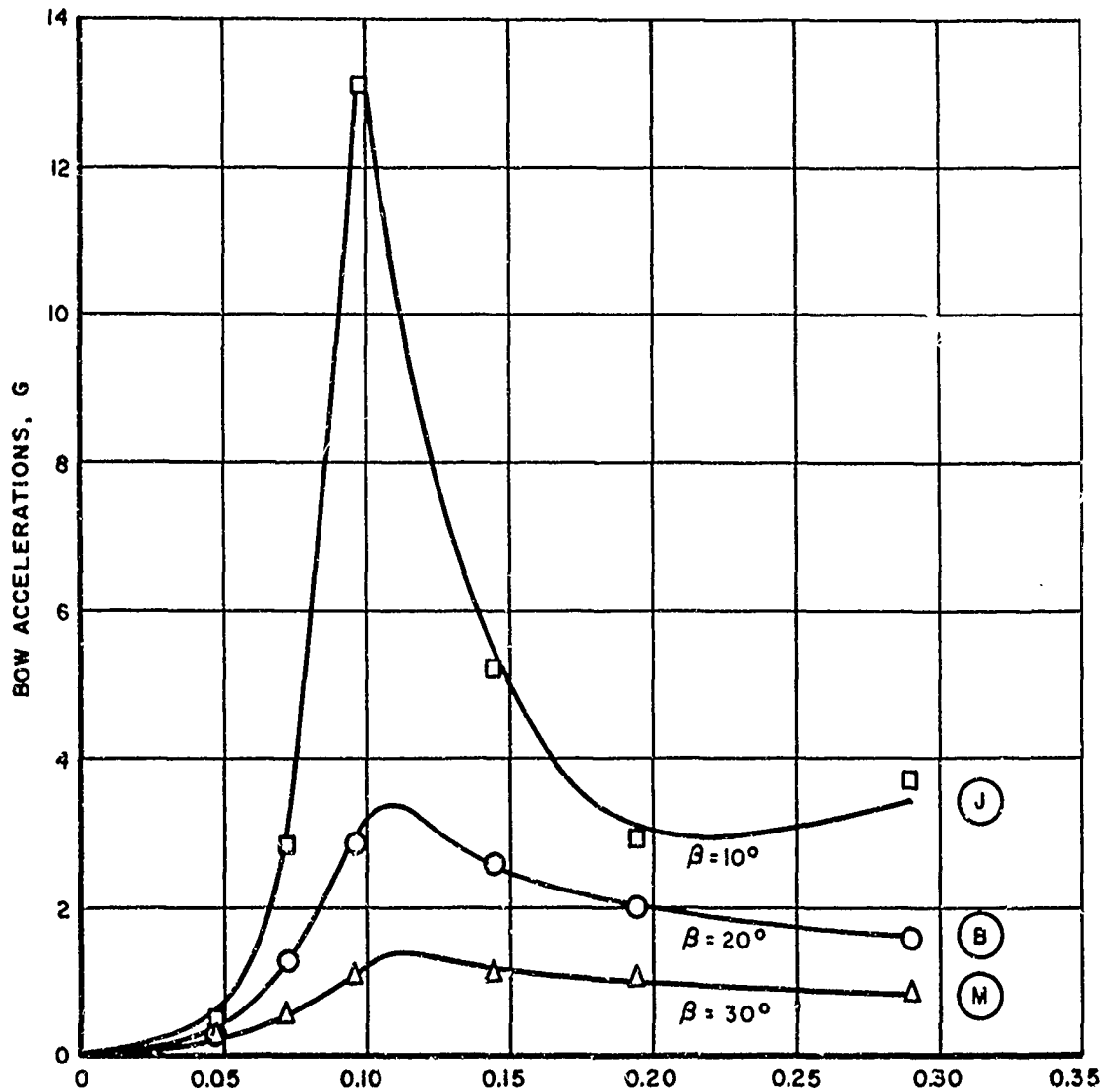


FIG. 64. EFFECT OF DEADRISE ON BOW ACCELERATIONS AT $V/\sqrt{L} = 6$
 ($L/b = 5$, $C_d = 0.608$, $\tau = 4^\circ$, $H/b = 0.111$)

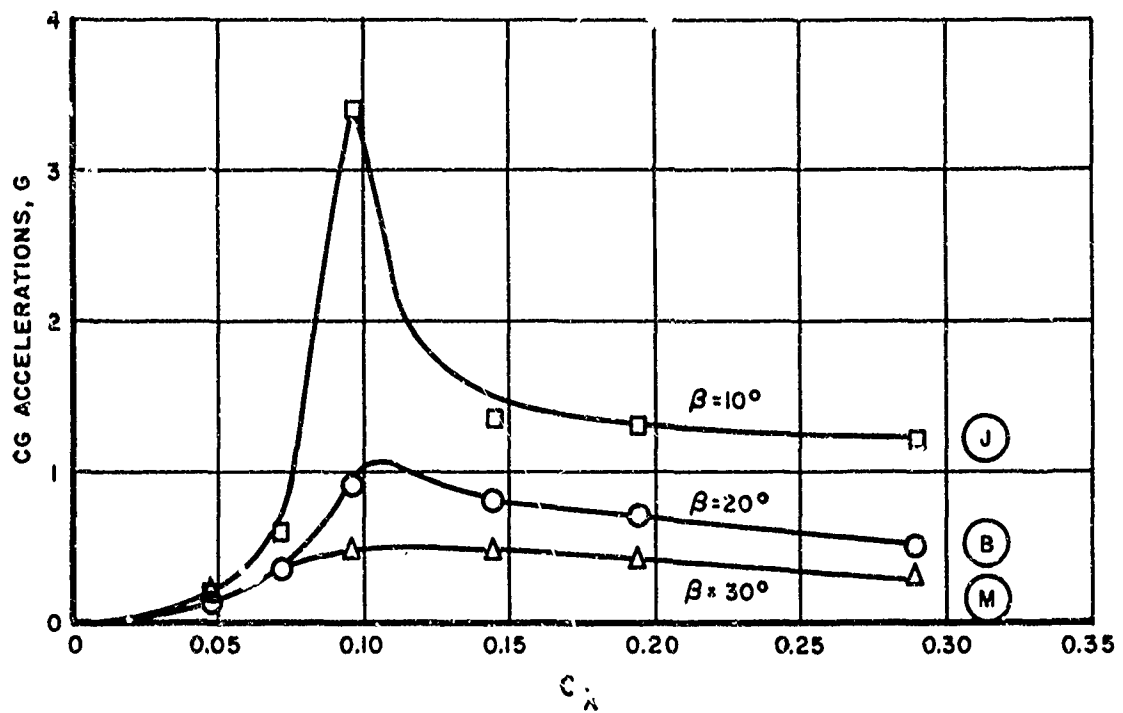


FIG. 65. EFFECT OF DEADRISE ON CG ACCELERATIONS AT $V/\sqrt{L} = 6$
 ($L/b = 5$, $C_A = 0.608$, $\tau = 4^\circ$, $H/b = 0.111$)

UNCLASSIFIED

Security Classification

DOCUMENT CONTROL DATA - R & D

Security classification of title, body of abstract and indexing annotation must be entered when the overall report is classified

1. ORIGINATING ACTIVITY (Corporate author) Davidson Laboratory Stevens Institute of Technology		2a. REPORT SECURITY CLASSIFICATION Unclassified	
		2b. GROUP	
3. REPORT TITLE A-SYSTEMATIC STUDY OF THE ROUGH-WATER PERFORMANCE OF PLANING BOATS			
4. DESCRIPTIVE NOTES (Type of report and, inclusive dates) Final (March-December 1968)			
5. AUTHOR(S) (First name, middle initial, last name) Gerard Fridsma			
6. REPORT DATE November 1969		7a. TOTAL NO. OF PAGES viii + 38 p.	7b. NO. OF REFS
8a. CONTRACT OR GRANT NO. N00014-67-A-0202-0010		9a. ORIGINATOR'S REPORT NUMBER(S) R-1275	
b. PROJECT NO. SR 009 01 01			
c.		9b. OTHER REPORT NO(S) (Any other numbers that may be assigned this report)	
d.			
10. DISTRIBUTION STATEMENT This document has been approved for public release and sale; its distribution is unlimited. Application for copies may be made to the Defense Documentation Center, 5010 Duke St., Cameron Station, Alexandria, Va. 22314. Reproduction of the document in whole or in part is permitted for any purpose of the U. S. Government.			
11. SUPPLEMENTARY NOTES		12. SPONSORING MILITARY ACTIVITY Naval Ship Research and Development Center Washington, D. C. 20007	
13. ABSTRACT A series of constant-deadrise models, varying in length, was tested in smooth water and regular waves to define the effects of deadrise, trim, loading, speed, length-beam ratio, and wave proportions on the added resistance, on heave and pitch motions, and on impact accelerations at the bow and center of gravity. Each of these parameters was varied independently of the others so as to obtain a proper evaluation of the effects of changing a single quantity. The results, presented in the form of response characteristics, cover a wide range of operating conditions; and show, quantitatively, the importance of design parameters on the rough-water performance of planing hulls.			

UNCLASSIFIED

Security Classification

A-31409

UNCLASSIFIED
Security Classification

14 KEY WORDS	LINK A		LINK B		LINK C	
	ROLE	WT	ROLE	WT	ROLE	WT
Planing Hulls Hydrodynamic Impact Marine Craft Prismatic Surfaces Motions Resistance in waves Linearity						